UNIVERSITY OF CALIFORNIA,
IRVINE

Production of High Specific Activity Radioisotopes via the Szilard-Chalmers Method, Using the UC-Irvine TRIGA® Reactor

DISSERTATION

Submitted in partial satisfaction of the requirements

For the degree of

DOCTOR OF PHILOSOPHY

In Chemical and Biochemical Engineering

By

Leila Safavi-Tehrani

Dissertation Committee:

Professor Mikael Nilsson, Chair

Professor Joyce Keyak

Professor Martha Mecartney

2016

DEDICATION

To the best person I will ever know, my Mother

TABLE OF CONTENTS

LIST OF FIGURES

LIST OF TABLES

ACKNOWLEDGMENTS

I would like to express my sincerest gratitude to every single person who made this journey possible and all the more joyful.

First and foremost, I would like to express my great appreciation to Professor Mikael Nilsson for patiently and insightfully guiding me through my graduate school experience. I have learned far more from your mentorship and this project than words can ever express and I will be forever indebted to you for all your unwavering support and guidance over the years.

A special thanks to Professor Joyce Keyak and Professor Martha Mecartney for your guidance, helpful comments and suggestions on my dissertation work and serving on my doctoral committee.

To Dr. George Miller for introducing me to the field of radiochemistry and nuclear chemistry back in 2010 when I was an undergraduate student and had no idea I would one day be working on radioisotope production for my Ph.D. Thank you for all your guidance and support throughout the years

To Jonathan Wallick who patiently trained me to become a reactor operator and always helped me with my experiments throughout the years at the UCI Reactor Facility.

To Professor Eric Mcfarland and all the members of the DOW center for sustainable engineering and innovation at the University of Queensland, for giving me the opportunity to join the center as a visiting scholar and evaluate the techno-economics of my research project. I learned so much from your mentorship, guidance and work ethic.

Thank you to Professor Ali Mohraz, Graduate Student Advisor, Professor A.J. Shaka and all the Chemical Engineering and Materials Science department staff: Yi-San Chang-Yen,

Beatrice Mei, Grace Chau, Janine Le and Steve Weinstock for your support and guidance throughout the years.

A special thanks to my friends: Ladan Boustani, you've been through it all with me since middle school, Media Neek who's made the last couple years at UCI memorable, and all my past and present colleagues from the Nilsson research group: Andy Jackson, Quynh Vo, Christian Bustillos, Tro Babikian, Jaclynn Unangst, Randy Ngelale, Rose Pier, Edward Jenner, Ko Nee, Jeremy Pearson, Michael Gray, Alex Braatz, Cory Hawkins, Jisue Moon, Alan Tam, Amber Hennessey and Raul Ocampo every single one of you made this journey all the more enjoyable I could not have imagined going through this without you.

A special thanks to Maryam and Shadi Alesafar your love and support throughout the years especially when I moved to California was essential in getting me to where I am today, I am forever grateful.

Thank you to Elahe and Shahab Rafiee for inviting me into your family and making my experience in Brisbane so memorable.

I would like to thank my family without your love, support, patience and guidance I would never be where I am today. Particularly I would like to thank, my sister Azadeh Safavi you always have a way of lightening the mood when I take life to seriously. My Aunt Marjan Najmabadi, Amin Najmabadi and Hossien Najmabadi, your love and support in every aspect of my life has been essential, thank you for always being there.

I am grateful for my dog Mooshi who has always been by my side through all the late nights and weekends I was working on this project.

Last but definitely not least I would like to thank my parents especially my Mother Afarin Safavi, words can never express how grateful I am for everything you have done for me, none of this would be even remotely possible if it wasn't for your love, continuous support, guidance and sacrifices. I am forever indebted.

I would like to thank U.S. Nuclear Regulatory Commission through the Faculty Development Grant contract no. NRC-HQ-11-G-38-0037 and the Department of Energy: DOE AWARD DE-NE-0000361 (2010-2012) Reactor Minor Upgrade Program for the funding of this project.

CURRICULUM VITAE

Leila Safavi-Tehrani

Education

2010	B.S. in Chemistry, University of California, Irvine
2013	M.S. in Chemical Engineering, University of California, Irvine
2016	Ph.D. in Chemical Engineering, University of California, Irvine

Field of Study

Production of High Specific Activity Radioisotopes via the Szilard-Chalmers Method, Using the UC-Irvine TRIGA® Reactor.

Journal Publications

Safavi-Tehrani L, Miller G, Nilsson M. Production of High Specific activity Radiolanthanides for Medical Purposes using the UC Irvine TRIGA reactor. J Radioanal Nucl Chem 2015;303:1099-103. Available online: DOI: 10.1007/s10967-014-3486-2

Safavi-Tehrani L, Miller G, Nilsson M. Continuous Production of High Specific Activity Radiolanthanides using the Szilard-Chalmers method (In preparation).

Safavi-Tehrani L, Nilsson M, McFarland E. Techno-economic Analysis of Radioisotope Production (In preparation)

Safavi-Tehrani L, Miller G, Nilsson M. Review Paper: Application and Production of Radioisotopes (In Preparation).

Safavi-Tehrani L, Miller G, Nilsson M. Radioisotope Production Using Novel Holmium Acetylacetonate Polyvinyl Alcohol XAD-4 Resins (In preparation)

Patents

Safavi-Tehrani L, Miller G, Nilsson M. High Efficiency Continuous Flow Production of Radioisotopes (Provisional)

Selected Conferences

Oral Presentations:
Safavi-Tehrani L, Miller G, Nilsson M. Production of High Specific Activity Radiolanthanides for Medical Purposes. American Chemical Society, Philadelphia 2012
Safavi-Tehrani L, Miller G, Nilsson M. Production of High Specific Activity Radiolanthanides for Medical Purposes. Test Research and Training reactors, San Diego 2012
Safavi-Tehrani L, Miller G, Nilsson M. Production of High Specific Activity Radiolanthanides for Medical Purposes Using the UCI TRIGA® Reactor.
Asia Pacific Symposium on Radiochemistry, Japan 2013
Safavi-Tehrani L, Miller G, Nilsson M. Production of High Specific Activity Radiolanthanides for Medical Purposes using the Szilard-Chalmers Method. Radiochemical Conference, Czech Republic 2014

Poster Presentation:
Safavi-Tehrani L, Miller G, Nilsson M. Production of High Specific Activity Radiolanthanides for Medical Purposes, Actinides
Separation, Salt Lake City, Utah 2015

Student Attendee:
Safavi-Tehrani L, Women in Nuclear Conference. Austin, Texas 2015

Invited Panelist:
Safavi-Tehrani L. TeraWatts, TeraGrams, TeraLiters 2016 Workshop on Challenges and Opportunities for Future Sustainable Production of Chemicals and Fuels. Santa Barbara, California 2016

Honors and Awards

2015	University of Queensland, DOW Centre Scholarship
2014	U.S. Nuclear Regulatory Commission (NRC) Graduate Fellowship
2011	UCI Chemical Engineering Department Mentor Program Fellowship

ABSTRACT OF THE DISSERTATION

Production of High Specific Activity Radioisotopes via the Szilard-Chalmers Method, Using the UC-Irvine TRIGA® Reactor

By

Leila Safavi-Tehrani

Doctor of Philosophy in Chemical and Biochemical Engineering

University of California, Irvine, 2016

Professor Mikael Nilsson, Chair

Radioactive isotopes have become an important imaging, diagnostic and therapeutic tool in the medical field. For example, the neutron rich samarium isotope of ^{153}Sm has been proven to have desirable characteristics for treatment of bone cancer. However, for medical purposes, the radioisotope must be produced with high specific activity, i.e. low concentration of inactive carrier, so they are beneficial for therapy and the concentration of the metal ions does not exceed the maximum sustainable by the human body. The objective of the research study was to produce radioisotopes, specifically the lanthanides, with increased specific activity in a small-scale research reactor using the Szilard-Chalmers method. The preliminary experimental results showed a decrease of 34% in the amount of Lanthanide needed for a typical medical procedure[1]. An innovative experimental setup was also developed that instantaneously separated the radioactive recoil product formed during irradiation from the bulk of non-radioactive ions. The instant separation prevented the recoiled radioactive nucleus from reforming its original bonds within the target matrix and chemically separated it from the non-radioactive target matrix, resulting in a radioisotope product with increased specific activity. The novel experimental setup

resulted in further improvement of the radiolanthanide enrichment factors, and ultimately resulted in a decrease of 96% in the amount of lanthanide needed for typical medical applications. The methods for preparation and synthesis of the material used for irradiations, the results of enrichment factors and extraction yields in radioactive lanthanide solutions are discussed. The obtained results will be compared to previously published methods and their corresponding results.

CHAPTER 1: BACKGROUND AND INTRODUCTION

1.1 Radionuclides

A nuclide is an atom, which is characterized by the combination of protons and neutrons that comprise it. Radionuclides are atoms of an element that have an unstable combination of neutrons and protons. Each type of unstable radioisotope has exclusive radioactive decay properties (type of energy emission and half-life); stability is regained by emission of radioactive energy and transforming to a more stable state. There are a number of different types of radioactive decay (Table 1.1). The radioisotope decay rate is determined by the radioactive half-life, which is the time it takes for half of the radioactive nuclei to decay. The decay process can be just one or a combination of the decay types summarized in Table 1.1. The majority of radionuclides are artificially produced by transformation of a target nuclide into an unstable combination of protons/neutrons by bombardment with neutrons, protons deuterons, alphas, gammas or other types of nuclear particles [2].

Table 1.1: Types of radioactive decay.

Type	Characteristics	Example
Alpha Decay (α)	• Emission of an Alpha particle ($^{4}_{2}\mathrm{He}$) • Usually happens in larger heavier atoms	$^{238}_{92}\mathrm{U} \rightarrow {}^{234}_{90}\mathrm{Th} + {}^{4}_{2}\mathrm{He}$
Beta Decay (β^-)	• Emission of an β^- ($^{0}_{-1}\mathrm{e}$) particle • Accompanied by an anti neutrino • Conversion of a neutron to proton • Occurs in nuclei with high neutron to proton ratios	$^{153}_{62}\mathrm{Sm} \rightarrow {}^{0}_{-1}\mathrm{e} + {}^{153}_{63}\mathrm{Eu} + {}^{0}_{0}\nu^{-}$
Positron Decay (β^+)	• Emission of an β^+ ($^{0}_{1}\mathrm{e}$) particle • Accompanied by a neutrino • Conversion of a proton to neutron • Occurs in nuclei with high proton to neutron ratios	$^{13}_{7}\mathrm{N} \rightarrow {}^{0}_{+1}\mathrm{e} + {}^{7}_{6}\mathrm{C} + {}^{0}_{0}\nu$
Electron Capture	• The nucleus absorbs an electron converting a proton into a neutron • Seen in nuclides with high proton to neutron ratios	$^{145}_{62}\mathrm{Sm} + {}^{0}_{-1}\mathrm{e} \rightarrow {}^{145}_{61}\mathrm{Pm} + {}^{0}_{0}\nu$
Gamma Decay (γ)	• Electromagnetic radiation • Does not change the mass number or charge of the atom • Usually accompanies other types of decay (alpha, beta…)	$^{166}_{67}\mathrm{Ho} \rightarrow {}^{0}_{0}\gamma + {}^{166}_{67}\mathrm{Ho}$
Spontaneous Fission	• Unstable nuclei of heavy elements split into two smaller nuclei and 1-3 neutrons • The fission reaction is accompanied with the release of energy	$^{235}_{92}\mathrm{U} + {}^{1}_{0}\mathrm{n} \rightarrow {}^{89}_{36}\mathrm{Kr} + {}^{144}_{56}\mathrm{Ba} + 3\,{}^{1}_{0}\mathrm{n}$

Radioisotopes play an important role in the everyday life of people throughout the world. Radioisotopes are the key component of radiopharmaceuticals used in both diagnostic and therapeutic nuclear medicine; they are also widely used in industry and scientific research, therefore having reliable radionuclide production facilities is essential.

In addition to medical applications, radioisotopes have many applications in industry (Table 1.2), such as the use of Americium-241 in the commonly used smoke detectors, industrial radiography were a gamma source is used to test structural integrity of material in addition to gauging and measurement applications.

Table 1.2: Common industrial applications of radioisotopes[3].

Radioisotope	Use	Half-Life
Americium-241	Neutron Gauging Smoke Detectors	432.7 years
Cobalt-60	Gamma radiography Gauging Sterilization	5.27 years
Cesium-137	Radiotracer in soil Thickness gauging	30.07 years
Gold-198	Radiotracer in sewage and waste	2.7 days
Iridium-192	Gamma radiography Radiotracer in sand	73.8 days
Chromium-51	Radiotracer in sand	27.7 days
Tritiated water	Radiotracer for sewage and liquid waste studies	12.32 years
Ytterbium-169	Gamma radiography	32 days
Zinc-65	Radiotracer in mining waste water	243.87 days
Manganese-54	Radiotracer in mining waste water	312.1 days

For medical applications, radioisotopes are widely used to provide information on organs for diagnostic and preventative measures or therapeutic purposes such as cancer treatment. Target radionuclide therapy and radiation therapy are some of the well-known and widely practiced therapeutic applications of radioisotopes. Targeted radionuclide therapy uses a carrier molecule, labeled with a radionuclide, to target malignant tumors and deliver a therapeutic dose of radiation. Radiation therapy takes advantage of ionizing radiation to damage the cell's DNA and kill the cancer cells to prevent further growth and division of cancer cells[3].

Diagnostic applications of radioisotopes involve linking gamma emitting radioisotopes to biological molecules with site-specific characteristics. The gamma emission energy should be sufficient to escape the patient's body. Depending on the type of biological molecule, the radiopharmaceutical, which is usually administered by injection or orally, accumulates in the target tissue or organ. The gamma ray emission is detected by a gamma camera of some sort that

can view the target from various angles and build an image, which can be viewed by the physician to determine any unusual conditions[4].

The applicability of radionuclides in medicine strongly relies on the following key factors: 1) Achievable specific activity. The radionuclides should be obtained with high specific activity so a minimal concentration can be administered with maximum effect, to prevent chemical toxicity complications. 2) The radionuclides need to have a half-life long enough to allow for the diagnostic or therapeutic application, yet short enough to avoid excess radiation damage to the patient. 3) The radioisotope should have gamma emission energies suitable for diagnostic and imaging applications. 4) For therapeutic applications the radioisotope is required to have beta (1-10 mm range, 0.1-1 MeV) or alpha (50-80 micron, 5-8 MeV) emission energies suitable for radiotherapy. 5) The radionuclide should have coordination chemistry that permits attachment to bio-localization agents [5–11]. Table 1.3 summarizes radioisotopes used in the medical field along with their application and half-life.

Table 1.3: Common Radioisotopes used for medical applications[12].

Radioisotope	Medical Use	Half-life
Ac-225	Cancer treatment	10.0 d
Ac-227	Cancer treatment	21.8 y
Am-241	Osteoporosis detection Heart imaging	432 y
As-72	SPECT or PET	26 h
As-74	Biomedical applications	17.8 d
At-211	Cancer treatment	7.21 h
Au-198	Cancer treatment	2.69 d
Be-7	Berylliosis studies	53.2 d
Bi-212	Cancer Therapy Dosimetry studies	1.10 h
Bi-213	Cancer Treatment	45.6 m
Br-75	SPECT or PET	98 m
Br-77	Monoclonal antibody labeling	57 h
C-11	Radiotracer in PET scans	20.3 m
C-14	Radiolabeling for tumor detection	5730 y
Cd-109	Cancer Detection Pediatric imaging	462 d
Ce-141	Gastrointestinal tract diagnosis	32.5 d
Cf-252	Cancer treatment	2.64 y

Co-55	SPECT or PET	17.5 h
Co-57	Gamma camera calibration	272 d
Co-60	Cancer treatment	5.27 y
Cr-51	Cell labeling Dosimetry	27.7 d
Cs-130	Myocardial localizing agent	29.2 m
Cs-131	Radiotherapy	9.69 d
Cs-137	Blood irradiators PET Tumor treatment	30.2 y
Cu-61	SPECT or PET	3.35 h
Cu-62	Radiotracer	4.7 m
Cu-64	SPECT or PET Dosimetry Studies	12.7 h
Cu-67	Cancer treatment SPECT or PET	61.9 h
Dy-165	Radiation synovectomy	2.33 h
Eu-155	Osteoporosis detection	4.73 y
F-18	Radiotracer for brain studies PET	110 m
Ga-64	Treatment of Pulmonary diseases	2.63 m
Ga-67	Detection of Hodgkins/non-Hodgkins lymphoma	78.3 h
Ga-68	Thrombosis and atherosclerosis studies Cancer detection	68.1 m
Gd-153	Osteoporosis detection SPECT	242 d
Ge-68	PET	271 d
H-3	Labeling PET	12.3 y
Ho-166	Radiation synovectomy	26.8 h
I-122	Brain blood flow studies	3.6 m
I-123	Medical imaging	13.1 h
I-124	Radiotracer PET	4.17 d
I-125	Medical imaging	59.9 d
I-131	Radiation treatment Thyroid problems Medical imaging	8.04 d
In-111	Medical imaging Cellular dosimetry Treatment of leukemia	2.81 d
In-115m	Evaluation of inflammatory bowel disease	4.49 h
Ir-191m	Cardiovascular angiography	6 s
Ir-192	Cancer treatment	73.8 d
Kr-81m	Lung imaging	13.3 s
Lu-177	Heart diseases treatment Cancer therapy	6.68 d
Mn-51	Myocardial localizing agent	46.2 m
Mn-52	PET	5.59 d
Mo-99	Medical imaging	65.9 h
N-13	PET	9.97 m

	Myocardial perfusion	
Nb-95	PET Myocardial tracer	35 d
O-15	PET or SPECT	122 s
Os-191	Parent for Ir-191m generator, cardiovascular angiography	15.4 d
Os-194	Cancer treatment	6.00 y
P-32	Leukemia treatment Bone disease treatment Cancer treatment Radiolabeling	14.3 d
P-33	Labeling	25 d
Pb-203	SPECT or PET Immunotherapy Cellular dosimetry	2.16 d
Pb-212	Cellular dosimetry	10.6 h
Pd-103	Cancer treatment	17 d
Pd-109	Potential radiotherapeutic agent	13.4 h
Pu-238	Pacemaker	2.3 y
Ra-223	Cancer treatment	11.4 d
Rb-82	PET Blood flow tracer	1.27 m
Re-186	Cancer treatment	3.9 d
Re-188	Monoclonal antibodies Cancer treatment	17 h
Rh-105	Potential therapeutic applications	35.4 h
Ru-97	SPECT or PET	2.89 d
Ru-103	Myocardial blood flow Radiolabeling microspheres PET	39 d
S-35	Cellular dosimetry	87.2 d
Sc-46	Blood flow studies PET	84 d
Sc-47	Cancer treatment Radioimmunotherapy	3.34 d
Se-72	Brain imaging	8.4 d
Se-75	Radiotracer for brain studies	120 d
Sm-153	Cancer treatment Leukemia treatment	2.00 d
Sn-117m	Bone cancer pain relief	13.6 d
Sr-85	Brain scans	65.0 d
Sr-89	Bone cancer pain palliation Cancer treatment Cellular dosimetry	50 d
Sr-90	Generator system with Y-90 Immunotherapy	29.1 y
Ta-182	Bladder cancer treatment	115 d
Tb-149	Cancer treatment	4.13 h
Tc-99m	SPECT	6.01 h
Th-228	Cancer treatment	720 d
Tl-201	Clinical cardiology	73.1 h
Tm-170	Lymphoma treatment	129 d
W-188	Cancer treatment	69.4 d

Xe-127	Neuroimaging	36.4 d
Xe-133	SPECT Medical imaging	5.25 d
Y-88	Development of cancer tumor therapy	107 d
Y-90	Internal radiation therapy Cancer treatment	64 h
Y-91	Cancer treatment Cellular dosimetry	58.5 d
Yb-169	Gastrointestinal tract diagnosis	32 d

With respect to table 1.3 it can be seen that there are over 90 radioisotopes that have a wide variety of applications in the medical field. Therefore ensuring the availability of these radioisotopes with high specific activity and quality is essential.

1.2 Radiolanthanides for Medical Applications:

For the present study the primary focus was on radiolanthanide production, due to their desirable characteristics that are beneficial for both therapeutic and diagnostic medical applications. The lanthanide elements share similar chemistry and physical properties, they are often found in the +3 oxidation state and usually have coordination numbers greater than 6 [13]. Due to the similar characteristics lanthanide elements share, a general procedure can be applied for the synthesis and production of a variety of compounds and materials differing in the lanthanide element. The lanthanide cations (Ln^{3+}) have similar ionic radii to calcium (Ca^{2+}) but with a higher charge, facilitating them to have a high affinity for Ca^{2+} sites in biological systems, therefore having the potential to replace calcium in biomolecules and act as a potential Ca^{2+} inhibitor or probe[14,15]. In general, radiolanthanides have desirable characteristics for medical applications; they have a range of suitable half-lives and emission energies for both diagnostic and therapeutic applications[16–18]. Table 1.4 summarizes information regarding production, application and decay characteristics of some of the radiolanthanides used in nuclear medicine**.**

Table 1.4: Radiolanthanides commonly used for medical applications. (ae: atomic electron, sp: spallation, f: fission) [17]

Radioisotope	Application	Half-life	Main emission	Production route
Pr-143	Therapy	13.58 d	γ,β^-	$^{142}Ce(n, \gamma) \rightarrow \beta^-$,f
Nd-147	Therapy	10.98 d	γ,β^-	$^{146}Nd(n, \gamma)$, f
Pm-149	Therapy	2.212 d	β^-	$^{148}Nd(n, \gamma) \rightarrow \beta^-$
Sm-153	Therapy	1.946 d	γ,β^-	$^{152}Sm(n, \gamma)$
Gd-149	Therapy	9.2 d	γ,α,ae	$^{147}Sm(\alpha, 2n)$,Sp
Tb-149	Therapy	4.16 h	γ,α,	$^{152}Gd(p, 4n)$, $^{141}Pr(^{12}C, 4n)$,Sp
Tb-152	Therapy	17.5 h	γ,ae	$^{152}Gd(p, n)$, Sp
Tb-161	Therapy	6.91 d	γ,β^-	$^{160}Gd(n, \gamma) \rightarrow \beta^-$,
Dy-157	Imaging	8.1 h	γ,ae	$^{154}Gd(\alpha, n)$, $^{159}Tb(p, 3n)$, Sp
Dy-165	Therapy	2.33 h	γ,β^-	$^{164}Dy(n, \gamma)$
Dy-166	Therapy, in-vivo Generator	3.40 d	γ,β^-	$^{164}Dy(n, \gamma)$ $^{165}Dy(n, \gamma)$
Ho-161	Therapy	2.48 h	γ,ae	$^{159}Tb(\alpha, 2n)$, Sp
Ho-166	Therapy, in-vivo Generator	1.117 d	β^-	$^{165}Ho(n, \gamma)$ ^{166}Dy Generator
Er-160	Therapy	1.192 d	γ,ae	Sp
Er-165	Therapy	10.36 h	ae	$^{165}Ho(p,n)$
Er-169	Therapy	9.4 d	β^-	$^{168}Er(n, \gamma)$
Er-171	Therapy	7.52 h	β^-	$^{170}Er(n, \gamma)$
Tm-167	Imaging, therapy	9.24 d	γ,ae	$^{165}Ho(\alpha, 2n)$, Sp
Yb-166	Therapy	2.362 d	γ,ae	$^{169}Tm(p, 4n)$
Yb-175	Therapy	4.19 d	γ,β^-	$^{174}Yb(n, \gamma)$
Lu-177	Therapy	6.71 d	γ,β^-	$^{176}Lu(n, \gamma)$;$^{176}Yb(n, \gamma) \rightarrow \beta^-$

With reference to table 1.4 the majority of radiolanthanides have therapeutic applications and are produced by various methods such as neutron activation, particle accelerators, fission and spallation. The focus of the proposed study was on radioisotope production using a nuclear reactor via neutron capture.

Several of the neutron rich beta emitting lanthanide radioisotopes e.g. samarium-153 (^{153}Sm, $t_{1/2}$=46.32 h) and holmium-166 (^{166}Ho, $t_{1/2}$=26.83 h) have shown suitable characteristics for medical application[5,16,19,20]. Due to the proven medical applications in addition to desirable nuclear characteristics (cross section, half-life and decay properties) the ^{153}Sm and ^{166}Ho radioisotopes were the main focus of the study.

Samarium-153:

The stable Samarium-152 (^{152}Sm) isotope has a high thermal neutron cross-section (206 barns) it emits both beta energy particles useful for therapeutic applications and gamma ray emissions suitable for imaging purposes. The primary radiation emissions for ^{153}Sm are listed in Table 1.5. The energies listed for beta particles is the maximum energy, the average beta particle energy is 233 KeV [21].

Table 1.5: ^{153}Sm primary gamma and maximum beta energy emission values.

Emission type	Energy (keV)	% Abundance
Gamma	103	28.3
Beta	640	30
Beta	710	50
Beta	810	20

^{153}Sm has been successfully used in therapeutic radiopharmaceuticals for the treatment of painful bone metastasis associated with advanced cancers [22]. Unfortunately bone metastases develops in

up to 70% of patients diagnosed with prostate and breast cancer and up to 30% of patients diagnosed with lung, bladder and thyroid cancers [23]. There are major complications associated with bone metastases such as severe pain, spinal cord compression and pathological fracture, all of which significantly lowers the patient's quality of life [23]. ^{153}Sm chelated to ligands such as ethylene diamine tetramethyl phosphonate (EDTMP) to produce ^{153}Sm-EDTMP also known as Quadramet, has been reported as an effective radiopharmaceutical for the treatment of the bone pain associated with cancer [21,24]. The radiopharmaceutical is administered by injection of the ^{153}Sm-EDTMP into the patient's bloodstream, were EDTMP has a high affinity for bone tissue (hydroxyapatite) and it concentrates in areas of osteoblastic metastasis [25]. Once accumulated in the region of interest, the beta emitting ^{153}Sm delivers a therapeutic dose to the target and alleviates the pain associated with the metastasis. ^{153}Sm also emits a 103 KeV gamma ray suitable for imaging purposes and tracking the location of the radiopharmaceutical.

Holmium-166:

The stable Holmium-165 (^{165}Ho) isotope has a neutron capture cross section of 64 barns and similar to ^{153}Sm, ^{166}Ho decays by both beta emission and gamma photon emission. The primary radiation emissions for ^{166}Ho are listed in Table 1.6. The energies listed for beta particles are the maximum energy the average beta particle energy is 750 KeV.

Table 1.6: ^{166}Ho gamma and maximum beta energy emission values.

Emission type	Energy (keV)	% Abundance
Gamma	80.6	6.6
Beta	1774	48.7
Beta	1854	50

^{166}Ho has shown potential as a therapeutic radionuclide for applications such as synovectomy, bone palliation, bone marrow ablation and therapy of hepatic tumors [26,27].

Holmium-166 chelated to 1, 4, 7, 10-tetraaczocyclododecane-1, 4, 7, 10-tetramethylene-phosphonic acid (DOTMP) is a radiopharmaceutical used for bone marrow ablation and the treatment of myeloma. ^{166}Ho-DOTMP is a bone seeking radiopharmaceutical that localizes on bone surfaces, specifically in areas of active bone turn over, delivering a therapeutic radiation dose to the affected areas [28,29]. Another candidate radiopharmaceutical for radiation synovectomy is ^{166}Ho-ferric-hydroxide macro aggregate (FHMA) which is administered for the treatment of rheumatoid arthritis and decrease of joint pain [25,30]. ^{166}Ho microspheres are also used in radionuclide therapy for liver cancer therapy and kidney pre-surgical treatment [16,31]. The therapy consists of placing the microspheres near the tumor were a radiation dose is directly delivered to the malignant cells. Microspheres have been developed using varying compositions such as glass, resin and biodegradable polymer [31]. In addition to the few applications of ^{166}Ho in radiopharmaceuticals mentioned above, there are additional applications of ^{166}Ho in nuclear medicine summarized in Table 1.7.

Table 1.7: ^{166}Ho compounds used in medicine [32].

Compound	Application
^{166}Ho-FHMA	Synovectomy
^{166}Ho-Hydroxyapatite	Synovectomy
^{166}Ho-Glass microspheres	Hepatic tumor therapy
^{166}Ho-PLA microspheres	Hepatic tumor therapy Synovectomy
^{166}Ho-Boron-MA	Synovectomy Skin cancer therapy
^{166}Ho-Citrate Colloids	Synovectomy
^{166}Ho-CHICO (Chitosan)	Cancer therapy
^{166}Ho-EDTMP	Bone marrow ablation
^{166}Ho-DOTMP	Bone marrow ablation
^{166}Ho-HEEDTA	Bone Tumor therapy

1.3 Radioisotope Production:

Currently radioisotopes are produced by nuclear reactors or charged particle accelerators [10,16]. Typically neutron rich radioisotopes and those produced from nuclear fission by-products are produced in nuclear reactors while neutron-depleted radioisotopes are produced in charged particle accelerators.

One method of radioisotope production via nuclear reactors is from direct neutron activation by the (n,γ) reaction, (Eq. 1.1). A challenge encountered in reactor-produced radioisotopes is achieving high specific activity. Obtaining high specific activity radioisotopes via direct neutron activation requires: 1) Long irradiation times, not feasible for short lived radioisotopes. 2) High

neutron flux, which itself may lead to degradation and decomposition of the target due to irradiation effects. 3) Highly enriched irradiation targets, which are expensive.

$$^{A}_{Z}X + n \longrightarrow {}^{A+1}_{Z}X + \gamma_{prompt} \qquad \text{Eq.1.1}$$

An obstacle encountered with reactor produced radioisotopes is separation of radioisotopes with only ~1 amu difference in atomic mass. In the case of lanthanides this is an energy intensive and challenging task, since the lanthanide elements predominantly exist in the +3 valence state and all exhibit similar chemical characteristics[13]. Therefore production of high specific activity radioisotopes from direct (n, γ) reaction, using a low flux research reactor on the order of 10^{12} $n.cm^{-2}.s^{-1}$ with restricted periods of operation, is not favorable.

According to a study done in 2010 by World Information Service on Energy and the Nuclear Information and Resource Service [33], more than 80% of the radioisotopes used for therapeutic medical applications are produced by nuclear reactors, the remaining isotopes are made by particle accelerators, predominantly circular accelerators (cyclotrons) or linear accelerators (LINACS). The following is a brief overview of the most predominant radioisotope production routes currently used [34,35]:

1. Nuclear Reactors:

a) Production of radionuclides via direct (n,γ) reaction:

Radioisotopes can be produced in nuclear reactors [10,16,36] by exposing the target material of choice to the reactor neutron flux for a suitable amount of time (Figure 1.1). A wide range of radioisotopes can be produced via nuclear reactors. The specific activity achieved by this method is highly dependent on the cross section for neutron capture of the target, abundance and enrichment of the target isotope, the irradiation time and the neutron flux.

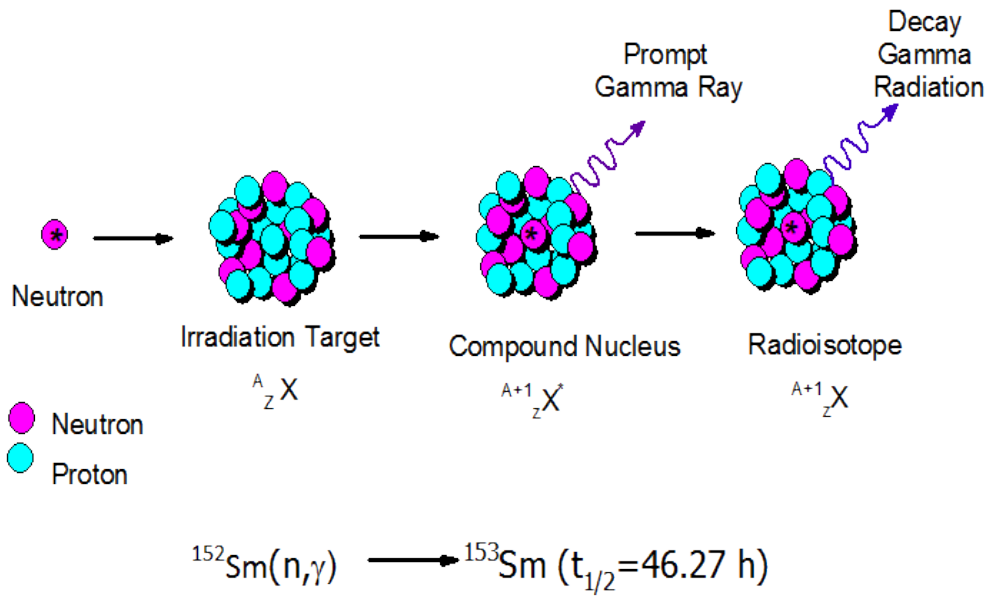

Figure 1.1: Schematic of radioisotope production via direct (n, γ) reaction mechanism.

With this production method the obtained radioisotope is not carrier free, meaning that the stable isotope carrier dilutes the resultant radioisotope product. For example the target isotope (^{152}Sm) and product radioisotope (^{153}Sm) are isotopes of the same element (samarium), and often-conventional separation techniques cannot be applied for the separation of the two isotopes due to the similarity in the chemistry they share. The presence of stable isotope carrier in the final radioisotope product is undesirable for medical application due to chemical toxicity effects, because a larger concentration of the final product must be administered to get the required medical radioisotope dose.

b) Production of no-carrier radionuclides via indirect (n,γ) reaction:

Production of high specific activity radioisotopes can be achieved using the indirect (n, γ) pathway (Figure 1.2). This method varies from direct neutron activation, by producing a short-lived radioisotope via direct neutron activation, that undergoes radioactive decay and produces

the longer-lived radioisotope of interest [10,36]. This radioisotope production method is desirable because it has the capability of producing carrier free radionuclides. Since the target radioisotope Ytterbium-176 (^{176}Yb) and the product radioisotope Lutetium-177 (^{177}Lu) are different elements, conventional chemical separation techniques can be more easily applied to obtain a carrier free radioisotope.

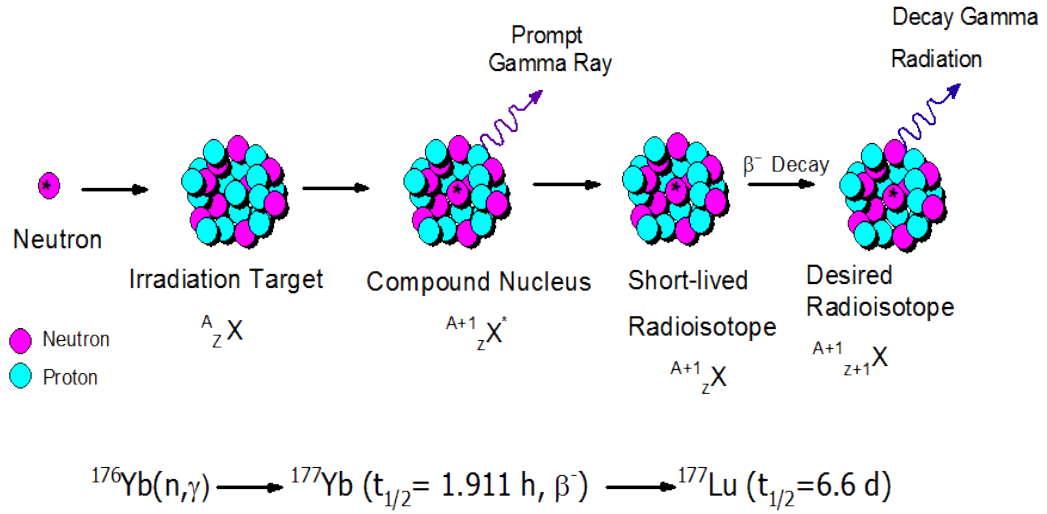

$$^{176}Yb(n,\gamma) \longrightarrow {}^{177}Yb\ (t_{1/2}= 1.911\ h,\ \beta^{-}) \longrightarrow {}^{177}Lu\ (t_{1/2}=6.6\ d)$$

Figure 1.2: Schematic of radioisotope production via the indirect (n,γ) reaction mechanism.

The indirect production route cannot be applied for the production of all radioisotopes in demand for medical application. The feasibility of this technique depends on the capability of producing a short-lived radioisotope precursor, which can undergo radioactive decay and produce the radioisotope of interest, which is of a different element from the target. The technique cannot be applied for the production of all radioisotopes since the intermediate short-lived radioisotope might not exist. This technique has been used for the production of high specific activity ^{177}Lu, which is a beta decay product of ^{177}Yb formed when ^{176}Yb captures a neutron [8,36,37].

c) Chemical Separation of fission produced radionuclides:

The fission-produced radionuclides (Figure 1.3) most often used in nuclear medicine are molybdenum-99, iodine-131 and xenon-133. These radioisotopes can be chemically separated from fission product mixture with effectively no stable isotope carrier present [36,38]. Nuclear fission chemical separation is the predominant way of obtaining Molybdenum-99 (^{99}Mo), which is used to manufacture technetium-99m generators. Technitium-99m (^{99m}Tc) is the most widely used isotope in nuclear medicine [39].

The majority of ^{99}Mo needed for ^{99m}Tc generators are produced by the fission of uranium-235 targets in nuclear reactors. The irradiated targets go through chemical processing and the purified ^{99}Mo is used for ^{99}Mo/^{99m}Tc generators used for medical application[39].

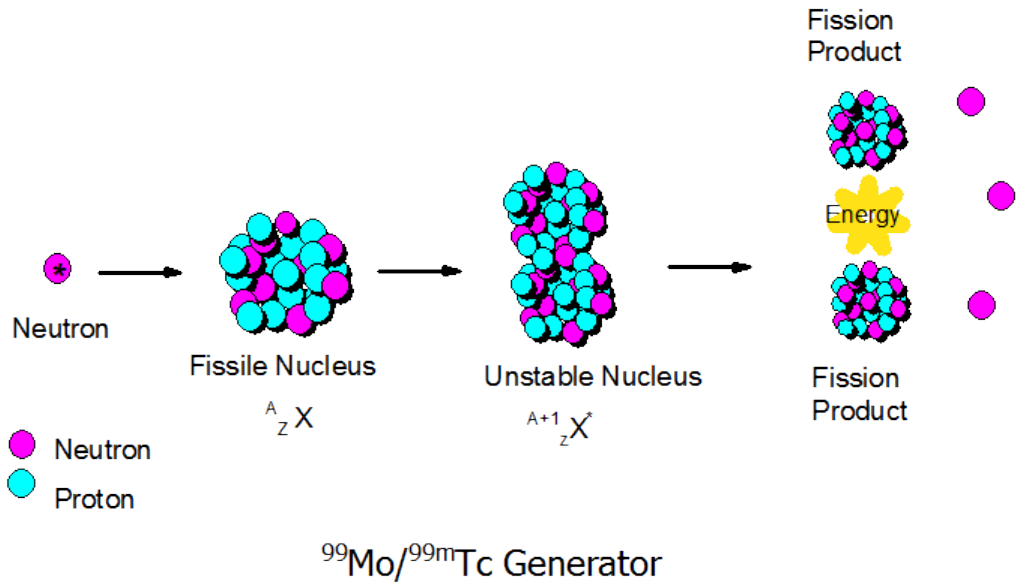

Figure 1.3: Radioisotope production from neutron fission.

Not all medically useful isotopes are present in the fission product mixture and in some cases common separation techniques cannot be easily applied to separate the desired radioisotope in practical quantities.

2. Charged Particle accelerators:

Accelerator produced radionuclides are generated by bombarding stable target material with accelerated charged particles such as protons (Figure 1.4). As a result of this collision, the produced radionuclide is neutron deficient and de-excites mainly by electron capture (EC) or positron emission (β^+) to form radioisotopes that can be used for medical applications[35,40,41].

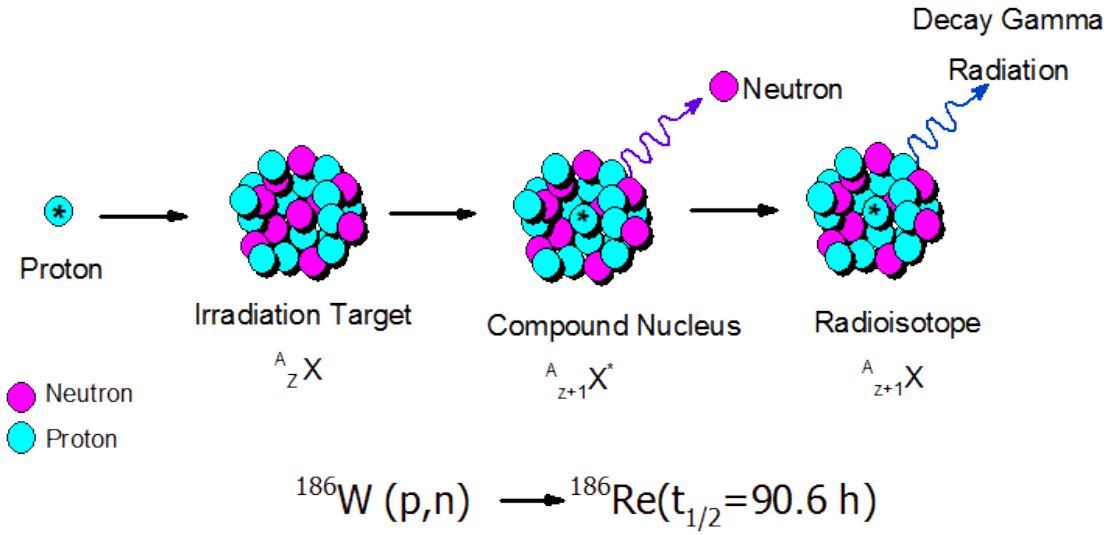

Figure 1.4: Production of radionuclides via charged particle accelerators.

With the use of particle accelerators for radioisotope production, the resulting radionucleus (tungsten-186, ^{186}W) is usually that of a different element than the target (rhenium-186, ^{186}Re) therefore chemical separation techniques can be applied to separate the target isotope from the radioactive isotope and obtain a carrier free product with high specific activity. This method is predominantly applied for the production of neutron deficient radioisotopes that decay by β^+ emission or electron capture.

With respect to the main methods discussed for radioisotope production, it can be seen that charged particle accelerators and nuclear reactors complement each other in radioisotope production techniques rather than compete. The Szilard-Chalmers method applied in the proposed study falls under the nuclear reactor radionuclide production route since it takes advantage of the (n, γ) reaction produced via nuclear reactors.

1.4 Szilard-Chalmers Method:

An alternative route to produce radionuclides with high specific activity utilizing nuclear reactors is the Szilard-Chalmers method [5,42–47]. In 1934 L. Szilard and T.A. Chalmers discovered they could isolate an iodine radioisotope from the neutron irradiation of ethyl iodide by taking advantage of the prompt gamma emission and recoil characteristics of the nucleus as a result of neutron capture. They named this discovery the Szilard-Chalmers effect [42]. This discovery was the starting point of the field of hot atom chemistry that formed a unique branch of nuclear and radiochemistry thereafter.

The Szilard-Chalmers process is a method to separate radioactive ions away from the bulk of the inactive material. The Szilard-Chalmers effect occurs as a result of the emission of a prompt gamma ray upon neutron capture, resulting in nuclear recoil of the radionuclide.

Following neutron capture of the target nucleus a new compound nucleus is formed with excitation energy equivalent to the binding energy plus the kinetic energy of the neutron. For most stable nuclei, the neutron binding energy is between 6-10 MeV were it increases up to Z=22 and then decreases[48]. De-excitation of the formed compound nucleus takes place within 10^{-16} seconds reaching its ground state within 10^{-9}-10^{-12} seconds by emitting a cascade of gamma rays. These gamma rays are considered prompt because following neutron capture the decay times are in the range of 10^{-9}-10^{-12} seconds which is shorter than the detection system resolving

time. After the emission of prompt gamma rays and de-excitation, the ground state reached is not necessarily stable and further radioactive decay via beta, alpha, gamma, electron capture or isomeric transition with a given half-life occurs [48]. The prompt gamma rays emitted results in the recoil of the neutron-capturing nucleus in an opposite direction from the emitted prompt gamma ray. The energy of the prompt gamma ray and the corresponding recoil energy is calculated according to equations 1.2 and 1.3 [48].

$$E_\gamma = E_T - E_R \quad \text{Eq. 1.2}$$

$$E_R = \frac{E_\gamma^2}{2m_A C^2} \approx \frac{E_\gamma^2}{2 \times A \times 931.5} \quad \text{Eq. 1.3}$$

With respect to equations 1.2 and 1.3, E_γ, E_R and E_T are the prompt gamma ray energy, recoil energy and transition energy values respectively, m_A is the mass of the capturing atom, A is the atomic number, C is the speed of light and 931.5 MeV/u is the conversion factor from mass scale to energy.

More specifically, the Szilard-Chalmers effect occurs such that upon neutron capture of the target radionuclide there is an increase in energy due to the binding energy of the neutron, the excess energy is released in the form of prompt gamma rays which imparts a certain amount of recoil energy to the target radionuclide. Depending on the mass of the target radionuclide and the energy of the prompt gamma ray, the recoil energy is often enough to break the chemical bonds holding the capturing radionuclide in the compound and eject it in the opposite direction. This means that the product radionucleus may be in a different chemical state that can be separated from the bulk of the target matrix. If the irradiation target is in contact with an immiscible capture matrix that can capture and separate the recoiling radionuclide from the bulk of the inactive target matrix, there is potential for obtaining the radionuclide with increased specific activity, compared to the radioisotope product obtained from the direct (n,γ) reaction (Figure

1.1). Figure 1.5 illustrates the Szilard-Chalmers process by using samarium acetylacetonate, which is a compound studied throughout this project, as a representation.

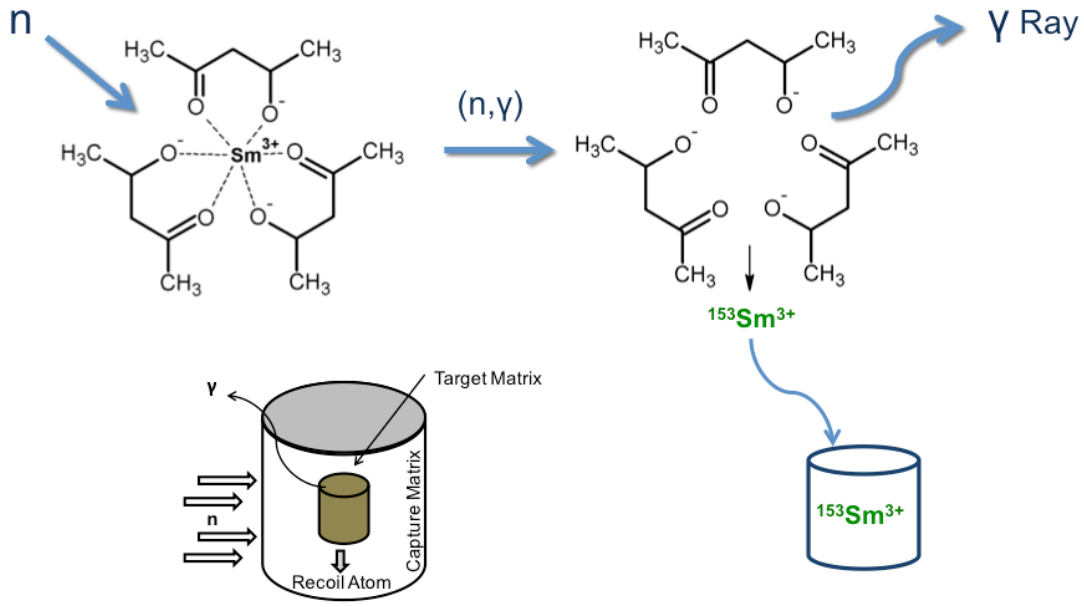

Figure 1.5: The Szilard-Chalmers Process. Samarium acetylacetonate compound undergoes neutron activation followed by ejection of the radioactive samarium atom from the acetylacetonate complex into the immiscible capture matrix.

With respect to Figure 1.5 it can be seen that upon neutron capture of the target ^{152}Sm isotope the ^{153}Sm radioisotope is formed. The ^{153}Sm radioisotope emits prompt gamma rays, which imparts a certain amount of recoil energy to the radioisotope. The imparted recoil energy is sufficient to break the bonds between the ^{153}Sm radioisotope and the acetylacetonate ligands, as a result ^{153}Sm radioisotope is ejected it in the opposite direction, were it can be captured and separated from the bulk of the inactive material.

Promising results have been obtained by previous studies using the Szilard-Chalmers method. Zeisler et al. studied the Szilard-Chalmers effect in holmium and praseodymium complexes and obtained enrichment factors between 3- 66 and 3-10 for holmium and praseodymium compounds

respectively[5,43]. They irradiated the compounds alongside their aqueous suspensions with neutrons and separated the radionuclide by solid-liquid extraction, ion exchange and HPLC techniques. A study done by Zhernosekov et al. on the Szilard-Chalmers effect in a Ho-DOTA complex resulted in enrichment factors ranging between 7.3-90. This study took advantage of ion exchange to separate cationic $^{165/166}Ho^{3+}$ from anionic [$^{165/166}$Ho-DOTA]$^{-}$ and then re-irradiation of the ionic $^{165/166}Ho^{3+}$ to determine the stable $^{165}Ho^{3+}$ present, in order to calculate enrichment factors[44]. Nassan et al. obtained enrichment factors up to 10^7 from neutron irradiated holmium tris-(cyclopentadienyl) compounds. This study used the following four separation procedures to separate organometallic holmium (III) tris-cyclopentadienyl from inorganic recoil species: 1) sublimation 2) Column chromatography 3) Paper chromatography 4) Thin-layer chromatography [46]. Jia et al. studied the Szilard Chalmers effect in rhenium compounds. This group irradiated inorganic rhenium target material, used the technique of leaching to remove the radioactive water-soluble ^{186}Re and then filtration to remove the rhenium carrier, resulting in enrichment factors between 1.29-7.54 [45]. Zhang et.al. Also looked into production of ^{186}Re and ^{188}Re via the Szilard-Chalmers method. This group synthesized a number of rhenium compounds and irradiated them with thermal neutrons for an hour. Post irradiation the recoiled rhenium was stripped from a dichloromethane solution of the irradiated compound using an aqueous phase. As a result an enrichment factor of 210 was obtained[49]. Hetherington et.al. studied the production of high specific activity copper-64. The copper phthalocyanine target was irradiated, post irradiation the target was dissolved in concentrated acid, then the mixture was poured into water, an excess of ammonium hydroxide was added to the mixture, and the cuprammonium ions were absorbed onto a chelating resin column. High specific activity ^{64}Cu was eluted from the resin using acid [50]. Tomar et. al. did studies on production of high specific activity of ^{99}Mo and ^{90}Y by

the Szilard-Chalmers reaction. The radionuclides were separated from the target by solvent extraction and ion exchange methods. The highest enrichment factors obtained for ^{99}Mo and ^{90}Y were 190 and 8.3 respectively [51]. Mausner et al. studied the Szilard-Chalmers process to improve the specific activity of tin (^{117m}Sn). They used tetraphenyl tin as the irradiation target and solvent extraction and ion exchange techniques to enrich the radioactive tin. The enrichment factors obtained for ^{117m}Sn were between 2.3 and 138 [47]. In these previous studies the experimental conditions and procedures for determination of enrichment factors were different. A number of patents have also been filed in regards to various radioisotope production routes and experimental conditions using the Szilard-Chalmers method [52–55] .

1.5 Prompt Gamma Analysis:

The Szilard-Chalmers process is based on the emission of prompt gamma rays upon neutron capture of the target isotope, resulting in the recoil of the radioisotope and separation from the bulk of the inactive material.

The neutron capture prompt gamma ray energy values for the radioisotopes of interest, were obtained from a compiled database available on the International Atomic Energy Agency (IAEA) website [56]. The prompt gamma ray energy values (E_γ) were used to calculate the corresponding recoil energy for ^{153}Sm and ^{166}Ho using equation 1.3.

The probability of emission of a prompt gamma ray was determined based on the partial gamma ray production cross-section σ_γ (Eq. 1.4). Were it is defined as the cross section per elemental atom to produce a particular gamma ray of energy E_γ upon irradiation with thermal neutrons [57].

$$\sigma_\gamma = \theta\sigma P_\gamma \qquad \text{Eq. 1.4}$$

Where θ is the natural abundance of the isotope of interest σ is the neutron capture cross section of the isotope and P_γ is the emission probability of the gamma ray (gammas emitted per capture)

with the indicated energy. The E_γ and σ_γ values were obtained from the database and used to calculate the recoil energies (Table 1.8). Figure 1.6 and 1.7 represent the partial gamma ray production cross-section as a function of the recoil energy for ^{153}Sm and ^{166}Ho respectively.

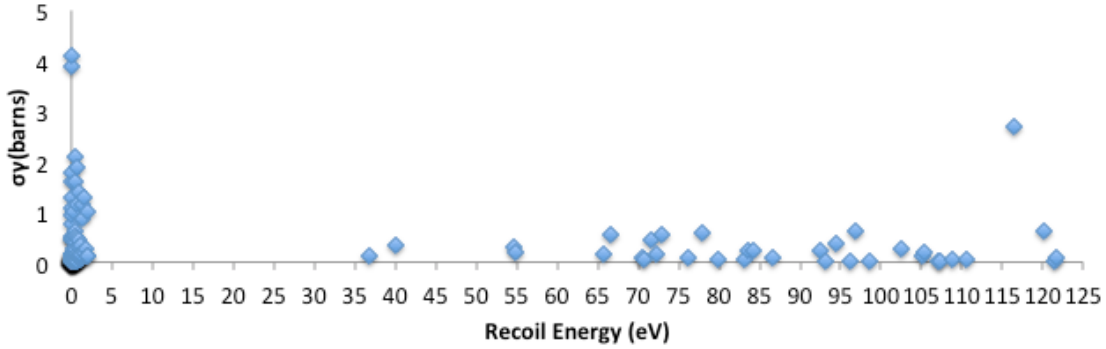

Figure 1.6: ^{153}Sm partial gamma ray cross section as a function of recoil energy.

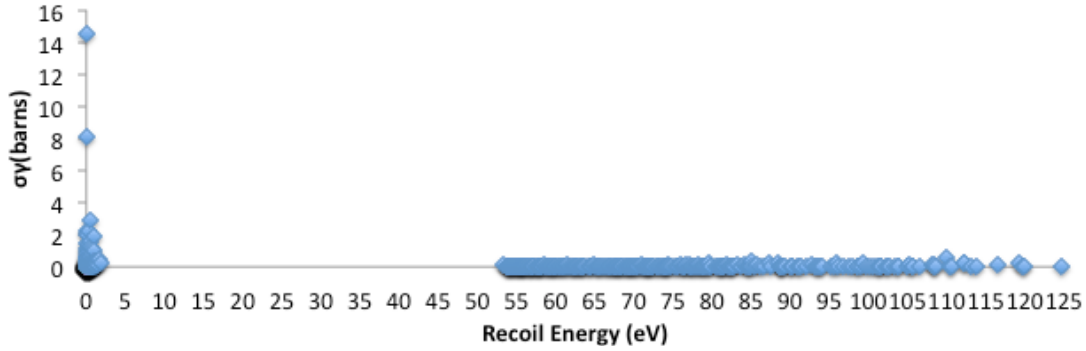

Figure 1.7: ^{166}Ho partial gamma ray cross section as a function of recoil energy.

Table 1.8: Summary of ^{153}Sm and ^{166}Ho prompt gamma and recoil energy data.

Isotope	# Prompt γ's	Min Prompt γ Energy (keV)	Max Prompt γ Energy (keV)	Min Recoil Energy (eV)	Max Recoil Energy (eV)
^{153}Sm	160	28.3	5868.3	.0028	121.7
^{166}Ho	536	19.8	6189.3	.0026	124.7

With respect to Table 1.8 ^{153}Sm has 160 prompt gamma rays with varying gamma ray partial cross sections. The prompt gamma ray energies range from 28.3-5868.3 KeV corresponding to a recoil energy range of 0.0028-121.7 eV. ^{166}Ho on the other hand has 536 prompt gamma rays with varying gamma ray partial cross sections. In the case of ^{166}Ho the gamma ray energies range from 19.8-6189.3 KeV corresponding to a recoil energy range of 0.0026-124.7 eV. With respect to Figures 1.6 and 1.7 it can be seen that a considerable number of prompt gamma ray emissions with varying probabilities correspond to recoil energies less than 5 eV while the remainder of the prompt gamma ray emissions corresponds to recoil energies ranging from 35-125 eV. According to Friedlander et al. "Neutron capture usually excites a nucleus to about 6-8 Mev, and a large fraction of this excitation energy is dissipated by the emission of one or more prompt gamma rays. Unless all the successive prompt gamma rays emitted in a given capture process have low energies, which is a relatively rare occurrence, the recoiling nucleus receives more than sufficient energy for the rupture of one or more bonds"[58]. Chemical bond energies are typically in the range of 1-5 eV [58] therefore the recoil energy imparted to the target nucleus often exceeds the magnitude of the bond energies resulting in the rupture of bonds holding the target radionucleus in the compound and ejecting it in the opposite direction.

1.6 Scope of the Dissertation

One method to improve the specific activity of radioisotopes produced from direct neutron activation, in low neutron flux research reactors with restricted operation times, is taking advantage of the nuclear recoil effect through the Szilard-Chalmers method[42]. The proposed method of radioisotope production using a small-scale research reactor provides the capability of producing radioisotopes with high specific activity, for use in local research labs and institutes and ultimately further optimization of the proposed method for medical radioisotope production.

In the presented study the Szilard-Chalmers effect in holmium and samarium compounds was investigated and attempts were made to improve their specific activities utilizing the unique experimental setup developed at the UC-Irvine TRIGA reactor facility. Therefore a collection of stable lanthanide compounds containing oxygen and nitrogen donor ligands were synthesized by adopting methods previously found in literature and designated as irradiation targets [5,43,51]. The lanthanide complex was required to be fairly insoluble and stable in the capture matrix of choice. In the proposed study water was the main capture matrix of choice, because it is not prone to damage in the radiation field, while offering a clean and readily available capture matrix. In addition to the experimental component, a techno-economical study was carried out as collaboration between UCI and The University of Queensland: DOW Center for Sustainable Engineering and Innovation, to look into the economics of various radioisotope production routes. The economical potential and financial benefits of current radioisotope production methods was carried out and compared with the proposed Szilard-Chalmers method for radioisotope production.

Specific Aims:

The overall goal of the study was to improve the specific activity and enrichment factors of reactor produced radioisotopes using the Szilard-Chalmers method, with the aid of the unique experimental irradiation setup at the UC-Irvine TRIGA reactor facility.

The Specific goals were to:

1. Identify and synthesize suitable lanthanide irradiation targets that offer: (i) simple chemical and molecular structures (ii) can afford high recoil yields as a result of the Szilard-Chalmers method (iii) can withstand exposure to the irradiation field without degrading and contaminating the capture matrix.

a. Synthesize stable lanthanide target complexes with organic oxygen and nitrogen donor ligands.
b. Look into target matrices with a large lanthanide containing surface area exposed to the capture matrix, to allow maximum recoil product transfer to the capture matrix.
    i. Production of ligand functionalized porous resins loaded with lanthanides.
    ii. Synthesis of lanthanide based microspheres.

2. Recognize capture matrices that have the following characteristics:
    a. Identify capture matrices which the lanthanide target matrix is insoluble in, such that the lanthanide atom capturing the neutron is released from its chemical bonded state and ejected irreversibly into the capture matrix
    b. Identifying simple capture matrices such as water that have little susceptibility to damage in the radiation field and can provide a clean and high specific activity radioisotope product.
    c. A capture matrix that has a high capacity for retention of the transferred radioisotopes.
3. Perform the Szilard-Chalmers process using the ideal target and capture matrix combinations. Compare different target/capture matrix systems to obtain the highest enrichment factor and specific activities.
4. Further enhance the experimental setup at the TRIGA reactor facility to achieve higher recoil yields and enrichment factors. Additionally identify effective separation techniques to separate the recoiled radioisotope from any stable isotope transferred to the capture matrix as a result of solubility or degradation of the target in the capture matrix.

5. Determine the feasibility to produce research quantities of high specific activity radioisotopes locally, and provide them for research and development to laboratories and research groups.
6. Optimize the radioisotope production process for larger facilities to scale up and ultimately produce radioisotopes for medical applications.
7. Perform a techno-economic analysis on radioisotope production and the various routes and techniques of production using nuclear reactors.

CHAPTER 2: TECHNO-ECONOMIC ANALYSIS OF RADIOISOTOPE PRODUCTION

2.1 Background

In order to rethink the value proposition of nuclear reactors a techno-economical analysis on radioisotope production was performed. The study was a collaborative study between the University of California Irvine and The University of Queensland's DOW Centre for Sustainable Engineering Innovation.

Radioisotopes will continue to play an important role in the everyday life of most people. Whether it's the use of radioactive Americium-241 in the commonly used smoke detectors, diagnosing and treating life threatening medical conditions of yourself or a loved one, calibration of detectors or development of nuclear batteries for deep space exploration; having reliable radionuclide production facilities are essential. Nuclear reactors or particle accelerators are necessary for medical radioisotope production. In the United States (U.S.) over 50,000 diagnostic and therapeutic procedures are performed daily that require the use of radioisotopes [59]. Nuclear medicine is currently suffering due to the limited infrastructure available for radioisotope production, coupled with aging facilities and the high cost associated with operation and maintenance of existing facilities [60–63]. In addition to the immediate and crucial issue of producing radioisotopes for the millions of medical diagnostic and therapeutic procedures performed worldwide yearly, there is a critical shortage of radioisotopes for research and development in various scientific fields. Furthermore clinical trials involving radioisotopes are also suffering because they require large quantities of radioisotopes that are not readily available or are very expensive. Radioisotope shortage can lead to decline in research and development of radioisotope products that can be used for the treatment and diagnosis of life threatening medical

conditions [64]. Technetium-99m and Iodine-131 are radioisotopes used for 80% of all nuclear medicine procedures, both of these radioisotopes are reactor produced as a result of neutron capture of a stable target[65]. The radioisotope shortage is an issue of concern because all the nuclear reactors supplying these radioisotopes, with the exception of Australia's Open Pool Australian Light water (OPAL) reactor, are over 40 years old and close to the end of their operational lifetime[64]. The issue of radioisotope shortage is an ongoing concern, which needs to be addressed. Building and commissioning new nuclear reactors can be costly and time consuming, which is the primary reason the U.S. has relied heavily on foreign reactors for radioisotope supplies. Although developing production facilities should be considered a solution in addressing radioisotope shortage for the long run, it cannot be considered as an immediate alternative to the pressing issue. Research and development of alternative methods for radioisotope production is important because of its contribution to the nuclear medicine field, in addition to various fields in industry and research.

Developing and optimizing methods for producing high-specific activity radioisotopes has a number of valuable outcomes and applications such as (but not limited to): 1) Local production of radioisotopes for research labs to incorporate in various research areas such as nuclear medicine 2) Developing the technology so larger facilities can scale up the method and supply radioisotopes on a larger scale. 3) Developing methods that do not require high scale processing and radioisotope-separating facilities typically required for production of high specific activity radioisotopes. In the present techno-economic analysis, the focus will be looking into determining: (i) the costs associated with using existing research reactors and building new reactors for radioisotope production (ii) the potential demand and revenue generated from radioisotope production.

2.2 Significance of Radioisotopes

Radioisotopes are the basis of radiopharmaceuticals and nuclear medicine and they have been used successfully for decades now. Table 2.1 summarizes some commonly used radioisotopes in the medical field along with their application and demand. Science and industry also use radioisotopes for many applications to gain information, such as gamma radiography and gauging or to improve productivity like gamma sterilization of medical products[66,67]. Therefore ensuring a stable and reliable source for radioisotope production is essential for the functionality of various fields that also hold significant economic importance.

Table 2.1: U.S. demand of common reactor produced medical radioisotopes [68].

Radioisotope	Activity per Procedure (mCi)	Maximum US Treatments per year	Maximum US demand (Ci)	Medical Use
Mo-99/Tc-99m	15-30 (Tc-99m)	20,000,000	1,500,000 (Mo-99)	Diagnostic imaging
Ir-192	10,000	400,000	14,000	High dose rate brachytherapy
I-131	30-200	200,000	11,000	Thyroid disease/cancer
Re-188	90	100,000	9000	Metastatic bone cancer
Sm-153	70	100,000	7000	Metastatic bone cancer
Re-186	40	100,000	4000	Metastatic bone cancer
Y-90	140	10,000	1300	Liver Cancer
I-125	50	10,000	500	Prostate cancer
Sr-89	4	100,000	400	Metastatic bone cancer
P-32	0.5	<10,000	<5	Cystic brain tumors

2.3 Radioisotope production

Radioisotopes are produced by nuclear reactors or charged particle accelerators[69]. Nuclear reactors account for the production of 80% of the radioisotopes used in medicine [33]. The radioisotope production methods are explained in detail in section 1.3.

2.4 Radiation Sources

The Australian OPAL reactor is a research reactor that opened in 2007. OPAL was primarily designed to produce commercial quantities of radioisotopes for use in nuclear medicine, research, scientific and industrial applications [70]. Reactors such as OPAL and similar facilities around the world are essential for generating neutrons that can be used to produce radioisotopes for therapeutic and diagnostic medicine, nuclear medicine research, materials research and industrial applications. As mentioned most of the reactors currently used for radioisotope production are getting close to their decommissioning age, thus developing and building reactors to ensure sustainable radioisotope production is crucial, especially for the medical field. Besides the fact that having reliable sources for radioisotope production is vital for many different applications, producing microgram-gram levels of radioisotopes generate a considerable amount of revenue and are considered a multi-billion dollar/year industry.

The United States Nuclear regulatory commission currently regulates 42 research reactors of which 31 are currently operational nuclear test and research reactors, also known as "non-power" reactors[71]. Currently there are 246 research reactors operational in 56 countries around the world[72]. These research reactors were primarily constructed and operated with government funding, and most likely the original capital costs have been paid for or justified for other purposes. Therefore production of radioisotopes can be considered a by-product that has the potential of generating a considerable amount of extra revenue for these facilities. These reactors have the potential to produce radioisotopes not only locally but also for neighboring cities and states.

Local production of radioisotopes using available test and research reactors is beneficial for a number of various reasons: 1) Addresses the issue of radioisotope shortage 2) Generates

substantial revenue for existing research reactor facilities 3) Local production can address the radioisotope transportation issue, which is highly regulated and costly 4) Also due to less overall transportation distance/time the quantity of the radioisotope decaying will also decrease, therefore a higher activity product will be delivered to the customer 5) Generating radioisotopes and making them readily available for research and development can aid in developing radiopharmaceuticals or further advancement of radioisotope use in industrial applications.

2.5 Economic Potential

The sustainability of radioisotope supply is an ongoing concern worldwide due to the decrease of reactors and the complications associated with transportation of the radioisotopes from the few functioning reactors. Production of radioisotopes contributes significantly to several sectors of economic significance such as healthcare and various industries [73]. Nuclear reactors in addition to radioisotope production are also used for electricity generation, and there has always been ongoing debates on whether the revenue generated from electric power generation is more valuable compared to the profit generated from radioisotopes and nuclear material. In 1991 the United States Council for Energy Awareness (USCEA) looked into the impact of nuclear power and radioisotope production on the national economy, they discovered that the annual revenue generated from radioisotope products/applications in the U.S. was $257 billion dollars and the revenue generated from nuclear power was $73 billion dollars [74,75]. Another Study conducted by Management Information Services Inc. for Organizations United (affiliated with the Nuclear Energy Institute) was performed to determine the 1995 economic and employment benefits of nuclear technologies. The results of this study is summarized in table 2.2[76].

Table 2.2: Summary of 1995 U.S. Economic and Job benefits associated with Nuclear Technologies [76].

Technology	Sales (Billions)	Jobs (Millions)	Taxes (Billions)
Nuclear Energy	$90.2	0.44	$17.8
Radioisotope Technologies	$330.7	3.95	$60.9
Total	$420.9	4.39	$78.7

Although these reports were generated over 20 years ago they are a good indication of the economic benefits associated with nuclear technologies and their potential demand.

The medical field accounts for the majority of radioisotope applications. According to an expert panel report on the "Forecast Future Demand for Medical Isotopes" for the U.S. Department of Energy, the diagnostic radiopharmaceutical market is forecasted to range from $2.7 billion to $18.7 billion by 2020. The therapeutic radiopharmaceutical market is forecasted to range from $244 million to $1.11 billion by 2020[64].

Information on the current and accurate production cost and selling price of radioisotopes is not readily available. The economic conditions differ from region to region therefore the prices of radioisotopes produced under the same technology may differ depending on the country and area of production. The price and cost of radioisotopes is dependent on a number of different factors such as status of radioisotope producing reactors, demand and cost of production among other factors. Therefore the economic information presented in this study was obtained from various sources.

According to a 2012 report from the U.S. Government Accountability office, the U.S. Department of Energy (DOE), which provides 300 different isotopes for commercial and research applications, needs better planning for setting prices and managing production risks[77]. Table 2.3 summarizes the DOE's revenue of eight of its top selling isotopes in the fiscal year 2011 (the report lacks information on the quantity of each isotope sold).

Table 2.3: Revenue of the eight top selling DOE isotopes in fiscal year 2011[77].

Isotope	2011 Revenue
Strontium-82	$11,560,000
Californium-252	$7,657,000
Helium-3	$3,255,000
Germanium-68	$1,910,000
Nickel-63	$576,000
Strontium-90	$297,000
Actinium-225	$263,000
Lithium-6	$223,000
Total	$25,741,000

With respect to Table 2.3 it can be further verified that radioisotope production has the potential of generating a substantial amount of revenue.

Another radioisotope that has both economical and medical potential is the ^{153}Sm radioisotope. The ^{153}Sm radioisotope has proven desirable characteristics for the treatment of metastatic bone cancer [20,24,78,79]. According to a Canadian study in 2013, treatment cost-savings would accrue if ^{153}Sm was used for the treatment of bone metastases compared to traditional palliative treatments, providing suffering patients with equal or better care and clinical outcomes (Table 2.4) [80].

Table 2.4: Economic benefits of using ^{153}Sm for treatment of bone metastases [80].

Treatment Type	Product Cost per Patient	Treatment Cost Per Patient
Traditional Palliative treatments	N/A	$26,075
Treatments using ^{153}Sm	$4,500	$11,680

Replacement of traditional palliative treatments with treatments using ^{153}Sm resulted in system savings of $14,395 per patient. The study took into consideration an estimated 755 patient treatments. In 2012, the total ^{153}Sm product cost and total ^{153}Sm treatment cost for 755 patients was $3,397,500 and $8,818,400 respectively. If traditional palliative treatments were applied the treatment cost for 755 patients would be $19,686,625. Therefore an investment of $3,397,500 in

^{153}Sm for 755 patients results in savings of $10,868,225 compared to traditional treatments, resulting in a return of investment (ROI) of 220 %.

As illustrated above, radioisotope production can also be economically beneficial to entities such as the health care industry by proposing alternative treatment options resulting in equal or better clinical results for the patients while being the cheaper option, similar to the mentioned study were the product cost for using ^{153}Sm was considerably lower than traditional palliative treatments. Another example that depicts the use of nuclear technology to be both more effective and economically favorable is in the detection of pipeline leaks. Traditional detection methods range between $0.5-$1 million and can take up to six months, were as with the use of nuclear technology it can be detected in a time span of a couple of days or weeks and the cost is significantly lower, ranging between $25,000-$50,000 [76].

A financial burden for radioisotope production facilities are the hot cells necessary for radioisotope separation processes post irradiation, which are the most expensive part of the separation process. In 2008 the Missouri University Research Reactor (MURR) estimated that it could cost between $30-$40 million to construct a hot cell facility for Molybdenum-99 production at MURR[81]. Therefore if new technologies could be adopted that do not need advanced hot-cells for post irradiation radioisotope separation it can contribute greatly to radioisotope production economics.

2.6 Proposed Radioisotope Production Method

Szilard Chalmers Process:

An alternative route to produce radionuclides with high specific activity using nuclear reactors is the Szilard-Chalmers method [42–45,47,82] (Figure 2.1). The method is detailed in section 1.4.

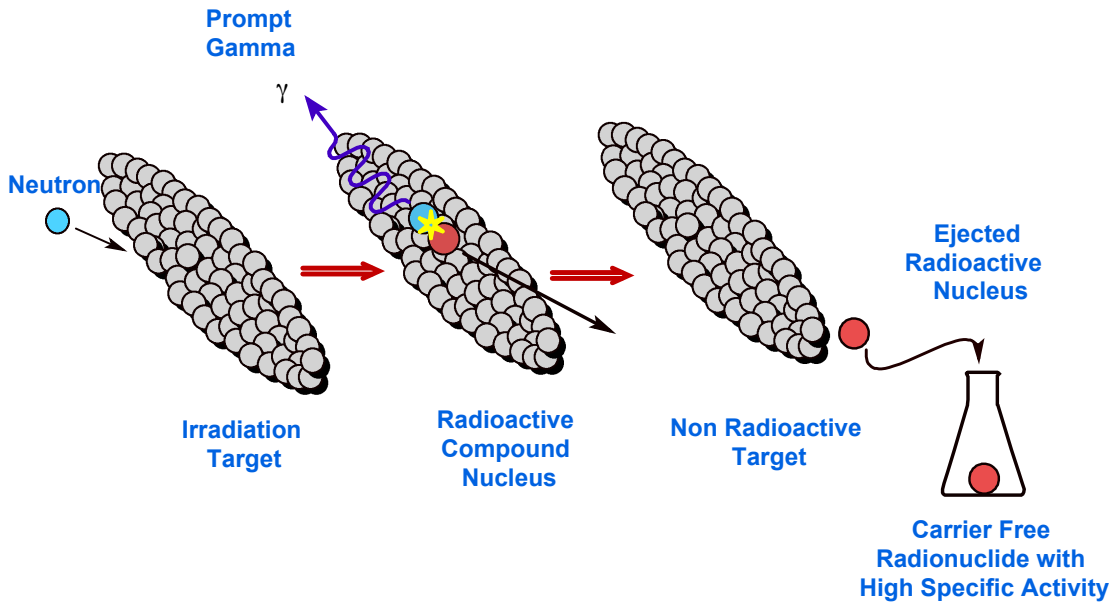

Figure 2.1: The Szilard-Chalmers effect as a result of prompt gamma recoil.

In this section techno-economic evaluation of the production of radioisotopes with high specific activity in a small-scale research reactor using the Szilard-Chalmers method is discussed, while also looking into building new reactors for radioisotope production.

As a result of the analysis the following concerns are addressed:

Shortage: By using available research reactors currently not being used at full capacity or building reactor facilities that can be used for radioisotope production.

Transportation: with 246 research reactors worldwide and 31 operational in the U.S alone, local production and distribution of radioisotopes can easily take place.

Radioisotope Processing and Separation: The Szilard-Chalmers process separates the radioisotope from the bulk of the nonradioactive target, this methodology not only addresses the costly expense of having advanced hot-cells for post irradiation radioisotope separation

and handling, but it also produces radioisotopes with increased specific activity which is essential for most applications, specially for medical purposes.

Increasing the revenue of research reactors: Production of radioisotopes could generate revenue for existing research reactors that are not currently being used at their full capacity. Financial incentive for building Nuclear Power production plants that can also facilitate radioisotope production.

Decrease of radiation exposure to personnel and public: With radioisotope separation occurring during irradiation as a continuous process, there is no need for reactor personnel to handle and transport the radioactive product for processing and separation post irradiation.

2.7 Results and Discussion

Producing radioisotopes via nuclear reactors typically involves neutron bombardment of an irradiation target for a predetermined amount of time. Post irradiation the target is removed from the reactor core and transported to radioisotope separation and processing facilities that are not necessarily always on the reactor facility site (Figure 2.2).

The following are some drawbacks of the mentioned production route

- Long irradiation times to obtain required specific activity
    - Costly
- Transportation of the irradiation target to radioisotope separation and processing facilities
    - Costly ($100-$20,000)
    - Higher risk of personnel and public exposure to radiation
    - Loss of radioactivity due to decay
- Effectiveness of radioisotope separation and enrichment processes if the target and radioisotope are the same element ($^{152}Sm+n \rightarrow {}^{153}Sm$)

- Low specific activity product
- Production of radioactive chemical waste
- High cost of building and operating radioisotope separation and processing facilities
- Loss of radioactivity due to decay

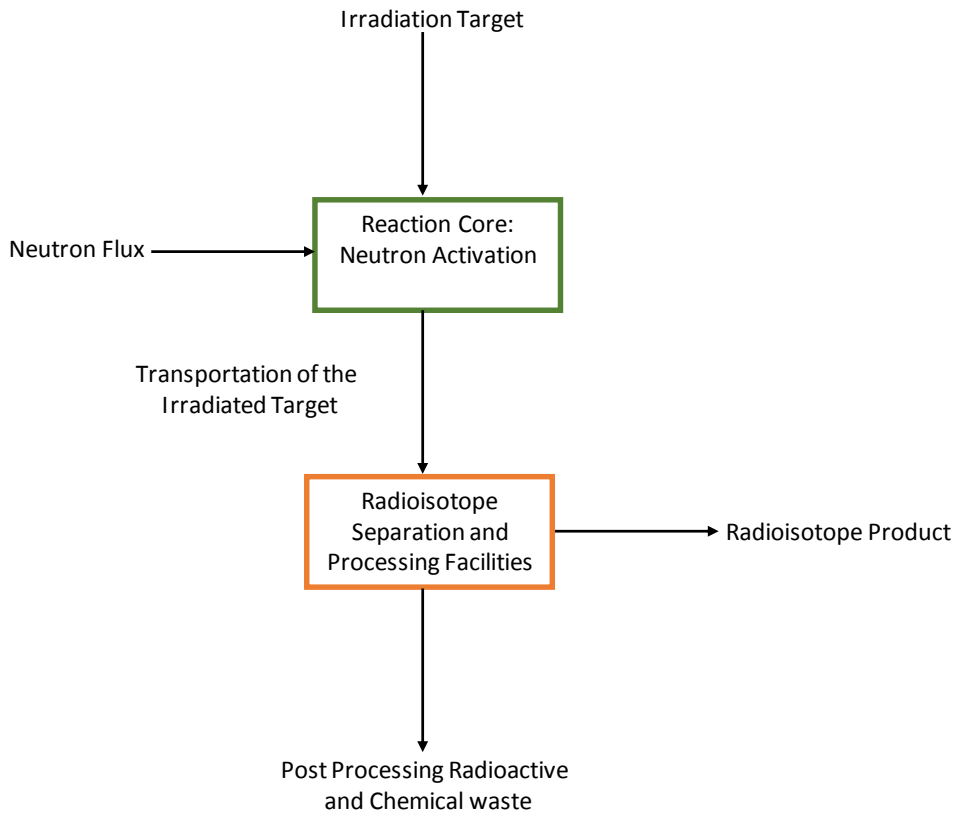

Figure 2.2: Reactor produced radioisotope production process diagram.
Radioisotope production occurs via neutron activation of the target. Post irradiation the irradiated target is transferred to separation and processing facilities for recovery of the radioisotope product.

The Szilard-Chalmers radioisotope production model via a continuous flow system (Figure 2.3) can produce radioisotopes with increased specific activity, while addressing typical challenges associated with reactor-produced radioisotopes. Similar to typical radioisotope production, the

target is exposed to a neutron flux; additionally the irradiation target is in continuous contact with a capture matrix for the duration of the irradiation. The role of the capture matrix is to collect the recoiled radioisotope produced as a result of the Szilard-Chalmers (S-C) effect. The radioisotope product is collected in a shielded reservoir outside the reactor core. There is an additional filtration step between radioisotope production and the collection reservoir to filter out any target material that may have transferred into the capture matrix. Essentially the radioisotope separation process occurs during irradiation in the reactor facility.

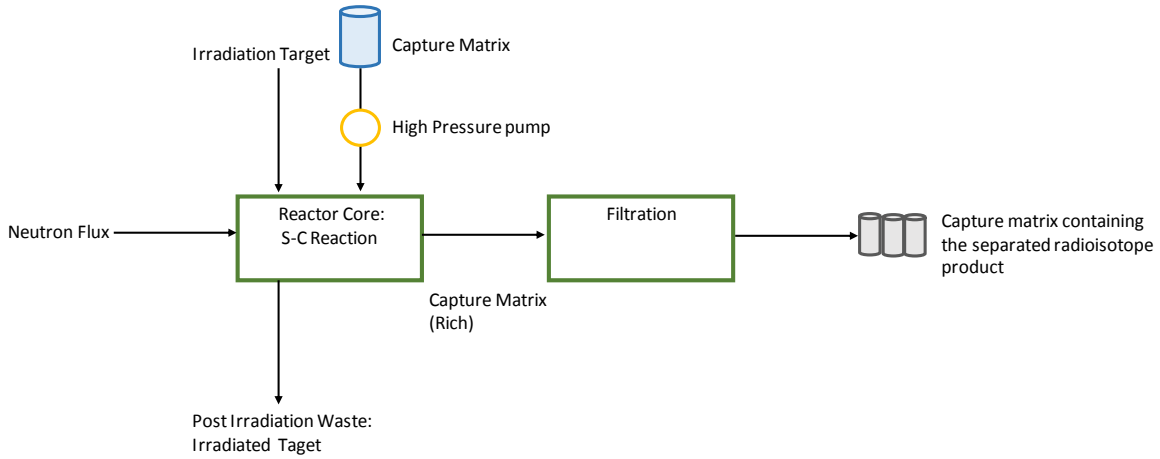

Figure 2.3: Radioisotope production by the Szilard-Chalmers Process diagram. Radioisotope production occurs by neutron activation coupled with the Szilard-Chalmers (S-C) reaction. The radioisotope product is collected and separated during irradiation via a capture matrix.

The following are some benefits of this production route

- Production of a radioisotope product with increased specific activity
- No need for handling and transportation of highly radioactive material for separation and processing
- Costly and exotic radioisotope separation facilities are not required

The following are matters that need to be addressed for further enhancement of radioisotope production using the Szilard-Chalmers method

- Development of irradiation targets that can withstand exposure to the radiation field without degrading in the capture matrix and diluting the specific activity.
- Development of irradiation targets that are thin and have a high surface area exposed to the capture matrix, such that the recoil range of the radionuclide exceeds the thickness of the target and can be easily ejected into the capture matrix.
- Determining the target behavior and specific activity as a result of scale up when using a higher neutron flux and longer irradiation time.

Regardless of the production route, radioisotope production requires nuclear reactors. Building a reactor entails a considerable amount of capital investment. Such an investment can be justified if the radioisotope product has more value compared to production and processing costs. Table 2.5 summarizes the technical information and estimated costs associated with building and operating a research reactor similar to the OPAL reactor.

Table 2.5: Reactor cost predictions based on an OPAL type reactor [83].

Life Span	40 years
Construction time	5 years
Operating days per year	300 days
Neutron Flux	$4x10^{14}$ n/cm^{2}s
Power Level	20 MW
Cost	$350 million (2004) with a cumulative interest of 26% would be equivalent to $441 million in 2015
Capacity Factor	%85
Discount Rate	10%
Annual Operating Costs	$21 million
Annual Revenue to Repay Capital+Yearly Operating Costs	$81.6 million

While building reactors needs to be considered for the long run sustainability of radioisotope production, a readily available option in response to radioisotope shortage is to utilize the 246

research reactors operational in 56 countries around the world[72] (31 operational in the U.S.) for radioisotope production. Most of these reactors are not used to their full capacity therefore can be used to produce radioisotopes, which in turn can generate substantial revenue for these facilities. Different types of research reactors exist with varying radioisotope production capacities and capabilities. Table 2.6 provides a range of production capabilities and associated costs for a range of U.S. research reactors.

Table 2.6: Reactor Costs associated with U.S. research reactors [84].

Total number of research reactors	42
Number of research reactors over 35 years old	40
Number of research reactors less than 35 years old	2
Neutron Flux (n/cm^2s)	1.0×10^8 -2.5×10^{15}
Annual Reactor Operations Cost ($)	7000-65,000,000

For example Molybdenum-99, the most widely used radioisotope in the diagnostic medical field with an estimated 10 million tests per year and 3-4 billion dollars cost to patient annually, is reactor produced [34]. Currently the world supply of ^{99}Mo is heavily dependent on a few reactors that are scattered around the world. The majority of these reactors are over 40 years old and are getting close to the decommissioning stage [60]. Table 2.7 summarizes information regarding these radioisotope-producing reactors, which supply the majority of ^{99}Mo used for medical diagnostic applications worldwide.

Table 2.7: Information on the reactors providing the majority of ^{99}Mo world supply[83–85].

Country	Name	Type	Initial Cost ($)	Annual Cost ($)	Capacity (Ci-6 day)/y [29]	First Criticality	Max flux Thermal ($n.cm^{-2}.s^{-1}$)	Days/Year Operating
Canada	NRU	Heavy Water	41 M	15.5 M	187,200	11/3/57	4.00E+14	273
Netherlands	HFR	Tank in pool	--	18.5 M	187,200	11/9/61	2.70E+14	308
Belgium	BR-1	Graphite	7 M	271 K	156,000	5/11/56	2.00E+12	200
Poland	MARIA	Pool	--	--	66,000	12/18/74	3.50E+14	200
France	OSIRIS	Pool	--	--	62,400	9/8/66	2.70E+14	252
South Africa	Safari	Tank in pool	4.5 M	5 M	130,700	3/18/65	2.40E+14	308
Australia	OPAL	Pool	350 M	21 M	42,900	8/12/06	4.00E+14	364

With reference to Table 2.7 it can be seen that the world supply of ^{99}Mo is heavily dependent on 7 reactors, were six of them are over 40 years old and close to decommissioning age.

The National Research Council (US) Committee on Medical Isotope Production without highly enriched Uranium, developed the cost estimates associated with ^{99}Mo production[81]. The committee recognized that there was no single cost for ^{99}Mo/^{99m}Tc generators in the supply chain because the radioisotope production sites are located in various countries therefore operate using different currencies and have varying costs associated with materials, labor, facilities and services. In general they found that most companies consider cost breakdown of radioisotope production to be proprietary information.

The estimates made for ^{99}Mo/^{99m}Tc production were as follows:

1. Cost of producing ^{99}Mo at the production facility in 2008: $225 for a 6-day curie with a cost variation of ±40%

2. Price of ^{99}Mo/^{99m}Tc 10-Curie generator in 2005: $1900 with a cost variation of ±25%.
3. Price for ^{99m}Tc dose in 2008: $11 per dose of ^{99m}Tc sodium pertechnetate with a price variation of ±20%.

In 2006 the global ^{99}Mo supply and demand was 12,000 6-day curies per week, were between 5000-7000 of the global demand met the United States needs. With a cost of $225 for a 6-day curie the overall cost of producing ^{99}Mo to meet the 2006 global demand would be approximately $141,000,000 annually.

In order for the use of research reactors intended for radioisotope production to be considered economically viable, the cost for radioisotope production must be less than the cost of the generated radioisotope product.

Due to reasons previously mentioned financial information regarding radioisotopes was not readily available and many factors come into play when pricing radioisotopes.

As discussed in preceding sections, ^{153}Sm is another radioisotope with proven application in the medical field. The ^{153}Sm radioisotope is a therapeutic radioisotope used for the treatment of painful bone metastases. Considering the production capability of an OPAL type reactor and the estimated worth of the ^{153}Sm radioisotope a significant amount of revenue can be generated as a result of ^{153}Sm production (Table 2.8). Based on the capabilities of an OPAL type reactor, a one-hour irradiation of 100g of pure ^{152}Sm target material can generate up to 13,000 Ci resulting in potential revenue of $832 million dollars. The price estimation of ^{153}Sm is based on a Canadian study done on the economic benefits of ^{153}Sm, were the product cost of ^{153}Sm was $4500 for approximately 70 mCi [80]. The cost associated with using existing research reactors for radioisotope production will most likely always be less than the value of the radioisotope product therefore generating revenue.

Table 2.8: Production economics of ^{153}Sm based on an OPAL type reactor [68,80].

Radioisotope	**Samarium-153**
Price ($/Ci)	$64,000
Max ^{153}Sm produced per 1 hr irradiation of 100 g ^{152}Sm target (Ci)	13,000 (EOI)
Max ^{153}Sm produced per 1 hr rradiation of 100 g ^{152}Sm target (mg)	29.6 (EOI)

Proof of concept experiments described in the following sections, were initially performed to study the Szilard-Chalmers method of radioisotope production, with a focus on samarium and holmium compounds [1]. The preliminary experimental results showed a decrease of 34% in the amount of lanthanide needed for a typical medical procedure, indicating enrichment and enhancement of the specific activity of the radioisotope of interest. After proven success with the preliminary experiments a unique experimental flow loop set-up was developed at the University of California Irvine (UCI) TRIGA® reactor facility (Detailed in Ch. 5). The innovative experimental setup instantaneously separated the radioactive recoil product formed during irradiation from the bulk of non-radioactive ions. The instant separation prevents the recoiled radioactive nucleus from reforming its original bonds with the target matrix and chemically separates it from the non-radioactive target matrix, resulting in a radioisotope product with a decreased amount of stable isotope carrier and an increased specific activity. The experimental results using the flow loop setup showed a decrease of up to 96%, depending on the target, in the amount of lanthanide needed for a typical medical procedure.

2.8 Conclusion

The use of nuclear reactors for radioisotope production, whether using existing reactors or building new reactors, specifically for radioisotope production, will address issues such as radioisotope shortage and transportation of radioactive material while also generating significant

revenue for these facilities. Adaptation of the Szilard-Chalmers method results in a radioisotope product with increased specific activity compared to reactor produced radioisotopes via direct (n, γ) reaction. High specific activity is essential for most radioisotope applications especially medicine. The proposed method decreases radioisotope production costs because: 1) there is no need for costly radioisotope separation and processing facilities since the radioisotope is obtained in the separated product form during irradiation 2) Shorter irradiation times are required to achieve the same desired specific activity 3) Prevents the formation of unwanted by products as a result of unnecessary exposure of the target radioisotope to the neutron flux.

In the analysis, the costs associated with operating existing research reactors both worldwide and in the U.S. for radioisotope production in addition to determining the capital needed to build a reactor for radioisotope production, were determined. The potential revenue some radioisotopes can generate if produced were also determined. Further studies need to be performed to determine the demand for radioisotopes in various fields and the economical potential for radioisotope production. The most favorable scenario is to use existing infrastructure to produce radioisotopes while developing and building new reactors that can meet the future demand of radioisotopes worldwide.

CHAPTER 3: TARGET MATERIAL SYNTHESIS AND CAPTURE MATRICES

3.1 Introduction

The objective of the study was to investigate the feasibility of producing radioisotopes with increased specific activity in a small-scale research reactor using the Szilard-Chalmers method. According to Friedlander et al. the following three general conditions need to be satisfied for radioisotope enrichment to be possible by the Szilard-Chalmers method: 1) the radioactive atom in the process of its formation must be broken loose from its parent molecule. 2) It must neither recombine with the molecular fragment from which it separated from nor rapidly interchange with inactive atoms in other target molecules. 3) A method for separation of the target compound from the radioactive material in its new chemical form must be available [58]. For this purpose a number of well defined, temperature and air stable complexes of samarium and holmium were synthesized. Ideally the Lanthanide (III) complexes must stay intact and not dissociate to free metal ion and ligand unless undergoing the Szilard-Chalmers effect. Therefore the candidate lanthanide complexes should have high thermodynamic stability and kinetic inertness. Lanthanides are considered hard acids and preferably coordinate to hard bases such as oxygen and under certain conditions nitrogen [86]. Organic ligands with nitrogen and oxygen donor atoms such as 8-hydroxyquinoline and acetylacetone [43,82,87], which show complexation affinity towards lanthanides were chosen to form thermodynamically stable and kinetically inert complexes with samarium and holmium. The lanthanide compound should also be radiolytically stable and not degrade in the capture matrix as a result of exposure to the radiation field. Lanthanide complexes with organic ligands can afford radiolytic stability to some degree (depending on neutron flux and irradiation time) due to low neutron absorption cross sections of the atoms involved in the typical framework of organic ligands (basically C,H,O and N) [44].

Chemical stability is also another important factor to consider when choosing the irradiation target material. The target should not decompose as a result of exposure to high temperatures or evolve gas that would pressurize and pose risk to the integrity of the containment vessel [34]. The Szilard-Chalmers effect was studied on the synthesized lanthanide compounds with two different experimental setups and conditions.

The following describes the various target materials considered and their synthesis procedure in addition to the capture matrices used, followed by description of the experimental setups and conditions used.

3.2 Lanthanide Compound Synthesis:

The following lanthanide complexes were synthesized according to previous literature methods with slight modifications (Figure 3.1)[82,87].

Lanthanide Acetylacetonate:

5 mmol of lanthanide nitrate hydrate (Ho, 99.9% Strem Chemicals; Sm, 99.9% Acros Organics) was dissolved in enough 0.01M HCl (36.5-38%, EMD Chemicals), added drop-wise, to dissolve the lanthanide nitrate salt. The solution was evaporated and the resulting residue was dissolved in 20 mL of ultrapure water (18.2 MΩ) and removed from heat. 20 mmol of pentane-2,4-dione (acetylacetone) (pentane-2,4-dione, 99% Acros Organics) was added to the mixture under constant stirring. The pH of the mixture was adjusted to 6 by the addition of 0.5 mL 14.5M ammonia (Ammonium Hydroxide, 29.14% Fisher Scientific) and upon slow addition of concentrated ammonia the complex precipitated. The precipitate was separated from the solution by vacuum filtration. The obtained precipitate was dried in an oven at 75 °C for 45 minutes.

Lanthanide Oxalate:

5 mmol of lanthanide nitrate hydrate (Ho, 99.9% Strem Chemicals; Sm, 99.9% Acros Organics) was dissolved in enough 0.01M HCl (36.5-38%, EMD Chemicals), added drop-wise to dissolve the lanthanide nitrate salt. The solution was evaporated to dryness and the obtained residue was dissolved in ultrapure water (18.2 MΩ). The lanthanide solution was treated with 20 mmol of oxalic acid (99.9% Fisher Scientific) under continuous stirring. Upon precipitate formation, stirring was stopped. The precipitate was separated from the solution by vacuum filtration and the obtained lanthanide oxalate powder was dried in the oven at 75 ^{O}C for 45 minutes.

Lanthanide 4-Aminobenzoate:

5 mmol of lanthanide nitrate hydrate (Ho, 99.9% Strem Chemicals; Sm, 99.9% Acros Organics) was dissolved in enough 0.01M HCl (36.5-38%, EMD Chemicals), added drop-wise, to dissolve the lanthanide nitrate salt. The solution was evaporated and the resulting residue was dissolved in 20 mL of ultrapure water (18.2 MΩ) and removed from heat. 16 mmol of 4-aminobenzoic acid (99% Sigma Aldrich) was added to the mixture under constant stirring. The pH of the mixture was adjusted to 6 by the addition of 0.5 mL 14.5M ammonia (Ammonium Hydroxide, 29.14% Fisher Scientific) and upon slow addition of concentrated ammonia the complex precipitated. The precipitate was separated from the solution by vacuum filtration. The obtained precipitate was dried in the oven at 75^{O}C for 45 minutes.

Lanthanide 8-Hydroxyquinolinate:

1 mmol of the lanthanide nitrate hydrate (Ho, 99.9% Strem Chemicals; Sm, 99.9% Acros Organics) was dissolved in 50 mL ethanol (95%, Gold Shield Chemicals). 4 mmol of 8-hydroxyquinolinate (99% Sigma Aldrich) was gradually dissolved in 50 mL of ethanol. The 8-hydroxyquinolinate ethanolic solution was added to the lanthanide solution under constant

stirring. The mixture was heated to boiling for 35 minutes. Precipitate formation was instantaneously visible. After 35 minutes the mixture was removed from heat, while stirring continued until the mixture was cooled down to room temperature. The resultant precipitate was separated from the mixture by vacuum filtration and dried in the oven at 75 ^{O}C for 45 minutes.

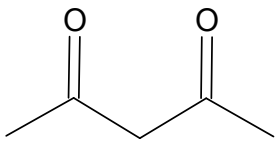

Acetylacetone

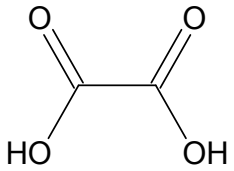

Oxalic Acid

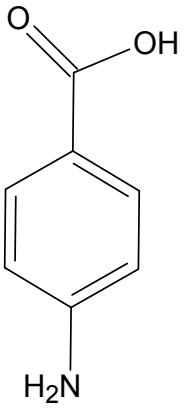

4-aminobenzoic Acid

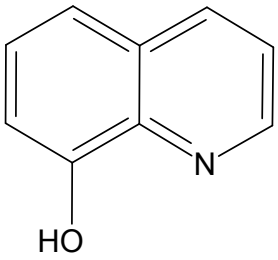

8-hydroxyquinoline

Figure 3.1: Lanthanide complexing ligands used for compound synthesis**.**

Characterization

For verification purposes the compounds that had known X-ray diffraction (XRD) spectra files published in the XRD database, were submitted to the UCI Laboratory for Electron and X-ray Instrumentation (LEXI) for analysis using the Rigaku Smart Lab X-ray diffractometer. The Samarium Oxalate and Samarium 4-aminobenzoate compounds had XRD spectra published in

the database therefore they were compared with the experimental XRD spectra obtained to verify the identity of the synthesized product.

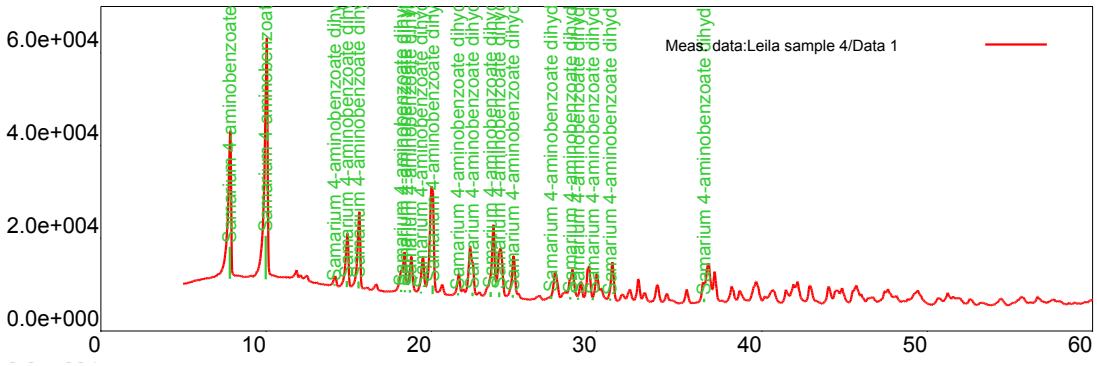

Figure 3.2: Powder X-ray diffraction pattern of Samarium 4-aminobenzoate.

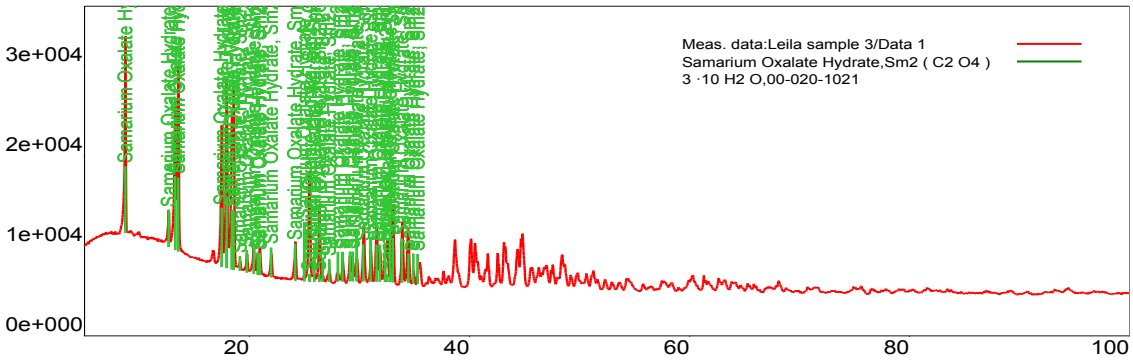

Figure 3.3: Powder X-ray diffraction pattern of Samarium Oxalate.

The experimental XRD spectra (red) matched closely with the spectra available from the XRD database library (green), indicating that the lanthanide compounds synthesized were in close agreement with the expected compounds (Figure 3.2-3.3). Since the overall focus of the study was radioisotope production via the Szilard-Chalmers method, synthesis of target material suitable for recoil studies via the Szilard-Chalmers process was essential. Therefore effort and resources were spent on characterization to a point where relative agreement between the expected compound and actual compound was achieved. Since the lanthanide compounds share

similar chemistry and the same general synthesis procedures were applied for the synthesis of both samarium and holmium compounds, it was assumed that the other compounds synthesized were in relative agreement with the predicted compound. Since the XRD spectra were not available in the database for all of the compounds synthesized, further analysis was carried out by neutron activation analysis for lanthanide content and compared to the predicted lanthanide content present in the compound based on predicted lanthanide-ligand combinations.

For neutron activation analysis the compound of interest alongside corresponding standard samples were irradiated at the UCI TRIGA reactor facility. Post irradiation the lanthanide compound and the standard samples were analyzed for the radiolanthanide activity using a high purity germanium (HPGE) detector (Canberra HPGe detector operated with GENIE software and calibrated for efficiency with a mixed Eckert Ziegler gamma source) at the representative gamma energy of the radioisotope of interest. The peak area at the representative energy was directly correlated with the lanthanide (samarium or holmium) content in the sample. The standard samples were used to construct a calibration curve, which was used to determine the lanthanide content in the synthesized samples. The experimental values were compared to the calculated theoretical values determined, based on the mass of the sample analyzed and predicted lanthanide/ligand combination to determine the composition of the synthesized compound (Table 3.1).

Table 3.1: Results from the Neutron Activation Analysis for the synthesized samarium and holmium compounds (Ln=Sm or Ho).

Compound	Complex model	Molar mass anhydrous based (g/mol)	Theoretical Ln found in compound (mg)	Experimental Ln found in compound (mg)	Percent difference
Holmium 8-Hydroxyquinolinate	$Ho(C_9H_6NO)_3$	597.38	7.80	6.70	14.10
Holmium Acetylacetonate	$Ho(C_5H_7O_2)_3$	462.25	1.80	1.50	16.67
Holmium Oxalate	$Ho(C_2O_4)_3$	428.99	5.00	5.20	4.00
Holmium 4-aminobenzoate	$Ho(C_7H_6NO_2)_3$	573.31	1.60	1.50	6.25
Samarium 8-hydroxyquinolinate	$Sm(C_9H_6NO)_3$	582.81	0.076	0.077	1.32
Samarium Acetylacetonate	$Sm(C_5H_7O_2)_3$	447.68	0.760	0.650	14.47
Samarium 4-aminobenzoate	$Sm(C_7H_6NO_2)_3$	558.74	0.750	0.610	18.67
Samarium Oxalate	$Sm(C_2O_4)_3$	414.42	0.940	0.810	13.83

With respect to Table 3.1 the percent difference between theoretical and experimental value for the lanthanide content present in the compounds of interest was between 1-19%. The value for the percent difference indicates that the predicted lanthanide-ligand combination was in relative agreement with the actual compound synthesized.

The molecular mass used for calculations were anhydrous based as opposed to taking into account the hydrate formation, since the number of H_2O molecules coordinated to the compound was not determined. The fact that the molecular weight of the hydrate was not used for theoretical calculations, contributes to the difference between the theoretical and experimental values calculated. Factors such as irradiation conditions, standard and sample preparation techniques and the associated errors, in addition to unforeseen outcomes associated with compound synthesis and the presence of impurities, are all contributing factors to the difference between theoretical and experimental calculations.

The purpose of the XRD and neutron activation analysis experiments were to determine if the lanthanide complexes synthesized were in agreement with the anticipated compounds. The lanthanide compounds were used as irradiation targets without any further purification or modification.

3. 3 Stability Constants:

The stability constant is a measure of the stability of the complex in solution. In the case of the mentioned compounds, it refers to the degree of association of the lanthanide and the organic ligand involved in the state of equilibrium. The higher the value of the stability constant, the larger the degree of association between the lanthanide and the ligand is, resulting in a greater degree of thermodynamic stability of the complex. Lanthanide ions in solution are usually surrounded by solvent molecules (H_2O) that compete with the ligand and can be replaced by them, the larger the stability constant is, the more stabilizing the ligand. The stability constants of the lanthanide complexes that were available in the literature are summarized in Table 3.2. Were log β is the cumulative stability constant.

Table 3.2: Stability constants of lanthanide compounds [88–90].

Lanthanide ion	Ligand	# of ligands	logβ
Sm^{3+}	8-Hydroxyquinoline (C_9H_7ON)	3	27.21[89]
Sm^{3+}	Acetylacetone ($C_5H_7O_2$)	3	12.23[90]
Ho^{3+}	8-Hydroxyquinoline (C_9H_7ON)	3	27.96[89]
Ho^{3+}	Acetylacetone ($C_5H_7O_2$)	3	14.13 [88,90]

The ionic atomic radius of the lanthanide elements decreases as the atomic number increases due to an effect known as lanthanide contraction, resulting from a poor shielding effect of the 4f electrons. The poor shielding results in the positively charged nucleus having a greater effect on the poorly shielded outer electrons leading to greater attraction to the electrons and ultimately

resulting in a decrease of the radius with the increase of the atomic number [91]. Due to the lanthanide contraction phenomena, there is typically an increase in the stability constants of the lanthanides with increasing atomic number. The increase of stability constants with increasing atomic number is evident from Table 3.2, were the holmium (Z=67) compounds have larger stability constants compared to samarium (Z=62) compounds with the same ligands.
The obtained stability constants (Table 3.2) were gathered from various literature sources and were not verified using the proposed experimental conditions used in the present study. In the upcoming sections the relationship between stability constants and enrichment factors will be considered.

3.4 Synthesis of Alternative Lanthanide Targets:

Background

The lanthanide irradiation targets used for the initial experiments were solid powders of samarium and holmium complexed with ligands containing oxygen or nitrogen donor atoms. The ideal irradiation target should be thin with a large surface area such that the recoil range of the formed radioisotope product, exceeds the thickness of the target and the product radioisotope can be ejected into the capture matrix[92]. With the mentioned experimental setup and procedure, detailed in the following sections, most likely only the radioisotopes formed on the surface of the packed powder target, in contact with the capture matrix had the opportunity to recoil, be ejected and separated from the target by the capture matrix. The recoil range of the radioisotopes produced below the surface in contact with the capture matrix is small compared to their distance from the capture matrix, leading to retention of the radioisotope in the target matrix. A large surface area of the target in contact with the capture matrix leads to an increase of the formed

radioisotope product having the opportunity to recoil into the capture matrix and be separated from the target, resulting in higher enrichment and an increase in specific activity.

In an effort to look into diverse irradiation targets (i) containing a high lanthanide content (ii) larger lanthanide containing surface area (iii) higher stability towards the irradiation field; the synthesis of additional target material that would fit into the mentioned criteria was investigated. Therefore functionalizing inert solid support resins with lanthanide selective ligands that adsorb lanthanides or coating porous high surface area solid support resins with the lanthanide of choice were considered as potential irradiation targets.

For this purpose XAD-4 polymeric adsorbent resins were chosen as a solid support (Figure 3.4). XAD-4 is a polymeric adsorbent solid support resin with suitable physical, chemical and thermal stability that can also withstand exposure to the radiation field. The non-ionic cross-linked polymer has adsorptive properties due to having both a continuous polymer phase and a continuous pore phase [93]. The characteristics of the resins are summarized in Table 3.3.

Table 3.3: Characteristics of XAD-4 polymeric adsorbent resin [93].

Resin	XAD-4
Matrix	Macroporous cross-linked aromatic polymer
Composition	Styrene divinylbenzene
Surface Area (m^2/g)	750
Average Pore Diameter (Angstroms)	50
Mesh Size (nominal)	20-60
Pore Volume (mL/g)	0.98
Physical form	White translucent beads

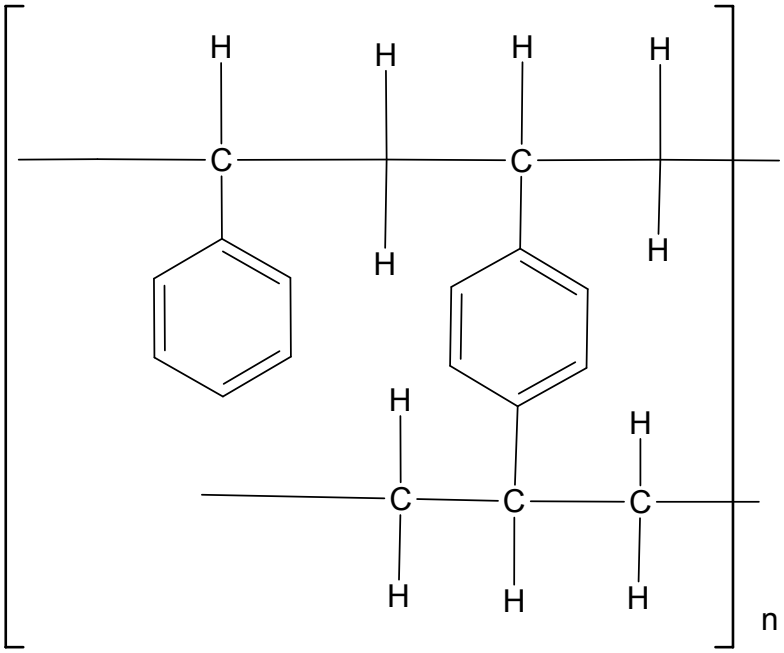

Figure 3.4: Chemical structure of XAD-4 polymeric resin.

XAD-4 has been used as an inert support for extraction chromatographic studies on the separation of actinides from lanthanides by impregnating the resin with selective extractant ligands such as 2,6-bis(5,6-diethyl-1,2,4-triazin-3-yl) pyridine (Ethyl-BTP) [94] or pre-concentration of Uranium on XAD-4 modified resin with the 8-hydorxyquinoline ligand [95]

An organic phase functionalized chromatographic resin loaded with lanthanides could be used as a potential irradiation target. For this purpose functionalizing resins with ligands of Bis-triazine pyridine (BTP) family was considered. The BTP ligands have shown selectivity and affinity towards trivalent actinides over trivalent lanthanides but these ligands show some affinity for the lanthanides especially in the absence of actinides. A characteristic that makes these ligands attractive as an irradiation target is their slow extraction kinetics, such that typically it takes hours for complete extraction of the trivalent metals. Once the metal-BTP complexes are formed they exhibit high stability therefore stripping of the metal ion is a challenging task. Developing an organic phase containing the BTP-Lanthanide as a candidate target matrix for testing the

Szilard-Chalmers method can potentially result in higher enrichment factors and specific activity. Upon neutron capture, the recoiling radiolanthanide would break apart from the BTP ligand and transfer to the aqueous capture matrix, as a result of the extremely slow extraction kinetics of the BTP ligands re-extraction of the radiolanthanide into the organic phase target would be slow. The Ethyl-BTP ligand (Figure 3.5) was synthesized based on reported literature methods[96,97]. Preliminary experiments were performed to impregnate the macroporous XAD-4 solid support with Ethyl-BTP followed by batch adsorption experiments to adsorb the lanthanide of interest onto the Ethyl-BTP functionalized resin based on reported literature methods [94,98]. Neutron activation analysis was performed on the lanthanide containing resin, based on these experiments the concentration of lanthanide adsorbed on the resin was too low for it to be a desirable irradiation target for Szilard-Chalmers studies. Therefore further experiments are necessary to adsorb a higher concentration of lanthanides on the functionalized resins.

2,6-bis(5,6-diethyl-1,2,4-triazin-3-yl) pyridine (Ethyl-BTP) Synthesis:

BTP ligands were synthesized according to the following procedure adapted from a study done by Wei et al. studying "Preparation of Novel Silica-Based Nitrogen donor Extraction Resins and their Adsorption Performance for Trivalent Americium and Lanthanides" [97]. The synthesis scheme was a two-step process.

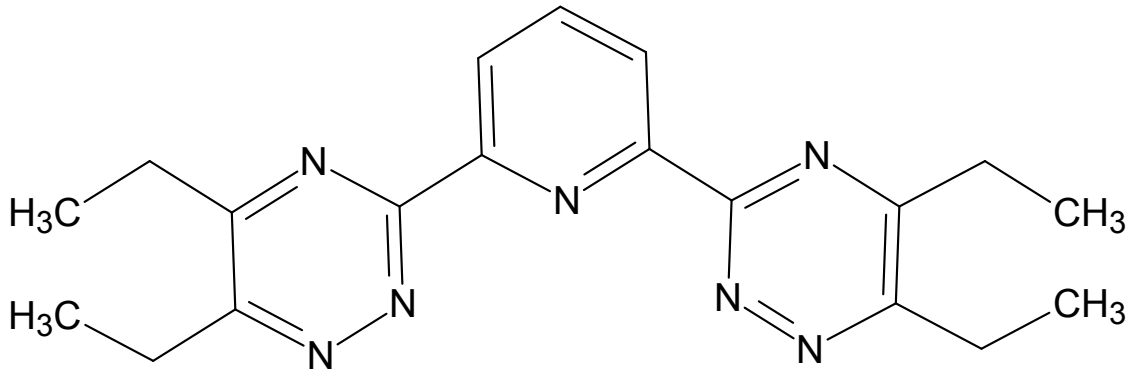

Figure 3.5: Chemical structure of 2,6-bis(5,6-diethyl-1,2,4-triazin-3-yl) pyridine (Ethyl BTP).

Ethyl-BTP Synthesis Step 1: Synthesis of 2,6-pyridine carboxamide hydrazine (Figure 3.6):

- 1.634 mmols (0.2110 g) of 2,6-pyridine dicarbonitrile (97%, Sigma Aldrich) (I) was allowed to react with 1.027 mL of hydrazine hydrate (50-60% reagent grade, Sigma Aldrich) in an aqueous medium at room temperature overnight
- The obtained 2,6-pyridine carboxamide hydrazine (II) was recrystallized from pure water.

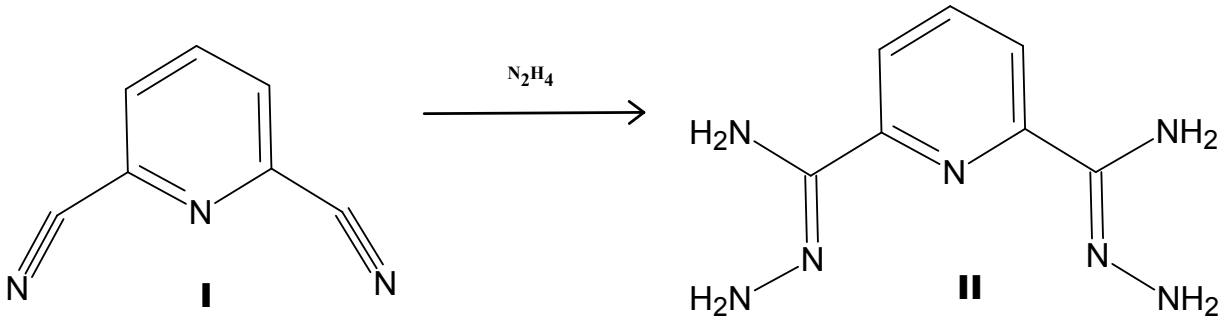

Figure 3.6: Ethyl-BTP synthesis scheme step 1.

Ethyl-BTP Synthesis Step 2: (Figure 3.7):

- 0.532 mmol of 2,6-pyridine carboxamide hydrazine (II) and 1.064 mmol of Hexane-3,4-dione (III) (95%, Sigma Aldrich) were allowed to react in an ethanol medium at refluxing temperature for 2.5 hrs to synthesize Ethyl-BTP (IV).
- The solid product was recrystallized from an ethanol medium, resulting in a yellow colored solid powder.

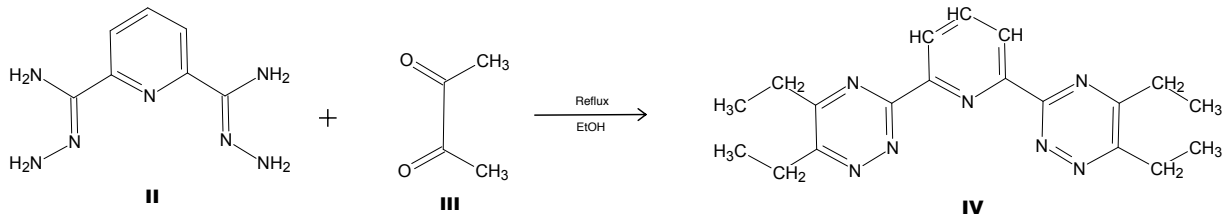

Figure 3.7: Ethyl-BTP synthesis scheme step 2.

The solid product was filtered and recrystallized from an ethanol medium. The obtained solid compound was characterized by mass spectrometry and nuclear magnetic resonance spectroscopy (NMR).

For NMR studies the Bruker GN-500 (500 MHZ, ^{1}H) spectrometer, equipped with a BBO probe at the UCI NMR facility was used. Figure 3.8 shows the $\{^{1}H\}$ NMR spectra of the synthesized Ethyl-BTP ligand with the corresponding color-coded peak assignment. The spectra showed three different proton signal groups. The experimental NMR spectrum was compared to the Ethyl-BTP spectrum from an NMR database [99]. The spectra from the database matched closely with the experimental NMR spectra obtained.

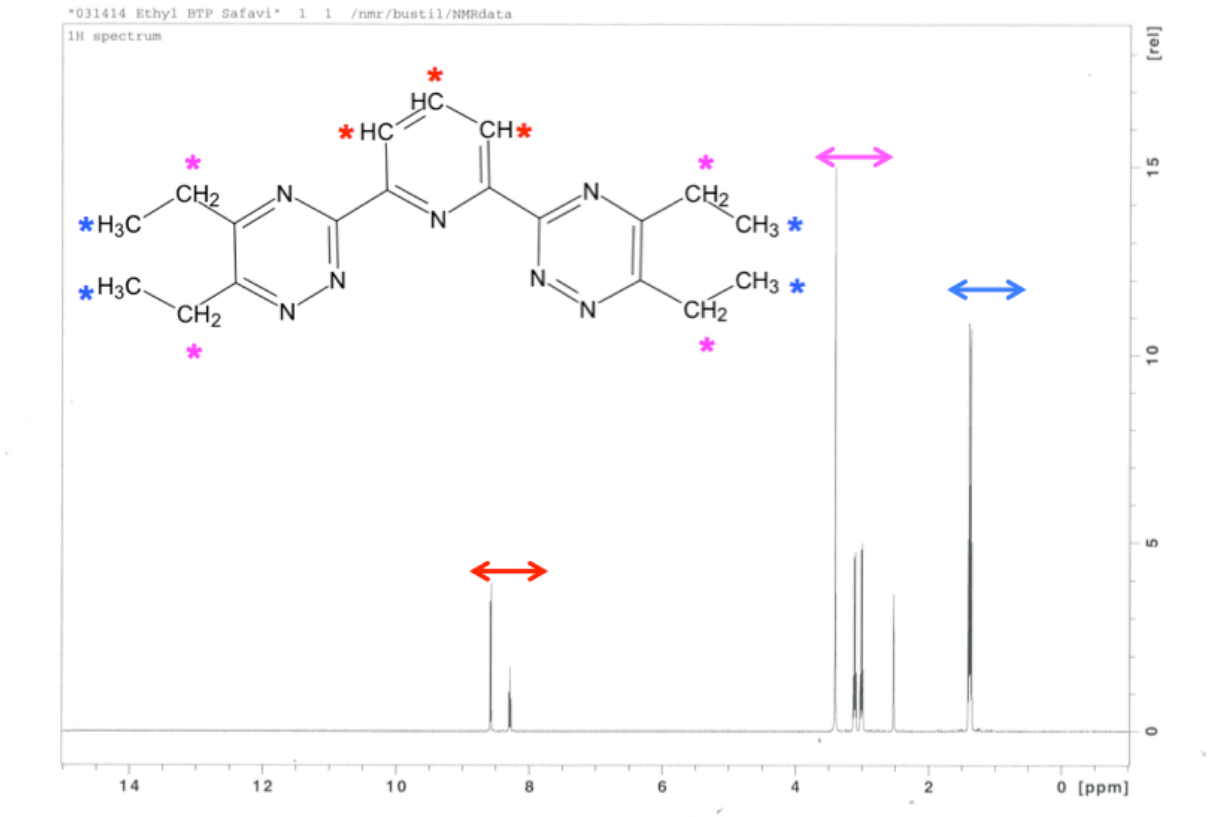

Figure 3.8: ^{1}H NMR Spectrum of Ethyl-BTP.

For further characterization of the Ethyl-BTP ligand, Electrospray ionization mass spectrometry was carried out using the positive ion mode of the ESI LC-TOF Micromass LCT 2 mass spectrometer operated with the MassLynx software, at the UCI mass spectrometry facility, for further characterization of the Ethyl-BTP ligand.

The theoretical molecular weight of Ethyl-BTP ($C_{19}N_7H_{23}$) was calculated to be 349.23 g/mol. With respect to Figure 3.9, two group of peaks are seen at m/z= 350.20 corresponding to the Ethyl-BTP ($[C_{19}N_7H_{23}]H^+$) and m/z=372.21 corresponding to the formed Ethyl-BTP sodium adduct ($[C_{19}N_7H_{23}]\,Na^+$) respectively (Figure 3.9).

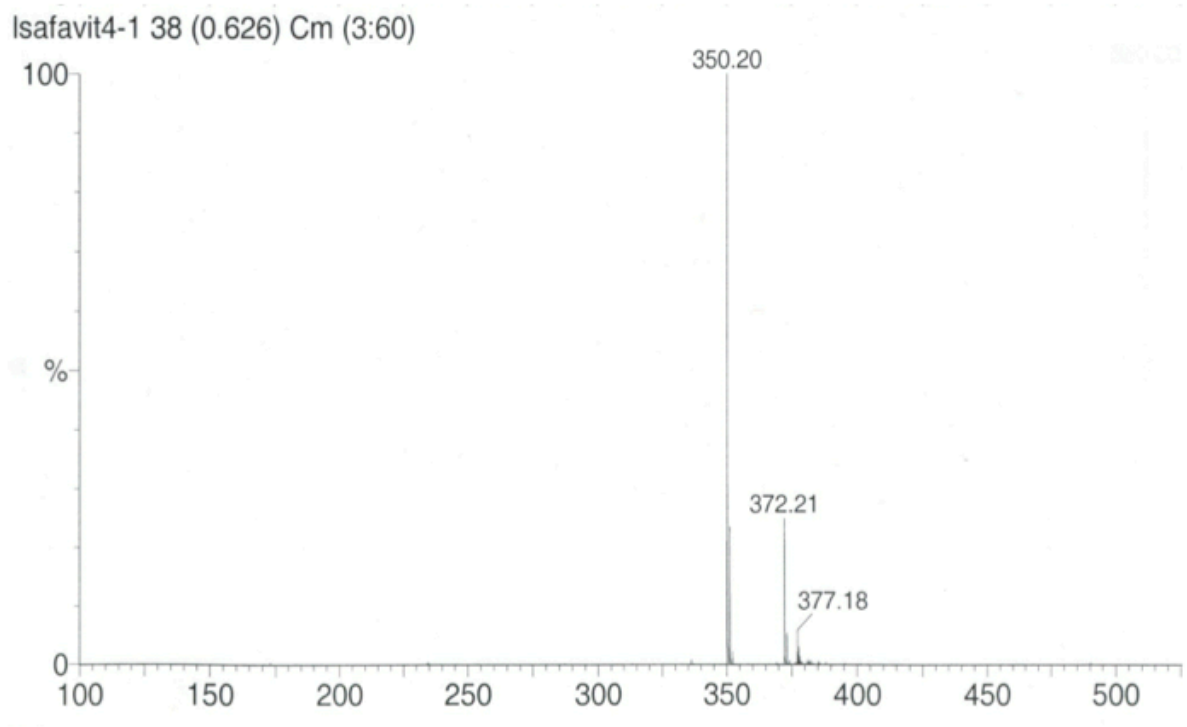

Figure 3.9: Mass spectrum of Ethyl-BTP.

With respect to the NMR and mass spectra it was concluded that the compound synthesized was Ethyl-BTP. The synthesized ligand was used to develop functionalized resins for lanthanide absorption.

Preparation of Ethyl-BTP Chromatography Resin:

To remove any contaminants and impurities from the solid support, the XAD-4 (Acros Organics) resin was cleaned thoroughly with methanol (99.9%, J.T. Baker), water, 1 M HNO_3 (70%, Sigma Aldrich), 1 M NaOH (1N, Fisher Scientific) then rinsed with water until a neutral pH was reached in the rinse solution. The resins were dried to constant weight before being used in experiments. The Ethyl-BTP functionalized resins were prepared by equilibrating 0.0432 g

Ethyl-BTP (MW: 349.43 g/mol) dissolved in 10 mL methanol (yellow solution) with 0.4040 g of the cleaned XAD-4 resin for 24 hours with constant stirring. The resin was separated from the solution and dried. To determine the amount of Ethyl-BTP taken up by the resin, the increase in weight of the resin post equilibration with Ethyl-BTP and drying of the resin was determined. There was an increase in weight of 0.0378 g (1.08E-04 moles) therefore more than 80% of the Ethyl-BTP present in the solution was adsorbed on the resin. The lanthanide uptake behavior of the Ethyl-BTP functionalized resin was studied by equilibrating 5 mL of 0.01 M Holmium (5E-05 moles) solution with the resin for 24 hours with constant mixing (1.24E-04 moles Ho/g ethyl BTP resin, 0.0204 g Ho/g ethyl BTP resin). Post equilibration the resin was separated from the solution and the holmium uptake of the functionalized resin was determined by neutron activation analysis and compared to other synthesized materials. The functionalized resins were irradiated at the UCI TRIGA reactor facility in the Lazy Suzan for 20 min at the 75 kW power level (neutron flux ~2.5×10^{11} $n.cm^{-2}.s^{-1}$) alongside calibration standards.

Post irradiation the holmium content adsorbed on the resins was determined by gamma analysis at the representative gamma energy for ^{166}Ho and compared to calibration standards.

Table 3.4: Holmium content of various synthesized target compounds.

Target/Compound	**g Ho/g target-compound**
Holmium Ethyl-BTP XAD-4 Resin	6.85E-05
Holmium Acetylacteonate PVA material	2.15E-02
Holmium Acetylacetonate PVA XAD-4 Resin	3.14E-02
Holmium 8-hydroxyquinolinate PVA XAD-4 Resin	7.21E-03
Holmium Acetylcacetonate	2.78E-01
Holmium 8-Hydroxyquinolinate	2.33E-01
Holmium Oxalate	3.98E-01
Holmium 4-Aminobenzoate	2.66E-01

Based on the experimental conditions stated above, a maximum of 0.0204 g of holmium could theoretically have been absorbed per gram of functionalized resin. Based on the neutron activation analysis of the Holmium Ethyl BTP resin 6.85E-05 g Ho was absorbed per gram of the functionalized resin (Table 3.4); approximately 300 times less than the maximum possible. The small amount of Holmium absorbed on the resin compared to the maximum amount possible, indicates that the functionalized resin were not optimized for the predicted holmium uptake, and further enhancement of the resin synthesis procedure is necessary so it can be used as a candidate irradiation target for Szilard-Chalmers studies.

For comparison purposes the amount of Holmium per gram of the Ethyl-BTP resin was compared to other holmium targets used throughout this study (Table 3.4). The holmium content was 450-3400 times less compared to the other target material used (Table 3.4). The amount of holmium in the target was directly proportional to the amount of radioactive ^{166}Ho produced as a result of irradiation and hence the amount of ^{166}Ho having the potential to recoil and be separated. Therefore the holmium Ethyl-BTP XAD-4 resin was not an ideal candidate for recoil studies and the Szilard-Chalmers method because the amount of ^{166}Ho activated and recoiled into the capture matrix would most likely be below the detection limit of the detector.

Holmium Acetylacetonate Polyvinyl Alcohol (HoAcAc PVA) material:

One class of material that was appealing as an irradiation target, and also considered as a promising agent for intra-arterial therapy and the treatment of liver malignancies was: radioactive holmium loaded poly(L-lactic acid) microspheres (Ho-PLLA-MS) [27,100–103]. These microspheres are loaded with holmium acetylacetonate (an irradiation target used throughout the proposed study, with promising results) and prepared by a solvent evaporation method [102,104]. Studies done by Vente et.al. concluded that Ho-PLLA-MS can endure neutron activation with a

nominal thermal neutron flux of 5×10^{12} $n.cm^{-2}.s^{-1}$ for 7 hours and still maintain their structural integrity [100].

Holmium microspheres were considered as an irradiation target candidate with desired properties for radioisotope production via the Szilard-Chalmers method. Studies were carried out by Nijsen et. al. for the production Ho-PLLA-MS via the solvent evaporation method [103]. The microspheres were prepared by dissolving Holmium Acetylacetonate (HoAcAc) (10 g) and poly(L- lactic acid) (6 g) in chloroform and dissolving poly-vinyl alcohol (PVA) in 1 L of boiling water. After the solutions were left to cool, the organic and aqueous mixtures were added together and stirred (500 rpm) for 40 hrs at room temperature while having a flow of nitrogen flushed over the mixture to accelerate the evaporation of the solvent [102,103]. The microspheres were collected, characterized and used for further experimentation. Bult et al. also studied the production of microspheres with ultra-high holmium content to be used for radioablation of malignances [104]. The microspheres were prepared similar to the above procedure carried out by Nijsen et al. except poly (L-lactic acid) was not used in the synthesis. For the proposed study, the Holmium Acetylacetonate Polyvinyl alcohol material was synthesized via an adapted route similar to Bult et al. were poly (L- lactic acid) was not used[104].

Synthesis of Holmium Acetylacetonate PVA material:

The HoAcAc PVA material was synthesized according to the following synthesis route adapted and scaled down from the method used by Bult et. al [104]. 0.3110 g HoAcAc synthesized (according to the synthesis method described for lanthanide acetylacetonate in section 3.2) was dissolved in 5.4 mL chloroform (99.9%, Mallinckrodt Chemicals) resulting in a cloudy pink solution (solution A). 0.6374 g of Polyvinyl alcohol (98-99% Hydrolyzed-low molecular weight, Alfa Aesar) was dissolved in 31.25 mL boiling water (solution B). Solution B was added to

solution A resulting in a 2 phase oil/water mixture. The emulsion was stirred at room temperature at a speed of (500-700 rpm) for 72 hours. After the solvent evaporated, a dense pink colored solid plastic like material was obtained, collected and washed 3 times with water and then dried at room temperature.

Due to the dense nature of the material there was difficulty collecting the solid post washing via filtration, as the filter would clog. Therefore the synthesized HoAcAc PVA material was not considered an ideal irradiation target for the current experimental setup. The experimental apparatus, setup and conditions are explained in detail in the following sections, but essentially the target is placed in a filter compartment where it is continuously contacted with the capture matrix. Post contact, the capture matrix is filtered into a sample collection flask. If the target material is dense and does not allow the capture matrix to pass through the filter it is not an ideal candidate to be used under the mentioned experimental setup.

To ensure the irradiation target allows the flow of the capture matrix through the filter for the duration of the experiment, another class of material was considered. Since the HoAcAc PVA material had suitable characteristics for an irradiation target, to address the dense nature of the material, coating of a porous solid support resin with the HoAcAc PVA material was considered. The XAD-4 resins previously used as an inert support in the Ethyl-BTP studies were considered as the solid support to be coated with the lanthanide compound. Similar studies using XAD-4 as an inert support was not found in literature.

Holmium Acetylacetonate Polyvinyl Alcohol XAD-4 (HoAcAc PVA XAD-4) Resins:

The synthesis route was adapted from the method used by Bult et. al [104]. Similar to the HoAcAc PVA material synthesis, 0.5130 g of HoAcAc was dissolved in 9.2 mL chloroform (solution A). 1.2664 g of PVA was dissolved in 90 mL boiling H_2O (solution B). Solution A was

added to solution B and 2.0394 g of cleaned XAD-4 resin was added to the emulsion and stirred at 500-700 rpm at room temperature for 72 hours until the majority of the solvent evaporated. The resultant pink colored resins were collected and dried (Figure 3.10, left)

Holmium 8-Hydroxyquinolinate Polyvinyl Alcohol XAD-4 (Ho8HQ PVA XAD-4) Resins:

The synthesis route was adapted from the production of HoAcAc PVA XAD-4 resins, detailed in the preceding section. 0.2212 g of Ho8HQ was dissolved in 9 mL chloroform (solution A). 1.4089 g of PVA was dissolved in 50 mL boiling H_2O (solution B). Solution A was added to solution B and 4.6829 g of cleaned XAD-4 resin was added to the emulsion and stirred at 500-700 rpm at room temperature for 72 hours. The resultant yellow colored resins were collected and dried (Figure 3.10, right).

Figure 3.10: HoAcAc PVA (right) Ho8HQ PVA (left) coated XAD-4 resins.

Characterization of PVA XAD material:

For the determination of the amount of holmium incorporated in the HoAcAc PVA, HoAcAc PVA XAD-4 and Ho8HQ PVA XAD-4 material, neutron activation analysis was performed. The amount of holmium per gram of material irradiated was determined and compared to other targets considered (Table 3.4). With respect to Table 3.4 it can be seen both HoAcAc PVA XAD-4 and Ho8HQ PVA XAD-4 resins have a considerable amount of holmium incorporated in them. The HoAcAc PVA XAD-4 resin had approximately 10 times less holmium per total gram of the resin compared to the holmium per gram of the pure HoAcAc powder. Ho8HQ PVA XAD-4 had approximately 30 times less holmium content incorporated per gram of resin compared to the holmium content per gram of pure Ho8HQ. The lower holmium content of the XAD-4 resins compared to the pure HoAcAc/Ho8HQ powders was anticipated since the powders were one of the components of the PVA XAD-4 resin and the majority of the HoAcAc and Ho8HQ PVA XAD-4 mass is attributed to the PVA and XAD-4 material. Although the HoAcAc PVA material had a considerable amount of holmium incorporated in the material, it was not chosen for Szilard-Chalmers studies due to the dense nature of the material and possible implications it could cause when tested with the filters used in the proposed experiments. The HoAcAc and Ho8HQ PVA XAD-4 resins were both chosen for further solubility and Szilard-Chalmers studies.

Scanning electron microscopy (SEM) coupled with energy dispersive X-ray spectroscopy (EDX) was also used to look at the surface topography and composition of the uncoated XAD-4, HoAcAc PVA XAD-4 and Ho8HQ PVA XAD-4 resins. The following samples were analyzed: (i) The uncoated XAD-4 resin (sample 1) (ii) The HoAcAc PVA XAD-4 resin (sample 2) (iii) The Ho8HQ PVA XAD-4 resin (sample 3). The spectra and analysis can be found in the

appendix (A.1). With respect to the EDX analysis, sample 1 (blank) did not show any presence of holmium. The points analyzed on sample 2 and 3 indicated the presence of holmium. The holmium peaks in sample 2 were more intense than sample 3, similar to the neutron activation results, indicating that sample 2 had a higher concentration of holmium adsorbed on the resins. With respect to the obtained SEM images it can be seen that the associated holmium peaks have varying intensity from point to point suggesting the holmium was not coated/distributed evenly on the resin. Therefore further enhancement of the synthesis procedure is necessary to obtain uniform holmium distribution on the resins.

3.5 Capture Matrices

The role of the capture matrix was to capture the recoiling radioisotope and separate it from the bulk of the inactive material (irradiation target) so a radioisotope product with increased specific activity could be obtained. Ideally the irradiation target should be insoluble in the capture matrix such that only the recoiling radioisotope is transferred to the capture matrix with minimum transfer of the stable isotope carrier. The capture matrix should have minimal susceptibility to damage in the radiation field. The capture matrix should not be dangerous to handle (flammable, extreme pH, volatile, toxic….) or need extreme and exotic conditions to work with. Also the capture matrix should be such that, post collection of the radioisotope product, it can be worked up easily for the intended application.

Water was the main capture matrix of choice for the experiments performed because it's not prone to damage in the radiation field, while offering a clean, non toxic, easy to work with and readily available capture matrix.

In an effort to obtain higher enrichment factors, additional aqueous capture matrices were considered. The capture matrix used in the experiments thus far had been water with a neutral

pH. The lanthanide ion has Lewis acid characteristics, in order to separate the recoiling radiolanthanide from the target, performing lanthanide chemistry in aqueous solutions at low pH (4 or lower) is preferred. The lower pH will prevent the potential formation of lanthanide oxide/hydroxides due to extensive hydrolysis of the lanthanide ion [105]. Therefore the effect of lower pH capture matrices on the enrichment factors and experimental results was studied. Preliminary experiments were conducted with a 10^{-4} M HNO_3 capture matrix (pH=4). Further investigation needs to be performed to look at issues such as solubility of the irradiation target at lower pH and how the enrichment factor can be further optimized under these conditions. Experiments with 10^{-4} M HNO_3 capture matrix was performed on the holmium 8-hydroxyquinolinate, holmium acetylacetonate and samarium 8-hydroxyquinolinate compounds with the same irradiation and experimental conditions described in chapter 5.

CHAPTER 4: PRELIMINARY SZILARD-CHALMERS STUDIES

4.1 Introduction

Two sets of experimental conditions were used for the study. The first set of experiments (Chapter 4) were preliminary proof of concept experiments. For these experiments centrifugal filter tubes were used such that the lanthanide containing powder target was placed in the filter compartment and the capture matrix (water) was added to the target, basically sitting on top of the insoluble target. The target in contact with the capture matrix was irradiated (static irradiation). Post irradiation the capture matrix was separated from the target and analyzed for Szilard-Chalmers studies. After success with proof of concept experiments, a second set of experiments (Ch. 5,6 and 7) were conducted using a flow test loop set up at the reactor facility. For the second set of experiments, the irradiation target (lanthanide powder or resin) was placed in a filter compartment, housed in a container connected to a reservoir containing the capture matrix (H_2O or 10^{-4} M HNO_3). During irradiation the target was continuously contacted with fresh capture matrix, post contact the capture matrix was collected and analyzed for Szilard-Chalmers studies. The experimental conditions are further explained in the upcoming sections.

4.2 Pre-irradiation Solubility Tests:

The ideal irradiation target and capture matrix combination is one were the irradiation target is insoluble in the capture matrix. Insolubility of the target in the capture matrix is essential to prevent the transfer of stable isotope to the capture matrix and dilution of the specific activity of the radioisotope product. Therefore solubility studies were essential in determining favorable target and capture matrix combinations.

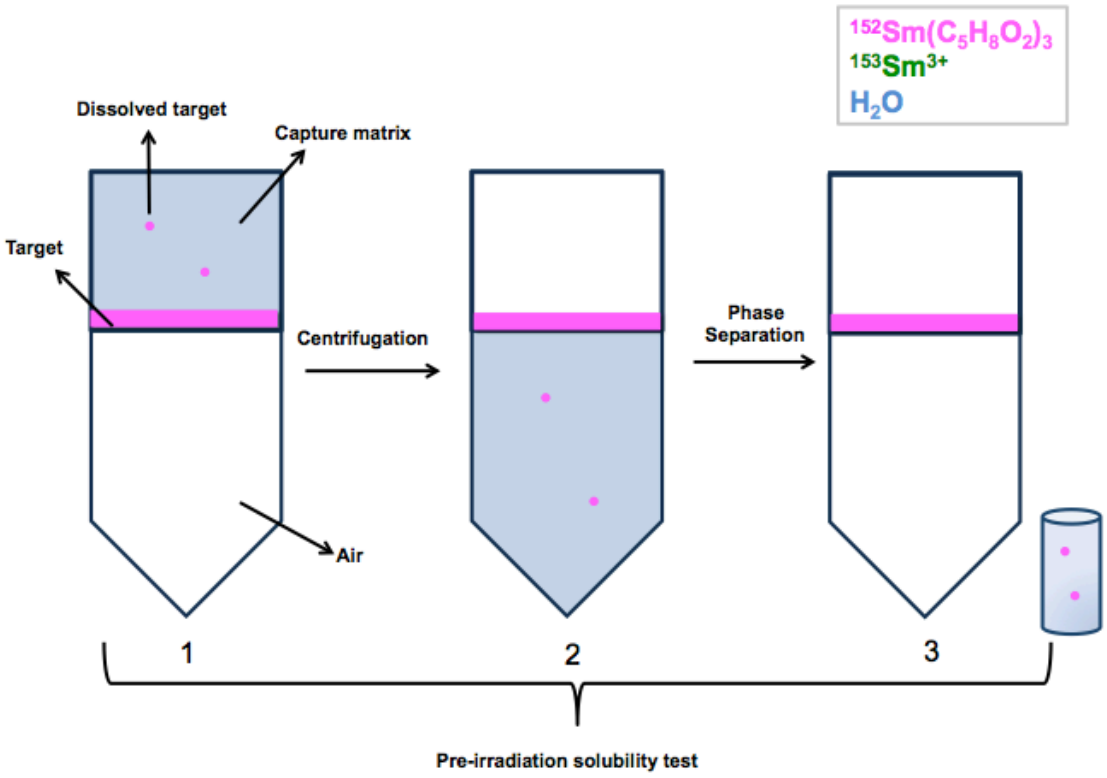

Figure 4.1: Pre irradiation solubility test schematic representation. (1: irradiation target in contact with the capture matrix. 2: irradiation target separated from capture matrix. 3: separated capture matrix analyzed for target solubility).

Prior to irradiation, the solubility of the lanthanide complex in the water capture matrix was determined (Figure 4.1:1,2&3). For this purpose 50-100 mg the lanthanide-containing target solid was thoroughly mixed with 0.5 mL of ultra-high purity H_2O, post contact the solution was separated from the solid using a centrifugal filter tube (EMD Millipore) (Figure 4.2). A second wash of the solid was obtained using the same procedure. The solid and the washes were submitted for neutron activation analysis in order to determine the degree of solubility of the lanthanide target in H_2O.

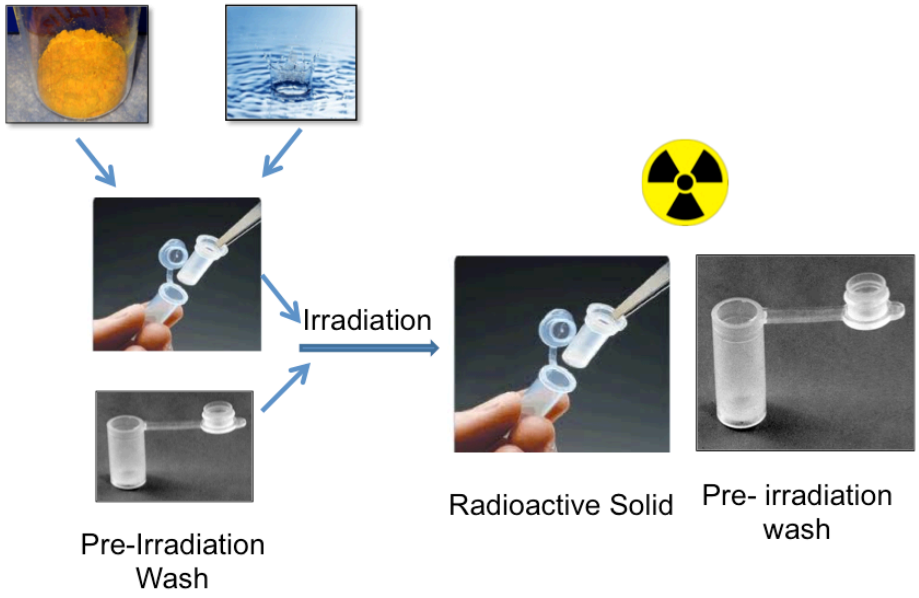

Figure 4.2: Pre-Irradiation solubility test experimental procedure.

4.3 Recoil and Irradiation:

Prior to installation of the unique continuous flow irradiation system at the UC-Irvine TRIGA reactor facility, preliminary studies on the nuclear recoil and the Szilard-Chalmers effect for radiolanthanide production was investigated using the following method: 50-100 mg of the lanthanide-containing target was mixed with 0.5 mL of H_2O on the filter of a centrifugal filter tube (Figure 4.3, Figure 4.4:4). The solid in contact with the water capture matrix was irradiated at the UC-Irvine TRIGA reactor facility for 20 min at the 25 kW power level (neutron flux ~8×10^{10} $n.cm^{-2}.s^{-1}$)

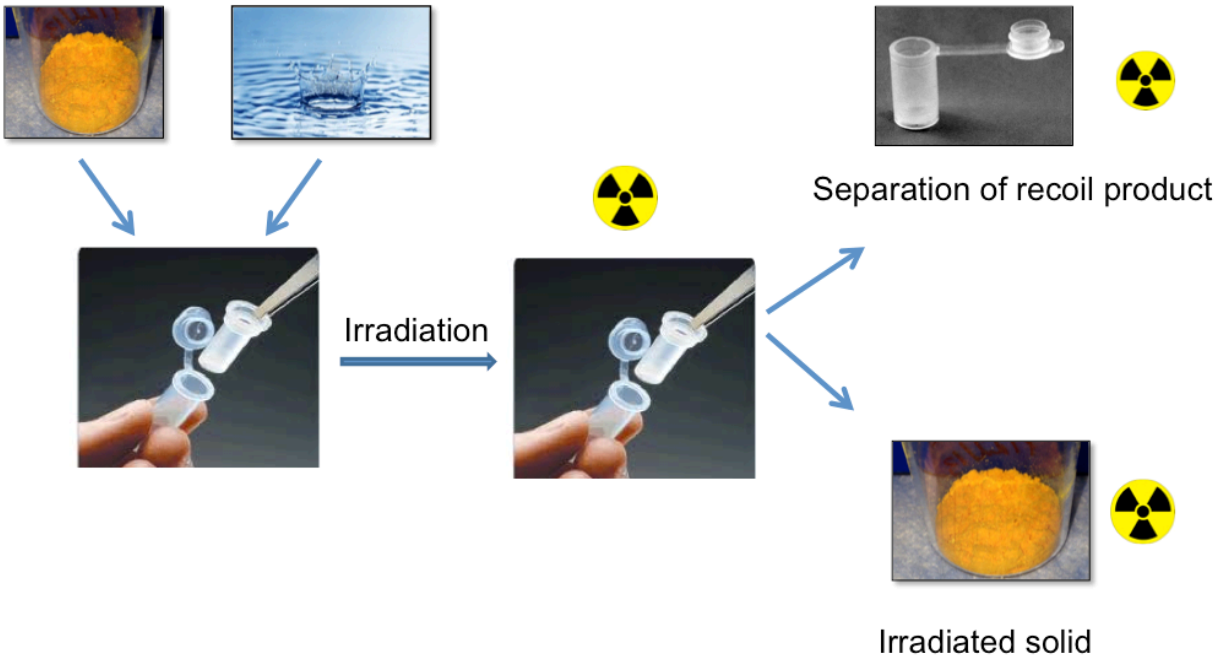

Figure 4.3: Recoil and Szilard-Chalmers studies experimental procedure.

4.4 Post Irradiation Sample Handling:

Post irradiation the samples were left to cool to allow any short-lived radioisotopes to decay before transfer to the laboratory for treatment and analysis. The capture matrix was filtered and separated from the irradiation target in order to separate any recoiled radiolanthanide (Figure 4.4: 4,5&6). The solid irradiation target and the corresponding capture matrix were collected for analysis of the activity of the radiolanthanide of interest. The pre-irradiation solubility test samples along with corresponding calibration standards were also analyzed for radioactive lanthanide content without further treatment. The irradiated samples were analyzed for radiolanthanide activity using an HPGe detector at the representative gamma energy of the radiolanthanide of interest. The ^{153}Sm activity of the samarium samples were measured at the gamma energy of Eγ=103 keV and ^{166}Ho in the holmium samples were measured at Eγ= 81 keV.

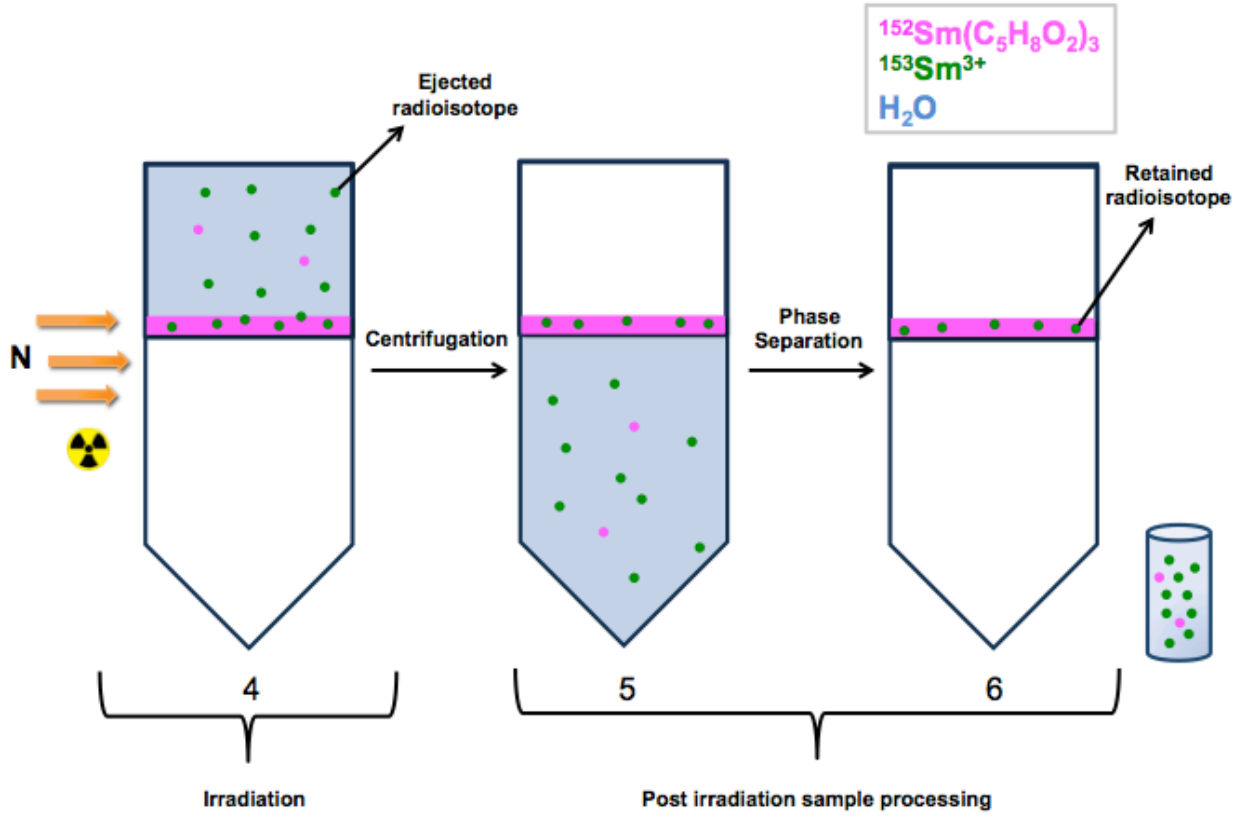

Figure 4.4: Szilard-Chalmers process, separation via solid-liquid extraction. (Irradiation target: Samarium Acetylcaetonate $Sm(C_5H_8O_2)_3$, Capture Matrix: Water. 4: Irradiation target in contact with capture matrix-Neutron activation for Szilard-Chalmers studies. 5: Post irradiation separation of irradiation target and capture matrix. 6: Analysis of the separated capture matrix containing the radioisotope product).

4.5 Determination of Stable Isotope Content in Capture Matrix:

The capture matrices containing radioactive ^{153}Sm and ^{166}Ho were allowed to decay to near background levels and then re-irradiated at the same flux and irradiation time as the initial irradiation in order to determine the stable ^{152}Sm and ^{165}Ho content in the capture matrices and in turn determine the enrichment factors. Thus the activity found after the second irradiation reflects the amount of stable isotope present in the capture matrix. No post treatment of samples was made, and they were analyzed for radiolanthanide activity using the HPGe detector with the same conditions as the samples from the first irradiation.

4. 6 Results and Discussion

Solubility and Recoil of the Lanthanide Complexes:

The percent activities of the nuclide of interest in the different samples (wash, target, capture matrix) are shown in Table 4.1. All the samples for a particular compound were irradiated as a group, along with standards for calibration purposes and direct comparisons of activities. In samples that were not treated post irradiation by separation (e.g. as in the case of target and capture matrix) the activity of the radiolanthanide was directly related to the total concentration of the corresponding lanthanide. The count rate measured in each sample was normalized to a single point in time to account for decay during measurements. Both pre-irradiation washes were determined to give an indication of the solubility of the lanthanide complex in the capture matrix (H_2O). The second wash was obtained to determine if the lanthanide activity detected in the first wash was actually due to solubility of the lanthanide containing target or due to factors such as impurities or the presence of the un-complexed lanthanide that came off in the first wash .The percent activity of the radiolanthanide retained in the solid compound was indicative of the amount of the produced radiolanthanide that did not recoil into the capture matrix and was retained in the target. Radiolanthanides that recoiled out but reformed bonds with the solid compound, or underwent isotopic exchange with the target isotopes would also appear as retained. The percent activity in the capture matrix indicates the amount of radioisotopes transferred to the capture matrix during irradiation that did not reform bonds with the target matrix. Activity in the capture matrix may also reflect dissolution of the target matrix rather than recoil. Samarium acetylacetonate shows slight indication of solubility, which decreases with the second wash. The ^{153}Sm activity detected in the capture matrix indicates the possibility of the Szilard-Chalmers effect and recoil of the target radioisotope into

the capture matrix. Samarium 4-aminobenzoate was soluble in water as was holmium 4-aminobenzoate, with both washes indicating the same amount of solubility; therefore these compounds were not good candidates under the proposed experimental conditions. The samarium and holmium oxalate compounds were found to be insoluble in water with minimal activity detected in both pre-irradiation washes. The majority of activity remained retained in the solid target. The activity detected in the capture matrix was enough to consider samarium or holmium oxalate as potential candidates for further studies of the Szilard-Chalmers reaction with different experimental environments to enhance the recoil effect. The low yield in the capture matrix indicates that the oxalate compounds had either high stability, such that the recoil energy was not capable to overcome the binding energy holding the compound together or that the compounds had fast kinetics such that as soon as the target radioisotope was ejected away from its original position it instantly reformed bonds within the target matrix. The solubility of samarium 8-hydroxyquinolinate in water was low and the retention of the ^{153}Sm in the target was large. The ^{153}Sm activity detected in the capture matrix may be attributed to both solubility and the Szilard-Chalmers effect. Holmium 8-hydroxyquinolinate showed low solubility in the first wash and decreasing solubility in the second wash, with the majority of the activity retained in the target. The ^{166}Ho activity detected in the capture matrix indicates the possibility of recoil of ^{166}Ho from the target into the capture matrix. Between the Sm and Ho compounds tested, samarium acetylacetonate and holmium 8-hydroxyquinolinate showed the highest indication of the Szilard Chalmers effect. Hence, these compounds were chosen for enrichment factor determination.

Table 4.1: Extraction yield and retention values of the studied radiolanthanides in the wash, target and capture matrix.

Compound	% Activity in Wash 1	% Activity in Wash 2	%Activity in Target	% Activity in Capture matrix
Samarium Acetylacetonate	7.0±2.3	2.1±1.3	46.2±7.6	44.7±6.9
Samarium 4-aminobenzoate	27.3±3.0	26.8±2.9	23.0±2.7	22.9±2.6
Samarium Oxalate	<1	<1	98.7±5.4	1.2±0.3
Samarium 8-Hydroxyquinolinate	<1	<1	90.4±9.5	9.2±2.2
Holmium 8-Hydroxyquinolinate	1.4±0.9	<1	93.7±9.5	4.4±1.5
Holmium 4-aminobenzoate	7.0±1.6	7.7±1.7	71.0±6.5	14.3±2.3
Holmium Oxalate	<1	<1	99.7±3.8	<1

Determination of Enrichment Factors:

The irradiated holmium 8-hydroxyquinolinate and samarium acetylacetonate samples were allowed to decay to near background levels, and then re-irradiated at the same flux and irradiation time as the first irradiation for the purpose of determining the enrichment factors (Eq. 4.1). No post-treatment of the samples were made, as the aim was to determine the amount of ^{152}Sm or ^{165}Ho in the samples, respectively. Thus, the activity found after the second irradiation would reflect the amount of non-radioactive (target) lanthanide isotopes found in the capture matrix. If the re-irradiation produces the same number of radioisotopes in the capture matrix as the first irradiation, i.e. $^{A+1}_{Z}\mathrm{X}(1\text{st irradiation}) = {}^{A+1}_{Z}\mathrm{X}(2\text{nd irradiation})$, then there was no isotope enrichment and the activity from the first irradiation was from the dissolution and/or

degradation of the target matrix. The assumption is that the target isotope (^{152}Sm or ^{165}Ho) was not consumed to any significant degree during the irradiation. On the other hand if ${}^{A+1}_{Z}\mathrm{X}(\text{1st irradiation}) > {}^{A+1}_{Z}\mathrm{X}(\text{2nd irradiation})$ radioisotope enrichment has occurred. In this case the radioisotopes in the capture matrix from the first irradiation are due to the Szilard-Chalmers reaction and not activation of cold atoms present in the capture matrix due to either solubility or degradation of the target in the capture matrix. Equation 4.1 was used to determine the enrichment factor (EF) such that if the ratio of produced radioisotopes ${}^{A+1}_{Z}\mathrm{X}$ to the number of the inactivated target isotopes ${}^{A}_{Z}\mathrm{X}$ in the capture matrix was greater than the number of radioisotopes produced ${}^{A+1}_{Z}\mathrm{X}$ to the number of inactive target isotopes ${}^{A}_{Z}\mathrm{X}$ in the target (i.e. $\frac{{}^{A+1}_{Z}\mathrm{X}(\text{capture matrix})}{{}^{A}_{Z}\mathrm{X}(\text{capture matrix})} > \frac{{}^{A+1}_{Z}\mathrm{X}(\text{target})}{{}^{A}_{Z}\mathrm{X}(\text{target})}$) enrichment of the radioisotope has occurred by the Szilard Chalmers Reaction.

$$\text{Enrichment Factor (EF)} = \frac{{}^{A+1}_{Z}\mathrm{X}(\text{capture matrix})}{{}^{A}_{Z}\mathrm{X}(\text{capture matrix})} \Big/ \frac{{}^{A+1}_{Z}\mathrm{X}(\text{target})}{{}^{A}_{Z}\mathrm{X}(\text{target})} \qquad \text{Eq. 4.1}$$

An EF >1 indicates that the ratio of ${}^{A+1}_{Z}\mathrm{X}/{}^{A}_{Z}\mathrm{X}$ was higher in the capture matrix than in the target matrix, therefore the specific activity was enhanced and there was indication of radioisotope enrichment. The enrichment factors for samarium acetylacteonate and holmium 8-hydroxyquinolinate are summarized in the following table (Table 4.2).

Table 4.2: Maximum Lanthanide Enrichment Factors.

Compound	**Enrichment factor**
Samarium acetylacetonate	1.19
Holmium 8-hydroxyquinolinate	1.51

4.7 Conclusions

The results showed potential for enhancing the specific activity of radiolanthanides using a small- scale research reactor. The proposed simple production route of radiolanthanides using the Szilard-Chalmers method resulted in an enrichment factor of 1.51 for ^{166}Ho compared to irradiating without a capture matrix. This corresponds to a decrease of 34% in the amount of holmium needed for a typical medical procedure. Although this is a modest decrease, it is a step in the right direction. The low enrichment factor could be attributed to the following: (i) degradation of the target as a result of exposure to ionizing radiation during the irradiation, leading to break-down of the target and release of the stable isotope into the capture matrix and hence lower enrichment factors; (ii) delay in separating the irradiated target from the capture matrix leading to the recoiled atom having time to reform its original bonds or possibly isotopic exchange with the stable isotope (iii) unfavorable location of the recoiling atom in the target; the recoil energy may be enough to eject the radioisotope but the radioisotope may not reach the capture matrix leading to further retention of the radiolanthanide in the target.

The re-irradiation method used for stable isotope determination was not the most accurate and ideal method because the exact irradiation conditions, as the first irradiation cannot be achieved. Factors such as prior reactor use, neutron flux fluctuations, fuel burn up and reactor operator performance are among conditions that influence the irradiation conditions.

CHAPTER 5: CONTINUOUS FLOW/SZILARD-CHALMERS RADIOISOTOPE PRODUCTION

5.1 Introduction

The proposed experimental conditions in chapter 4 resulted in enrichment factors that corresponded to an average decrease of 34% in the amount of lanthanide needed for a typical medical procedure. Following the preliminary proof of concept experiments, the irradiation setup was enhanced in order to further optimize the enrichment factors and experimental conditions in addition to addressing some of the challenges encountered in the previous chapter, that lead to low enrichment factors. The proposed set up was such that the capture matrix flowed through the target continuously during irradiation and was then collected outside of the reactor core. The continuous flow instantaneously separated any radioisotope that had recoiled into the capture matrix, preventing potential, recombination, retention, isotopic exchange with the original target and successive neutron capture of the product radioisotope. Furthermore the setup was such that the irradiation target was placed in a filtering compartment, which allowed the capture matrix to filter out in all directions. Therefore the capture matrix was continuously contacted with the target material and filtered out through the bottom or sides of the filter unit, resulting in a higher concentration of separated radioisotopes (Figure 5.1). In chapter 4, the stable isotope content was determined by re-irradiation of the target and capture matrix with the same conditions as the first irradiation, this method proposed some complications. To address the issue an inductively coupled plasma mass spectrometer (ICP-MS Agilent 7500 CX, Software: Mass Hunter work station) was purchased for stable isotope analysis of the target and capture matrix.

In the previous setup (Ch. 4), the capture matrix was directly in contact with the top layer of the target (Figure 4.4:4), therefore the recoil range of the radioisotopes in the lower layers of the target was not enough to eject the radioisotope into the capture matrix to be separated, leading to low enrichment factors.

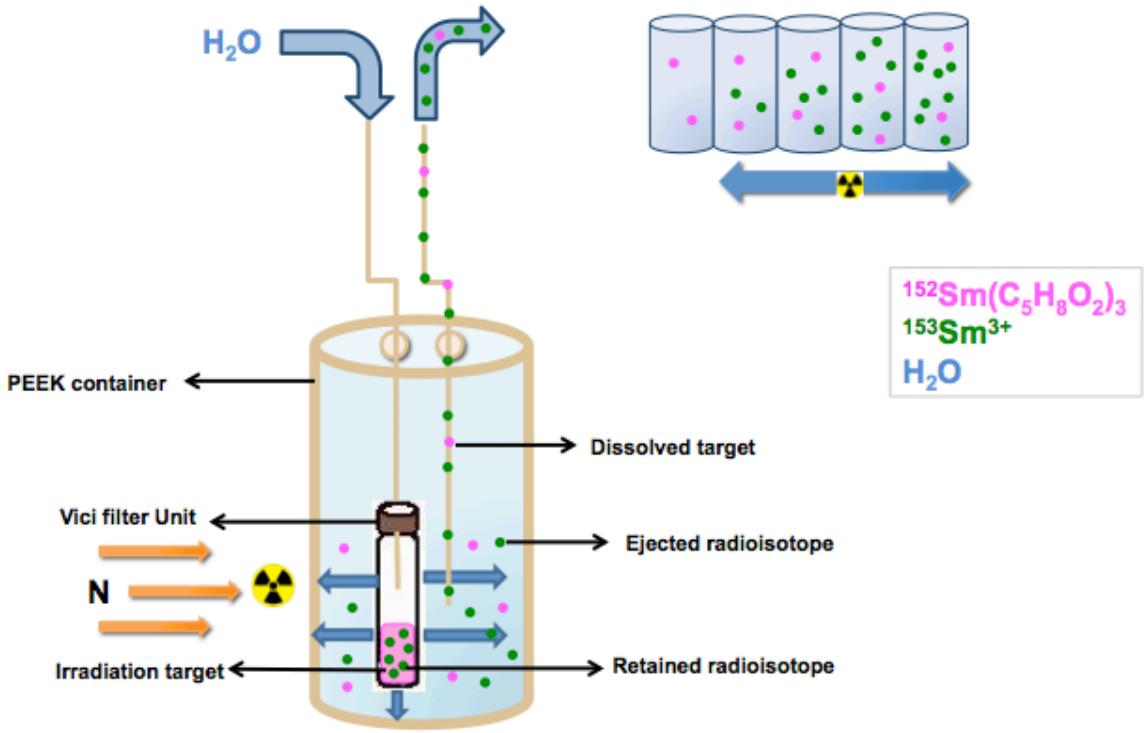

Figure 5.1: Illustration of the continuous flow process for radioisotope production and separation.

5.2 Experimental Setup

The experimental setup (Figure 5.1 & 5.2) consisted of a mobile phase filter (VICI) compartment holding the lanthanide target that was housed in a PEEK material container. The PEEK container had an inlet port that connected the filter compartment directly to a continuous fluid pump (LabAlliance, Series 1 pump), which continuously pumped the capture matrix through the target. The container had a separate outlet port that terminated in a collection reservoir and allowed sample collection. The PEEK container system was used for both pre-

irradiation solubility tests and recoil/irradiation studies in addition to post irradiation monitoring of the solid/capture matrix system. For irradiation purposes the setup included a hollow aluminum tube, also known as the flow loop terminus (FLT) that terminated in the outer ring position of the UC-Irvine TRIGA® reactor core (Figure 5.3).

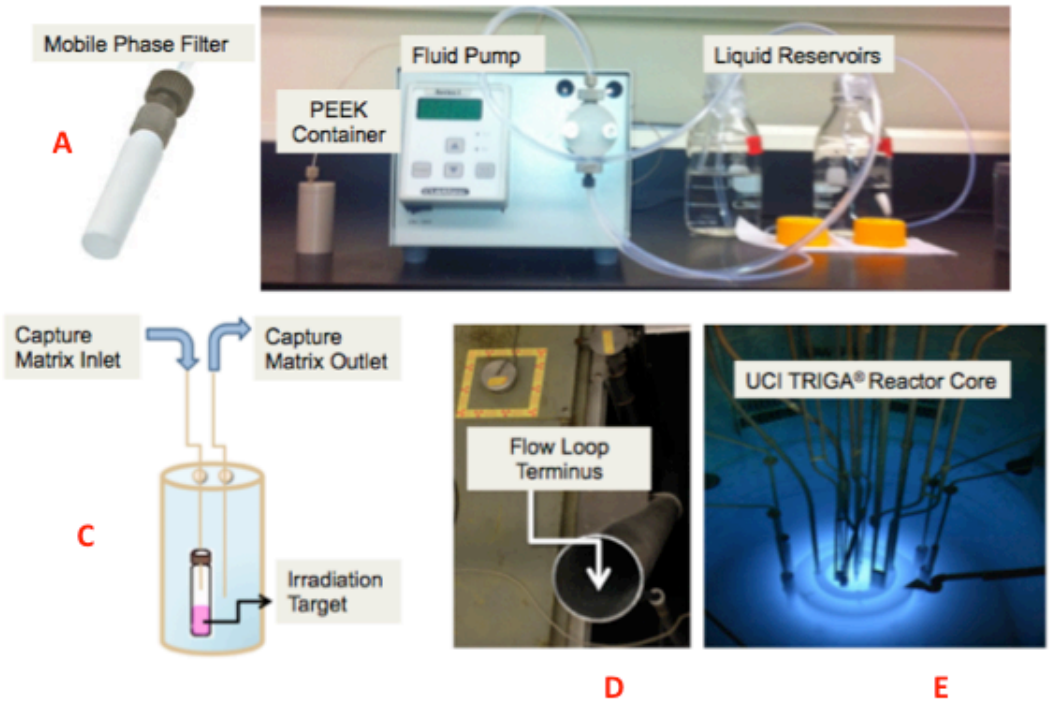

Figure 5.2: Experimental Setup for Continuous Irradiation and Separation of Recoil Product at UC-Irvine TRIGA ® Reactor. Fig. 5.2A-5.2E depict the embodiment of the experimental setup for a continuous-flow Szilard-Chalmers reaction. Fig. 5.2A is a perspective view of a mobile-phase filter for containing a target. Fig. 5.2B is a picture of the PEEK container with fluid pumps and liquid reservoirs for continuous-flow of the capture matrix. Fig. 5.2C is a diagram of the experimental setup for the continuous-flow Szilard-Chalmers reaction. Fig. 5.2D is a picture of the flow loop terminus exiting the reactor. Fig. 5.2E is a picture of the reactor core in the continuous-flow Szilard-Chalmers reaction setup.

For irradiation studies the PEEK container and the tubing associated with the system was lowered into the 20 ft long hollow aluminum tube (flow loop terminus) that terminated in core as a hollow fuel element located in core position G-28, with the PEEK container resting on the axial centerline of the core (Figure 5.3). During irradiation the lanthanide target was continuously

contacted with fresh capture matrix, post contact the capture matrix containing the recoiled ionic radionuclide was collected in sample vials surrounded by shielding. The setup allowed instantaneous separation of the capture matrix containing the recoiled nucleus from the bulk of the inactive material during irradiation. The rapid separation of the recoiled nucleus prevents it from reforming its original bonds with the target matrix and therefore prevents retention of the radionuclide in the irradiation target.

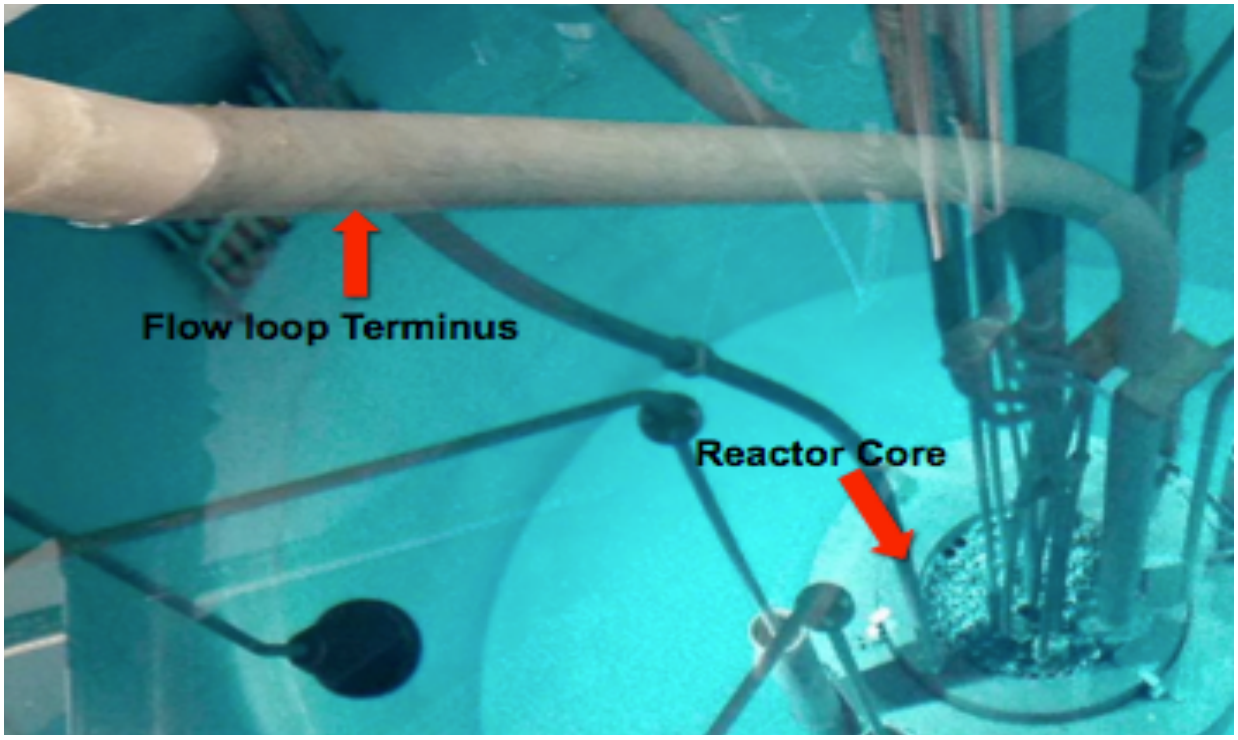

Figure 5.3: Flow loop terminus setup at the UC-Irvine TRIGA reactor.

5.3 Pre-irradiation Solubility Tests:

As previously mentioned the irradiation target should be insoluble in the capture matrix of choice. The solubility of each lanthanide-containing target was determined prior to each irradiation. The capture matrix was contacted with the lanthanide-containing target prior to insertion of the sample into the reactor core for irradiation. The samples were collected in two-

minute intervals and the pump was set to 3 ml/min. Post collection the samples were analyzed for the concentration of the stable lanthanide isotope using ICP-MS analysis (Figure 5.4).

5.4 Recoil and Irradiation Studies:

For the purpose of investigating the Szilard-Chalmers effect and recoil characteristics of the neutron activated lanthanide nucleus, the PEEK/Filter setup and sample used in the pre-irradiation solubility test was lowered into the reactor core and exposed to a specific neutron flux (20 min at the 75 kW power level, neutron flux ~2.5×10^{11} $n.cm^{-2}.s^{-1}$) for a predetermined amount of time, which was dependent on the lanthanides cross section, half-life and natural abundance. During irradiation fresh capture matrix flowed through the filter compartment containing the irradiation target, and was continuously contacted with the target at a rate of 3 ml/min. Post contact, the capture matrix containing the recoiled ionic radionuclide was collected in 2-minute intervals within appropriate shielding. Post irradiation, sample collection continued for a predetermined amount of time to ensure all capture matrix contacted with the irradiation target during irradiation was collected in addition to looking into post irradiation effects.
During each irradiation a set of lanthanide standards were also prepared and simultaneously irradiated in the lazy Susan for calibration and comparison purposes.

Post Irradiation Studies:

Post irradiation, 1 mL of each sample was transferred to a vial and analyzed for the radioactive isotope concentration using a high purity germanium detector (HPGe) at the representative gamma energy of the radioisotope (Figure 5.4). The lanthanide standards irradiated in the lazy Susan were also analyzed by the same technique. The HPGe detector was calibrated for efficiency, therefore using the detector efficiency and the count rate of each sample, the radioisotope activity and in turn the amount of radioisotope collected in each sample

was calculated. The collected samples were left to further decay to near background levels before being analyzed for stable isotope concentration using ICP-MS analysis. Each sample collected pre-irradiation, during irradiation and post irradiation were diluted by a factor of 100 using 2% nitric acid and analyzed alongside calibration standards for stable isotope concentration (Figure 5.4). For the determination of stable isotope concentration in the irradiation target, 10-50 milligrams of the target was dissolved and further diluted using nitric acid and analyzed alongside the other samples.

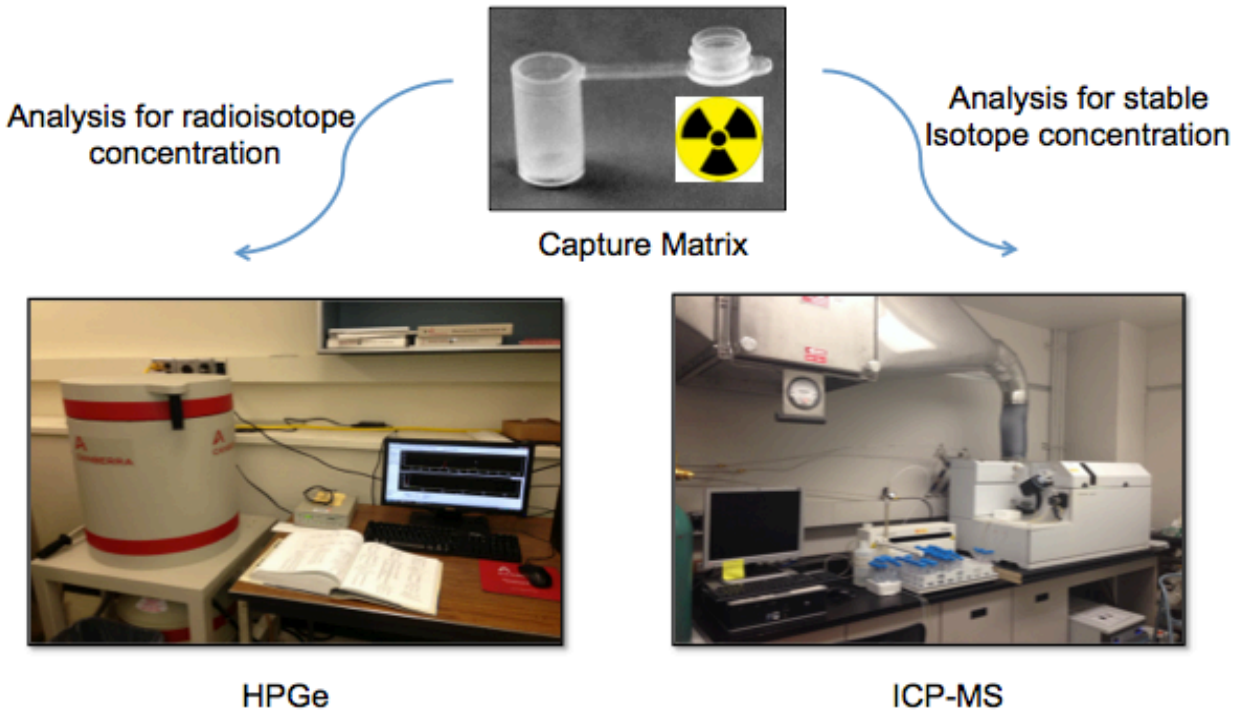

Figure 5.4: Capture matrix analysis for stable and radioisotope content.

5.5 Results and Discussion:

The following holmium compounds: HoAcAc, Ho8HQ were chosen as irradiation targets. HoAcAc and Ho8HQ were in powder form; the capture matrix used was ultrapure water (18.2 MΩ). The HoAcAc, Ho8HQ target and H_2O capture matrix combination resulted in the release of 7.83% and 1.99% respectively of the total stable ^{165}Ho isotope initially present in the

target into the H_2O capture matrix. In terms of radioisotope content separated via the capture matrix, in the HoAcAc irradiation 36.60% of the total ^{166}Ho radioisotope produced was found in the capture matrix. The Ho8HQ irradiation resulted in the separation of 6.29% of the total ^{166}Ho radioisotope produced, via the capture matrix.

The following table (5.1) summarizes the results of the pre, during and post irradiation behavior of the target with respect to the capture matrix of choice and irradiation conditions.

Table 5.1: Experimental results regarding holmium stable and radioisotope content as a result of the continuous flow setup.

Target	**HoAcAc**	**Ho8HQ**
Capture Matrix	H_2O	H_2O
Initial ^{165}Ho stable atoms in target pre-irradiation	2.77E+19	4.38E+19
Total ^{165}Ho stable atoms collected in capture matrix during irradiation	2.17E+18	8.71E+17
Total ^{165}Ho stable atoms remaining in target	2.56E+19	4.29E+19
Total ^{166}Ho radioactive atoms collected in capture matrix	2.70E+09	1.88E+10
Total ^{166}Ho radioactive atoms remaining in target	4.67E+09	2.79E+11
% Total radioactive ^{166}Ho found in capture matrix	36.60	6.29
% Total stable ^{165}Ho found in capture matrix	7.83	1.99
Highest Enrichment Factor	14.83	11.26

The following Samarium compounds: SmAcAc and Sm8HQ were chosen as irradiation targets. SmAcAc and Sm8HQ were both in powder form and the capture matrix used was water.

The SmAcAc, Sm8HQ target and H_2O capture matrix combination resulted in the release of 9.66% and 24.63% respectively of the total stable ^{152}Sm isotope initially present in the target into the H_2O capture matrix. In terms of radioisotope content separated via the capture matrix, from the SmAcAc irradiation 20.00% of the total ^{153}Sm radioisotope produced was found in the capture matrix. The Sm8HQ irradiation resulted in the separation of 67.23% of the total ^{153}Sm radioisotope produced via the capture matrix.

The following Table (5.2) summarizes the results of the pre, during and post irradiation behavior of the target with respect to the capture matrix of choice and irradiation conditions.

Table 5.2: Experimental results regarding samarium stable and radioisotope content as a result of the continuous flow setup.

Target	**SmAcAc**	**Sm8HQ**
Capture Matrix	H_2O	H_2O
Initial ^{152}Sm stable atoms in target pre-irradiation	1.76E+19	9.71E+17
Total ^{152}Sm stable atoms collected in capture matrix during irradiation	1.70E+18	2.39E+17
Total ^{152}Sm stable atoms remaining in target	1.59E+19	7.32E+17
Total ^{153}Sm radioactive atoms collected in capture matrix	2.57E+10	2.12E+09
Total ^{153}Sm radioactive atoms remaining in target	1.03E+11	1.03E+09
% Total radioactive ^{153}Sm found in capture matrix	20.00	67.23
% Total stable ^{152}Sm found in capture matrix	9.66	24.63
Highest Enrichment Factor	3.56	11.19

Figures 5.5-5.8 illustrate the stable isotope ($^{A}X=^{152}$Sm or ^{165}Ho) content found in the capture matrix pre, during and post irradiation (light blue) and the radioisotope ($^{A+1}X=^{153}$Sm or ^{166}Ho) content found in the capture matrix during and post irradiation (dark blue) for HoAcAc, Ho8HQ, SmAcAc and Sm8HQ respectively. Each data point on the graph resembles a sample collected for two minutes. The capture matrix samples collected pre-irradiation, before green mark, were only analyzed for stable isotope content, the samples collected after the green mark were analyzed for both stable and radioisotope content.

In the samples collected pre-irradiation (before lowering the sample into the reactor core, samples before green marker) the stable isotope content (light blue) was indicative of the solubility of the lanthanide target in the water capture matrix. The lanthanide targets tested, all showed similar behavior and trends in pre-irradiation solubility tests, irradiation, and post irradiation studies. The stable isotope concentration in the samples collected during irradiation (samples between green and red marker) was indicative of solubility or release of the stable isotope into the capture matrix as a result of breakdown of the target due to exposure to gamma irradiation while in the reactor core.

With respect to the data obtained for the lanthanide compounds tested, there was indication of radioisotope enrichment compared to the stable isotope. The pre-irradiation solubility tests exhibited the presence of the stable isotope in the capture matrix (Figures 5.5-5.8). The stable isotope concentration was higher in the first few samples collected pre-irradiation most likely due to the presence of impurities and any un-complexed lanthanide that washed out in the first few samples. The stable isotope concentration decreased with the progression of sample collection and remained relatively stable for the samples collected during irradiation, indicating a steady concentration of stable isotope was released into the capture matrix due to factors such as degradation of the target as a result of ionizing radiation that occurs during neutron irradiation. During irradiation while the stable isotope concentration remained relatively stable, the radioisotope concentration increased with increasing irradiation time and reached a maximum, and decreased after the reactor scrammed (Figures 5.5-5.8). Post reactor scram (samples collected after the red marker) there was a gradual decrease in radioisotope concentration, as expected since the target was no longer exposed to a neutron flux.

With respect to Figures 5.5-5.8 it can be seen that the radioisotope content (dark blue marker) increases with irradiation time and decreases as expected post irradiation. Comparing the samples collected during irradiation for stable isotope and radioisotope concentration it can be seen that the radioisotope content is increasing while the stable isotope concentration remains relatively constant, which is indicative of enrichment of the radioisotope. The radiolanthanide content detected in each sample indicates the possibility of recoil and capture of the radioisotope by the capture matrix. The activity may also be partially contributed to the activation of stable isotope present in the capture matrix due to break down or solubility of the lanthanide target and release of the stable isotope into the capture matrix during irradiation.

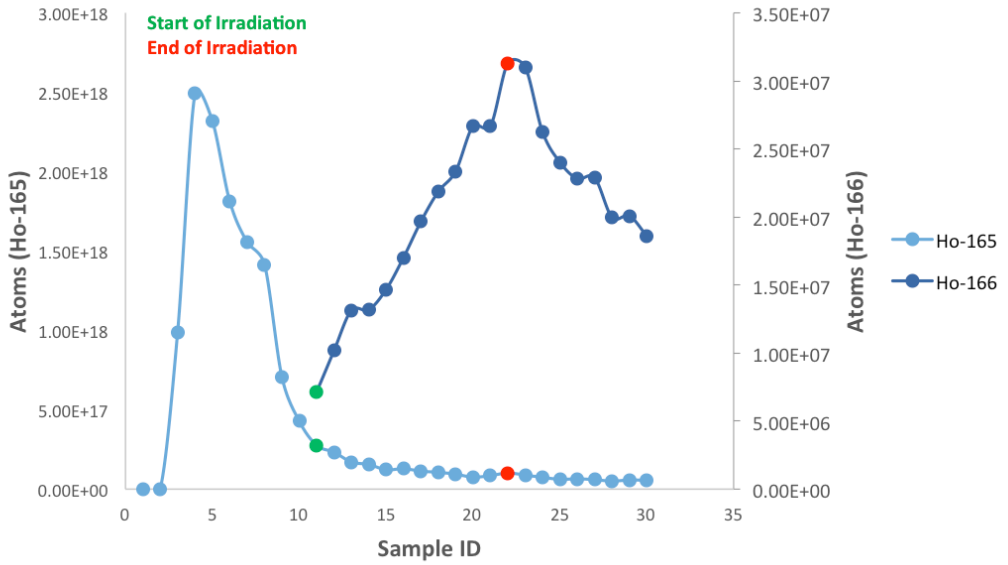

Figure 5.5: Holmium acetylacetonate target and water capture matrix. Stable Isotope (light blue) and Radioisotope (dark blue) behavior via the Szilard-Chalmers process coupled with the continuous flow setup.

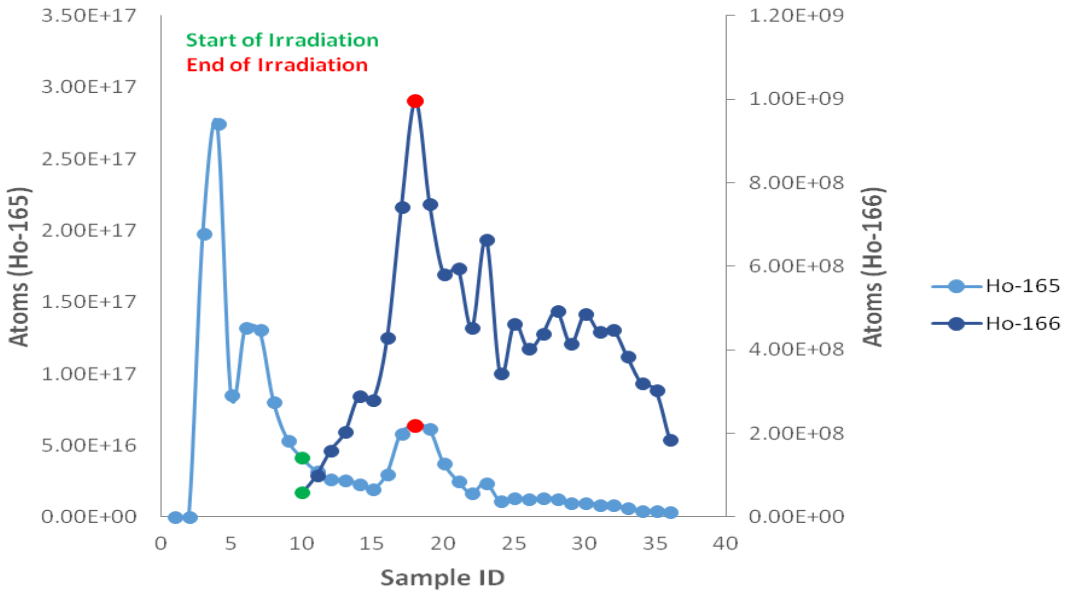

Figure 5.6: Holmium 8-hydroxyquinolinate target and water capture matrix. Stable Isotope (light blue) and Radioisotope (dark blue) behavior via the Szilard-Chalmers process coupled with the continuous flow setup.

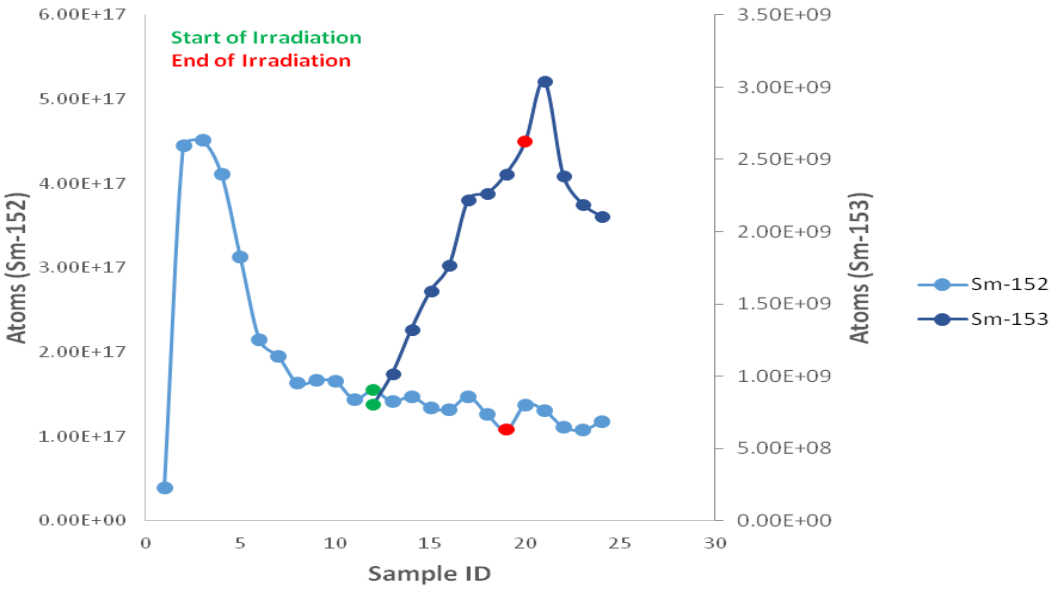

Figure 5.7: Samarium Acetylacetonate target and water capture matrix. Stable Isotope (light blue) and Radioisotope (dark blue) behavior via the Szilard-Chalmers process coupled with the continuous flow setup.

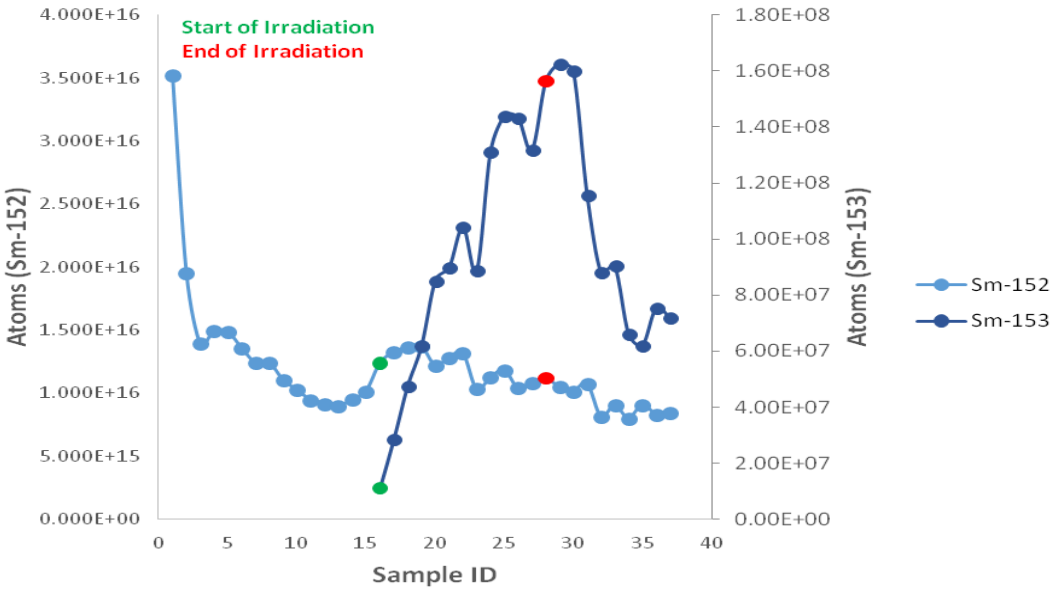

Figure 5.8: Samarium 8-Hydroxyquinolinate target and water capture matrix.
Stable Isotope (light blue) and Radioisotope (dark blue) behavior via the Szilard-Chalmers process coupled with the continuous flow setup.

With respect to the data obtained from ICP-MS and HPGe analysis of the samples and corresponding lanthanide irradiation targets, the enrichment factors were determined. The

enrichment factors were calculated using the same equations as in chapter 4 (Eq. 4.1) the enrichment factor for each sample collected was calculated. The maximum enrichment factors for the compounds tested are reported in Table 5.3.

Table 5.3: Summary of maximum enrichment factors for lanthanide compounds.

Target Compound	Radioisotope	Enrichment Factor
Holmium8-hydroxyquinolinate	^{166}Ho	11.26
Holmiumacetylacetonate	^{166}Ho	14.83
Samarium8-hydroxyquinolinate	^{153}Sm	11.19
Samariumacetylacetonate	^{153}Sm	3.56

With respect to Table 5.3 the holmium salts of acetylacetonate and 8-hydroxyquinolinate had higher enrichment factors compared to the samarium salts of acetylacetonate and 8-hydroxyquinolinate. Differences such as number and intensity of emitted prompt gamma rays and variations in recoil energy, cation radii and electronic configuration between holmium and samarium can all be contributing factors to the difference in enrichment factors between the same compounds of samarium and holmium under investigation.

The stability of the tested compounds may also be a contributing factor to the enrichment factors obtained. The stability constant is a measure of the degree of association between the lanthanide and the ligand. Larger stability constants result in a greater degree of stability of the complex and in turn ability to maintain its integrity when exposed to various conditions. Ho8HQ and Sm8HQ had similar literature values for cumulative stability constants (Table 3.2), 27.96 and 27.21 and similar enrichment factors 11.26 and 11.19 respectively. Higher stability of the compounds results in less break-down of the stable compound in the capture matrix and higher enrichment factors.

SmAcAc had the lowest stability constant (12.23) that could be a contributing factor resulting in the low enrichment factor (3.56) obtained compared to other compounds tested.

The results from the HoAcAc compound did not match the prediction of larger stability constant results in greater enrichment factors. HoAcAc had a lower stability constant (14.13) compared to Ho8HQ and Sm8HQ and a higher enrichment factor (14.83). To further verify the results for HoAcAc the experiment needs to be repeated. Also for future consideration, to verify the relationship between stability constants and enrichment factors, the stability constants should be obtained under similar experimental conditions to what was used throughout the study and compared to the literature values obtained. Kinetics also plays a role in enrichment factors, such that if a lanthanide-ligand combination has fast kinetics, it can contribute to lower enrichment factors. The fast kinetics can contribute to a higher probability of recombination of the recoiled radioisotope with the original compound ligands, resulting in retention. Therefore in addition to thermodynamic stability, kinetic stability is also a contributing factor to the degree of enrichment of the radioisotope of interest.

5.6 Conclusions

In the case of Ho8HQ and SmAcAc with enrichment factors of 11.26 and 3.56 respectively, there was a substantial improvement compared to our preliminary studies performed were the enrichment factors were 1.51 and 1.19 respectively [1]. For example an enrichment factor of 11.26 for Ho8HQ and 3.56 for SmAcAc results in 91% and 72% decrease in the amount of holmium and samarium needed for a typical medical procedure respectively. Although there has been considerable improvement in enrichment factors compared to our preliminary studies, the obtained enrichment factors need to be further improved for medical application. In order to obtain higher enrichment factors for the samarium and holmium, studies on alternative capture matrices and irradiation targets were carried out.

CHAPTER 6: CONTINUOUS FLOW/SZILARD-CHALMERS RADIOISOTOPE PRODUCTION WITH LOWER pH CAPTURE MATRIX

6.1 Introduction

Lanthanides are known to hydrolyze in the pH range of 6-7 [106,107]. Hydrated lanthanide cations can act as Bronsted acids by release of a proton from the bound water molecule, forming hydroxo complexes[108]. To prevent potential formation of lanthanide oxide/hydroxide precipitate due to hydrolysis of the metal ion[105], a capture matrix with lower pH (4 or less) was considered.

6.2 Experimental Procedures

For this purpose the chosen capture matrix was 10^{-4} M HNO_3 (pH=4) and the three irradiation targets from chapter 5 with the highest enrichment factors (HoAcAc, Ho8HQ and Sm8HQ) were chosen for experimental purposes and study of the Szilard-Chalmers effect with a lower pH capture matrix.

The experiments and analysis were carried out in the same manner as in chapter 5 using the continuous flow loop setup, only differing by the capture matrix used.

6.3 Results and Discussion

The HoAcAc, Ho8HQ target and 10^{-4} M HNO_3 capture matrix combination resulted in the release of 17.50% and 4.21% of the total stable ^{165}Ho isotope initially present into the capture matrix, which was an increase compared to when water was the capture matrix, and 7.83% and 1.99% of the total stable holmium isotope initially present in the HoAcAc and Ho8HQ targets were released respectively. For the holmium compounds tested, the increase in stable isotope was more significant compared to the increase in radioisotope content using the lower pH capture matrix therefore resulting in lower enrichment factors.

The Sm8HQ compound resulted in a lower percentage of stable isotope (15.42%) and lower percentage of radioisotope (14.79%) found in the 10^{-4}M HNO_3 capture matrix, compared to when water was used as the capture matrix, were 24.63% of the total stable isotope present in the target and 67.23% of the total radioisotopes produced was released in the capture matrix. Therefore due to the substantially lower radioisotopes released in the capture matrix, lower enrichment factors were obtained compared to when water was the capture matrix of choice. The following Table 6.1 summarizes the results of the pre, during and post irradiation behavior of the target with respect to the capture matrix of choice and irradiation conditions.

Table 6.1: Experimental results regarding stable and radioisotope content as a result of the continuous flow setup using 10^{-4}M HNO_3 as the capture matrix. ($^{A}X=^{152}Sm$ or ^{165}Ho, $^{A+1}X=^{153}Sm$ or ^{166}Ho)

Target	**HoAcAc**	**Ho8HQ**	**Sm8HQ**
Capture Matrix	10^{-4}M HNO_3	10^{-4}M HNO_3	10^{-4}M HNO_3
Initial ^{A}X stable atoms in target pre-irradiation	3.09E+19	4.38E+19	1.70E+18
Total ^{A}X stable atoms collected in capture matrix during irradiation	5.40E+18	1.84E+18	2.62E+17
Total ^{A}X stable atoms remaining in target	2.55E+19	4.19.E+19	1.44E+18
Total ^{A+1}X radioactive atoms collected in capture matrix	1.79E+10	1.19E+10	8.02E+10
Total ^{A+1}X radioactive atoms remaining in target	2.70E+10	8.23E+10	4.62E+11
% Total radioactive ^{A+1}X found in capture matrix	39.92	12.64	14.79
% Total stable ^{A}X found in capture matrix	17.50	4.21	15.42
Highest Enrichment Factor	6.05	4.54	1.37

Figures 6.1-6.3 illustrate the stable isotope content (^{A}X) found in the capture matrix pre, during and post irradiation (light blue) and the radioisotope content (^{A+1}X) found in the capture matrix during and post irradiation (dark blue) for HoAcAc, Ho8HQ and Sm8HQ respectively. The general trend for the samples collected during irradiation in chapter 5 was that during irradiation the stable isotope content remained relatively stable while the radioisotope content was increasing, that trend was not necessarily observed in this section. For HoAcAc and Sm8HQ (fig. 6.1 and 6.3) it can be seen that the stable isotope content varies from sample to sample during irradiation and does not appear stable during irradiation as it did in chapter 5. The Ho8HQ target

agreed more closely to the Ho8HQ results from chapter 5, were the stable isotope content remained relatively stable during irradiation, while the radioisotope content was continuously increasing.

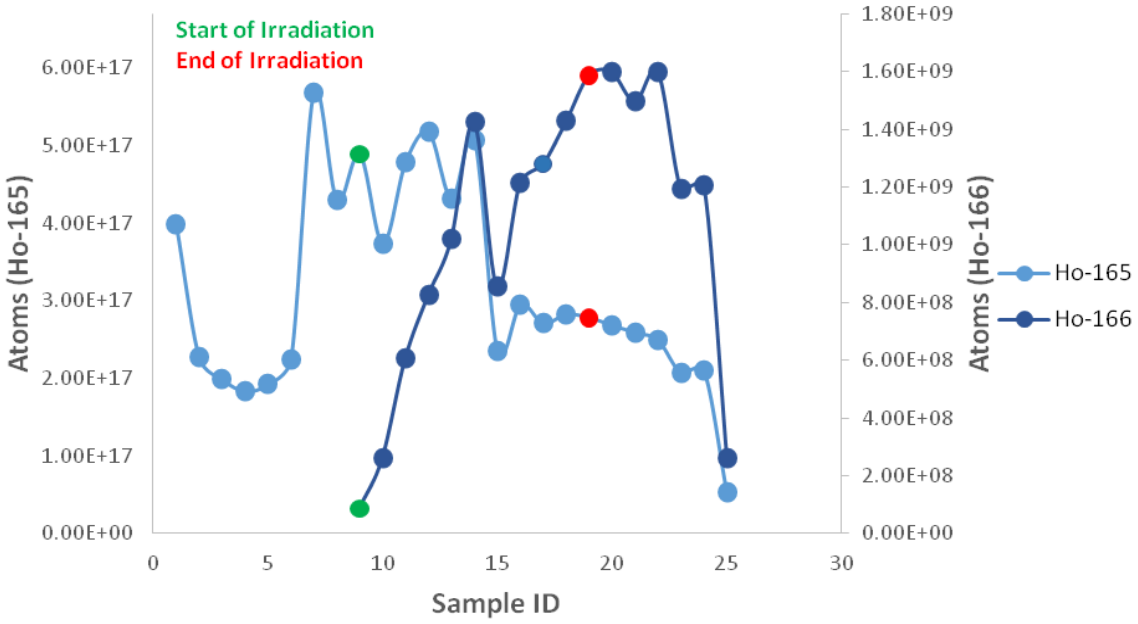

Figure 6.1: Holmium Acetylacetonate target and 10^{-4}M HNO_3 capture matrix. Stable Isotope (light blue) and Radioisotope (dark blue) behavior via the Szilard-Chalmers process coupled with the continuous flow setup.

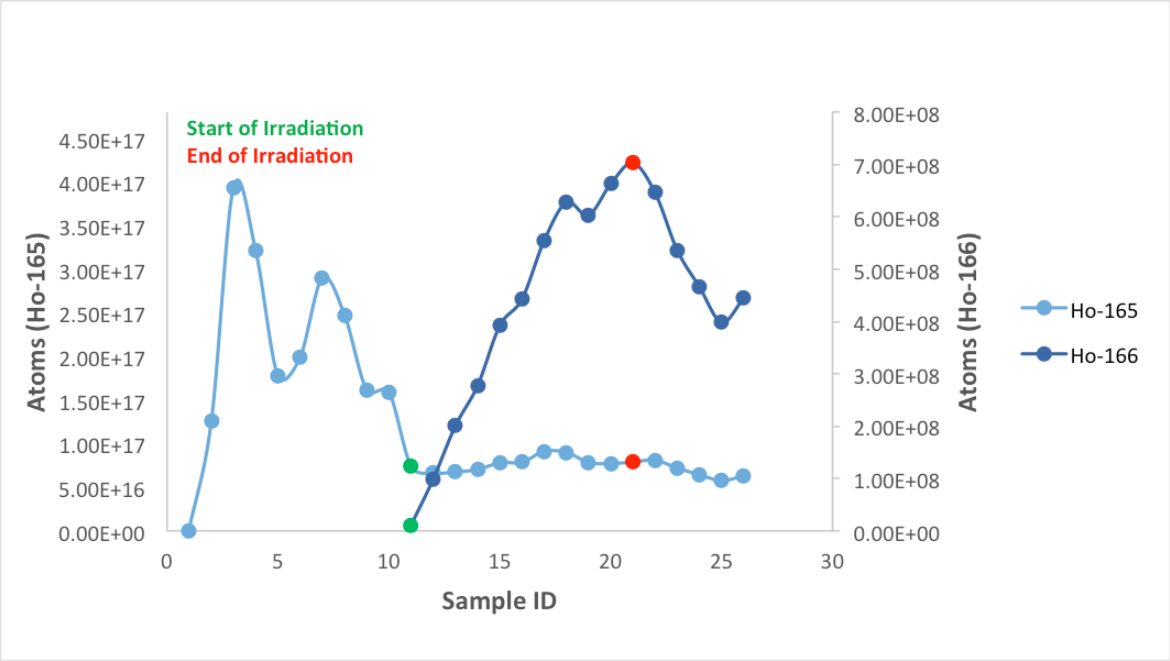

Figure 6.2: Holmium 8-Hydroxyquinolinate target and 10^{-4}M HNO_3 capture matrix. Stable Isotope (light blue) and Radioisotope (dark blue) behavior via the Szilard-Chalmers process coupled with the continuous flow setup.

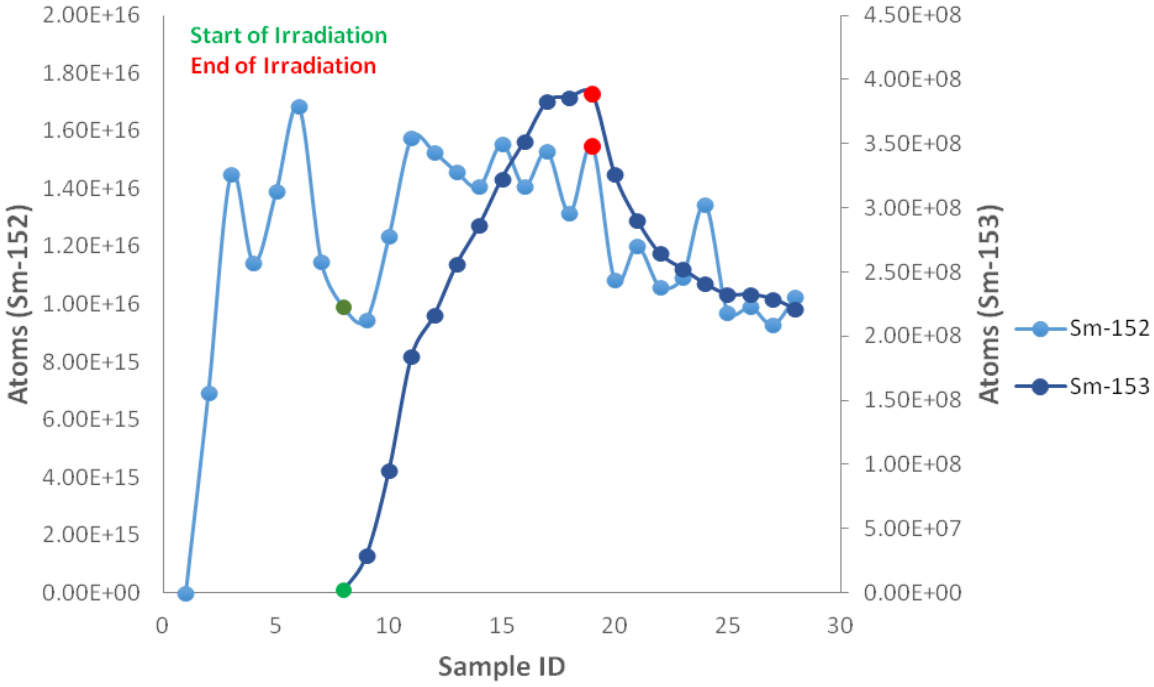

Figure 6.3: Samarium 8-hydroxyquinolinate target and 10^{-4}M HNO_3 capture matrix. Stable Isotope (light blue) and Radioisotope (dark blue) behavior via the Szilard-Chalmers process coupled with the continuous flow setup.

With respect to the data obtained from ICP-MS and HPGe analysis of the samples and corresponding lanthanide irradiation targets, the enrichment factors were determined. The enrichment factors were calculated using the same equations as chapter 4 (Eq. 4.1). The maximum enrichment factors for the compounds tested are summarized in Table 6.2.

Table 6.2: Maximum Enrichment factors for lanthanide compounds in 10^{-4}M HNO_3 capture matrix.

Target Compound	Enrichment Factor
Holmium 8-hydroxyquinolinate	4.54
Holmium Acetylacetonate	6.05
Samarium 8-hydroxyquinolinate	1.37

6.4 Conclusions

Comparing the enrichment factors (EF) obtained with HNO_3 capture matrix (Table 6.2) and H_2O capture matrix (Table 5.3) it can be seen that in the case of holmium acetylacetonate the enrichment factor decreased from 14.83 to 6.05, in the case of holmium 8-hydroxyquinolinate it decreased from 11.26 to 4.54 and in the case of samarium 8-hydroxyquinolinate decreased from 11.19 to 1.37. Therefore with respect to the obtained results it can be concluded that lowering the pH of the capture matrix results in a decrease in the enrichment factor. The decrease maybe due to further dissolution or breakdown of the target in the lower pH capture matrix compared to the water capture matrix, resulting in a higher concentration of carrier (stable isotope) being released and therefore lower enrichment factors. Further investigation of the effect of capture matrix pH on enrichment factor needs to be performed to determine the optimum conditions for choosing the capture matrix.

CHAPTER 7: CONTINUOUS FLOW/SZILARD-CHALMERS RADIOISOTOPE PRODUCTION ALTERNATIVE LANTHANIDE TARGETS

7.1 Introduction

Depending on the energy of the recoiling radionucleus and the environment of its surroundings, which effects the number of collisions it has with surrounding atoms hence resulting in its slow down, it can travel a certain distance.

The recoiled radionucleus baring kinetic energy is slowed down and eventually stopped through collision with other atoms. Therefore if the target is relatively thin or has a large lanthanide containing surface area in contact with the capture matrix, there will be an increased probability that the recoil range of the radionucleus exceeds the thickness of the target and therefore escapes into the capture matrix [92]. However if the recoiling radionuclide is located a farther distance from the target/capture matrix interface it is less likely capable of recoiling into the capture matrix due to its distance from the capture matrix and also it is more likely to collide with surrounding atoms resulting in further retention of the radionuclide in the irradiation target. Thus ideally the irradiation target should be very thin or have a large surface area covered with the target atom, that is in contact with the capture matrix, so the recoiled radionuclide can escape into the capture matrix and be separated from the irradiation target [109]. For this purpose, developing irradiation targets such as lanthanide containing-resins, microspheres, thin films and nanowires might afford such results.

The Ho-Ethyl-BTP XAD-4 resin, HoAcAc PLA material, HoAcAc PVA XAD-4 and Ho8HQ PVA XAD-4 resin were studied as potential irradiation targets for Szilard-Chalmers experiments. Experiments were performed to: determine the solubility of the target in the capture matrix, the lanthanide content of the target and observe the target behavior upon neutron activation.

7.2 Experimental Procedures

Neutron activation analysis was performed on the Holmium Ethyl-BTP XAD-4 resin, based on these experiments the concentration of lanthanide adsorbed on the resin was too low for it to be a desirable irradiation target for Szilard-Chalmers studies. Therefore, as future work, further enhancement of the synthesis route is necessary so a higher concentration of the lanthanide is absorbed on the functionalized Ethyl-BTP.

In order to determine the amount of holmium present in the synthesized PVA based target material, neutron activation analysis was carried out. The HoAcAc PVA, HoAcAc PVA XAD-4 and Ho8HQ PVA XAD-4 samples were irradiated for 20 min at the 75 kW power level (neutron flux ~2.5×10^{11} $n.cm^{-2}.s^{-1}$) alongside corresponding holmium standards, in the Lazy Susan section of the reactor core, at the UCI TRIGA reactor facility.

Due to the issue mentioned regarding filtration of the HoAcAc PVA using the centrifugal filter tubes, the solubility of the HoAcAc PVA and determination of how much holmium was transferred to each wash was not carried out.

7.3 Pre-irradiation Solubility Tests

The HoAcAc PVA XAD-4 and Ho8HQ PVA XAD-4 resins were analyzed for solubility using the Millipore centrifugal filter tubes, such that approximately 20 mg of the resin was placed on the filter and contacted with water for 20 minutes, the wash was filtered and transferred to an irradiation vial (Wash1). The resin was contacted with water a second time again for 20 minutes and the wash was transferred to another irradiation vial (wash 2). The Centrifugal tube containing the resin, wash 1, wash 2 were submitted for neutron activation analysis to determine the amount of holmium in each phase and in turn determine the solubility of the resin in the water capture matrix.

Table 7.1: Solubility and retention values of the studied lanthanide resins in the wash and target.

Compound	% Activity in Wash 1	% Activity in Wash 2	%Activity in Target
HoAcAc PVA XAD-4	1.71±0.54	1.01±0.28	97.82±4.25
Ho8HQ PVA XAD-4	0.98±0.54	0.52±0.39	98.51±7.60

With respect to Table 7.1 it can be seen that in the case of both HoAcAc PVA XAD-4 and Ho8HQ PVA XAD-4 over 96 % of the holmium remained retained in the solid target and there was minimal indication of solubility. In the case of the HoAcAc PVA XAD-4 it can be seen a total 2.72 % of holmium was found in the capture matrix with the first wash being higher with 1.71 % and the second wash lower with 1.01 % holmium transferred to the wash. The same trend was seen with the Ho8HQ PVA XAD-4 resin were a total of 1.50 % of holmium was found transferred to the capture matrix with the first wash being higher with 0.98 % and the second wash lower with 0.52 % holmium transferred to the wash. The higher holmium content in the first wash was most likely due to any uncomplexed holmium or impurities that washed out in the initial wash. In general the Ho8HQ compounds were less soluble in the capture matrix compared to the HoAcAc compounds. The lower solubility of the Ho8HQ compounds can be attributed to their higher stability constant compared to the HoAcAc compound (Table 3.2)

7.4 Neutron Activation Analysis

All three potential targets were irradiated to determine the lanthanide radioactivity per gram of irradiated material and the results were compared to the lanthanide radioactivity per gram of the original powder compounds of HoAcAc or Ho8HQ.

Table 7.2: Radioactivity per gram of various holmium irradiation target candidates.

Compound	**^{166}Ho Activity (Bq)/Mass of target material (g)**
HoAcAc powder	1.46E+07
Ho8HQ powder	9.14E+06
HoAcAc PVA	1.73E+06
HoAcAc PVA XAD-4	2.80E+06
Ho8HQ PVA XAD-4	5.69E+05

With respect to Table 7.2 the HoAcAc and Ho8HQ powders, which were used as an irradiation target in chapters 4,5 and 6 had the highest activity per gram of material, as predicted, since both were just one of the components used in the synthesis of the PVA and PVA XAD-4 targets. HoAcAc PVA XAD-4 had 38.2% higher activity per gram of target compared to the HoAcAc PVA target material. Irradiation of one gram of the HoAcAc PVA XAD-4 resin results in an increase in radioisotope production compared to the same mass of the HoAcAc PVA material. Due to the dense nature of PVA target it was not an ideal irradiation target candidate with the current irradiation setup, since the target is placed in a filter tube the dense nature of the PVA material prevents the capture matrix from filtering out into the collection container.

The HoAcAc PVA XAD-4 resin had higher activity per gram of material compared to the Ho8HQ PVA XAD-4 due to the different synthesis conditions. In the case of the Ho8HQ PVA XAD-4 resin, the ratio of XAD-4 resin to the Ho8HQ PVA mixture was higher, resulting in less holmium being adsorbed per gram of resin compared to the HoAcAc PVA XAD-4 resin. Since the coating of XAD-4 resins with a Lanthanide PVA mixture was not found in literature synthesis conditions were experimented with, in order to find the most suitable synthesis conditions. Post irradiation the resins were inspected visually for any degradation or apparent irradiation damage, the resin showed no visible sign of damage. Although the activity per gram

of the powder was considerably higher compared to the resins, the resins were still considered as irradiation targets for subsequent experiments. The high surface area, porosity, stability and insolubility of the resins were appealing factors to consider them for Szilard-Chalmers studies.

7.5 Szilard Chalmers Studies Results and Discussion

The HoAcAc and Ho8HQ PVA XAD-4 resins were both used as targets for solubility, irradiation/recoil and post irradiation studies using the same experimental conditions detailed in chapter 5, utilizing the continuous flow irradiation setup at the UCI reactor facility.

Table 7.3: Experimental results regarding Holmium stable and radioisotope content as a result of the continuous flow setup.

Target	**HoAcAc PVA XAD-4**
Capture Matrix	H_2O
Initial ^{165}Ho stable atoms in target pre-irradiation	2.20E+19
Total ^{165}Ho stable atoms collected in capture matrix during irradiation	2.73E+17
Total ^{165}Ho stable atoms remaining in target	2.17E+19
Total ^{166}Ho radioactive atoms collected in capture matrix	1.13E+09
Total ^{166}Ho radioactive atoms remaining in target	6.12E+09
% Total radioactive ^{166}Ho found in capture matrix	18.46
% Total stable ^{165}Ho found in capture matrix	1.24
Highest Enrichment Factor	24.36

In terms of target the HoAcAc PVA XAD-4 resin resulted in a higher enrichment factor compared to the HoAcAc and Ho8HQ targets in powder form. The higher enrichment factors were due to the higher stability of the resin when exposed to the irradiation field, resulting in less degradation and breakdown of the target. Therefore a smaller amount of stable isotope was released in the capture matrix and consequentially higher enrichment factors were obtained. The HoAcAc PVA XAD-4 resin and H_2O capture matrix combination resulted in the smallest percentage of stable isotope released in the capture matrix. Out of the total stable ^{165}Ho initially present in the target 1.24% was released in the capture matrix (Table 7.3).

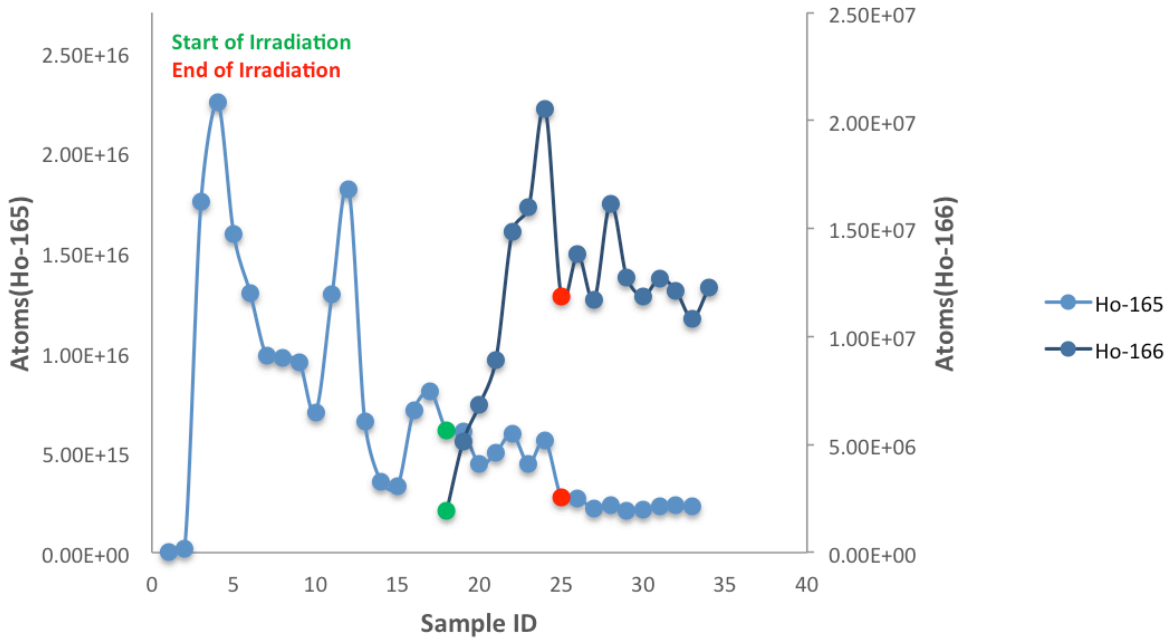

Figure 7.1: HoAcAc PVA XAD target and water capture matrix. Stable Isotope (light blue) and Radioisotope (dark blue) behavior via the Szilard-Chalmers process coupled with the continuous flow setup.

Post irradiation, the samples collected pre irradiation for solubility studies, during irradiation for Szilard-Chalmers effect studies and post irradiation samples were analyzed for stable isotope and radioisotope content and then compared to the stable isotope and radioisotope content of the target material for enrichment factor determination. Figure 7.1 illustrates the behavior of the samples collected pre, during and post irradiation. Stable isotope Ho-165 content and radioisotope content Ho-166 is depicted by the light blue and dark blue respectively. For the samples collected pre irradiation (prior to the green point) it can be seen there is an increase in ^{165}Ho followed by a decrease and another sharp increase. The inconsistent behavior and increase in Ho-165 can be attributed to the presence of impurities or any un-complexed lanthanides that were not washed out in the post synthesis workup of the resin. During irradiation (between green and red point) the Ho-165 carrier concentration is decreasing while the ^{166}Ho radioisotope concentration is increasing, indicating enrichment of the radioisotope product. Each sample is

collected for 2-minute time intervals and the stable and radioactive content are directly compared to each other, therefore the enrichment factor can be monitored to determine the optimum time and conditions during the experiment that yields the highest enrichment factor. Throughout the experiments carried out with the continuous irradiation setup, a similar trend in enrichment factors can be seen throughout all the samples collected. The enrichment factor continuously increases for the duration of the irradiation due to continuous radioisotope buildup and transfer to the capture matrix, the increase continues until usually 1-3 sample post irradiation and then decreases due to the end of irradiation and end of radioisotope production. With respect to the data obtained from ICP-MS and HPGe analysis of the samples and the corresponding lanthanide irradiation targets, the enrichment factors were determined. The enrichment factors were calculated using the same equations as in chapter 4 (Eq. 4.1). The maximum enrichment factor for the HoAcAc PVA XAD-4 target tested is summarized in Table 7.4.

Table 7.4: Maximum enrichment factor for HoAcAc PVA XAD-4.

Target Compound	**Enrichment Factor**
HoAcAc PVA XAD-4	24.36

7.6 Conclusions

The HoAcAc PVA XAD-4 compound irradiation with the continuous flow setup and water capture matrix, resulted in an enrichment factor of 24.36, which was a significant increase compared to the results obtained in Chapter 5 were the HoAcAc powder was the irradiation target (Enrichment factor= 14.83).

An enrichment factor of 24.36 obtained for the HoAcAc PVA XAD-4 target, results in a 96% decrease in the amount of holmium needed for a typical medical procedure.

The Ho8HQ PVA XAD-4 resin was tested twice using the continuous flow setup, due to complications with the setup and pump system the capture matrix was not fully contacted with the resin and was discharged through the top of the filter tube, as opposed to going through the target and collecting the recoiling species. The issue has been identified and currently steps are being taken to resolve the issue.

CHAPTER 8: CONCLUDING REMARKS

The enrichment factors obtained in the present study showed promising results. There was a significant increase in enrichment factors when switching to a continuous flow system (Chapter 5,6 and 7), compared to the static irradiation method used in the initial proof of concept experiments (Chapter 4). The unique continuous flow experimental setup allowed continuous flow of capture matrix through the target during irradiation and hence separation of the recoiled radionuclide from the bulk of the irradiation target. The setup allowed instantaneous separation of the capture matrix containing the recoiled isotope from the bulk of the inactive material preventing possible retention due to reformation of original bonds. In addition the experimental arrangement was advantageous in a sense that during one irradiation period a large sample range was collected, which allowed the monitoring of the enrichment factor behavior with irradiation time. Using this information the optimal conditions could be chosen for obtaining the maximum enrichment factor.

The Szilard-Chalmers method was studied using both, lanthanide powders as irradiation targets and lanthanide coated resins (HoAcAc PVA XAD-4), with respect to the obtained results the lanthanide coated resins, generated higher enrichment factors compared to the powder targets. The improved enrichment factors can be attributed to higher stability of the resin, larger lanthanide containing surface area in contact with the capture matrix and less degradation of the target due to exposure to the radiation field resulting in less stable isotope carrier released in the capture matrix and in turn higher specific activity.

Water and 10^{-4} M HNO_3 were both used as capture matrices. Water was used as a capture matrix for the lanthanide powder targets and the HoAcAc PVA XAD-4 resins. The lower pH HNO_3 capture matrix was chosen to prevent potential hydrolysis of the lanthanide. Under the stated

experimental conditions water was a more suitable capture matrix candidate, resulting in higher enrichment factors compared to HNO_3. The lower enrichment factor can be attributed to the breakdown of the lanthanide target in the HNO_3 capture matrix and release of the stable isotope carrier, resulting in lower specific activity and in turn smaller enrichment factors.

Although significant progress was made in terms of experimental setup, irradiation targets and enrichment factors, there is still need for improvement of the experimental conditions and further enhancement of the specific activity, so the produced radioisotopes can be potentially used for medical applications.

The following factors may be contributing to release of the stable isotope carrier in the capture matrix and retention of the radioisotope in the target that can lead to a decrease in enrichment factors (i) Radiolysis of the irradiation target due to exposure to ionizing radiation during neutron bombardment, leading to release of inactive atoms in the capture matrix and resulting in dilution of the radioactivity of the radioisotopes separable through recoil[110]. (ii) Insufficient recoil energy available to break the bonds of the target molecule and release the radioisotope into the capture matrix. For example ^{153}Sm emits 160 prompt gamma rays [56] upon neutron capture, resulting in recoil energies between 0.0028-121.7 eV. Electrostatic bond energies are on the order of a few electron volts. Thus in some cases the recoil energy is small compared to the bond energy of the target molecule and the radioisotope remains retained in the target (iii) Dissipation of the recoil energy through the molecule before the recoiling radioisotope has the opportunity to leave its immediate vicinity leading to retention of the radioisotope in the irradiation target[111].

The obtained results showed potential for enhancement of the specific activity of reactor produced radioisotopes via the Szilard-Chalmers method. The continuous flow system resulted

in enrichment factors that can reduce the amount of lanthanide needed for a typical medical procedure by 96%.

Furthermore using the proposed method compared to just irradiating the target alone (The typical method employed for reactor-produced radioisotopes) results, on average, in an increase of the specific activity by an order of magnitude (Specific Activity: Activity (Becquerel,Bq) of radioisotope (^{166}Ho) divided by grams of stable isotope (^{165}Ho)). Figure 8.1 illustrates the specific activity of the capture matrix, rich in radioactive ^{166}Ho, collected via the Szilard-Chalmers method compared to the specific activity of the same target irradiated without further processing.

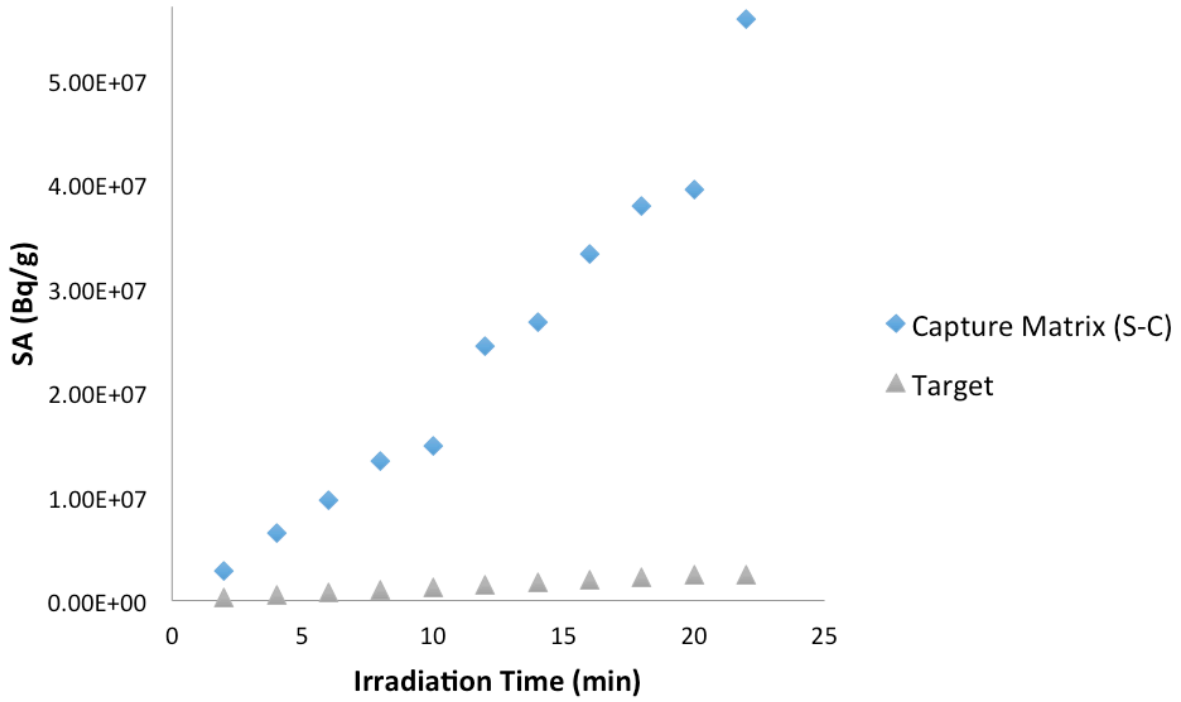

Figure 8.1: Specific activity (SA) of target, holmium acetylacetonate (HoAcAc), compared to the specific activity of the radioisotope rich capture matrix (H_2O).
Blue data points resemble the specific activity (Bq/g) of the capture matrix collected via the continuous flow setup coupled with the Szilard-Chalmers (S-C) method using a HoAcAc target. Grey data points resemble the specific activity of the HoAcAc target irradiated under the same conditions without any separation.

CHAPTER 9: FUTURE WORK

Looking into other potential irradiation targets is an area of interest for future studies. A challenge encountered in choosing a target material for Szilard-Chalmers studies is developing irradiation targets that are thin and have a high surface area exposed to the capture matrix, such that the recoil range of the radionuclide exceeds the thickness of the target and can be easily ejected into the capture matrix. Synthesis and development of irradiation targets need to be further explored such that irradiation targets are produced: (i) that can withstand exposure to the radiation field, without degrading in the capture matrix and diluting the specific activity (ii) irradiation targets with a large surface area containing the target isotope of interest, such as porous resins.

Also further considering capture matrices with pH levels optimal for radioisotope extraction and retention is of interest for future studies. In addition to exploring treatment of the capture matrix containing the radioisotope product post irradiation, using techniques such as solvent extraction and ion exchange to obtain a more pure radioisotope product.

Degradation of the irradiation target and release of the stable isotope carrier into the capture matrix is an ongoing issue that results in dilution of the specific activity and lower enrichment factors. Therefore investigation of the effect of gamma radiation that occurs during irradiation that can lead to degradation of the target is necessary.

Although initially the goal of the study was to produce radioisotopes for medical applications, the radioisotope production method can be further expanded to produce radioisotopes that are in high demand for other applications. One radioisotope that can specifically benefit from being produced via the Szilard-Chalmers method though the continuous flow system is: Plutonium-238 (^{238}Pu).

The ^{238}Pu radioisotope has a number of applications such as use in radioisotope power systems as a long-lived heat source to power space missions[112,113] or in nuclear powered cardiac pacemakers[114,115]. The decay heat of ^{238}Pu can be converted to electricity using a radioisotope thermoelectric generator (RTG)[112]. Currently ^{238}Pu is produced by neutron bombardment of large Neptunium-237 targets for periods of up to 1 year[116], according to the following mechanism (Eq. 9.1):

$$^{237}Np+n \rightarrow {}^{238}Np \rightarrow (\beta^-, 2.117 \text{ days}) \rightarrow {}^{238}Pu \quad \text{(Eq. 9.1)}$$

Such that the ^{237}Np with a neutron capture cross section of 170 barns captures a neutron to produce ^{238}Np which then beta decays with a half-life of 2.117 days to ^{238}Pu. A disadvantage of this production route is that the intermediate radioisotope of ^{238}Np has a large fission cross-section of 2600 barns therefore a majority (~85%) of the ^{238}Np has fissioned before decaying to ^{238}Pu. Applying the proposed Szilard-Chalmers method via the continuous flow setup can potentially address the challenges encountered in ^{238}Pu production.

The ultimate goal of the current study was to be able to successfully scale up the radioisotope production method and produce radioisotopes for medical, industrial, scientific and research purposes. Therefore studies need to be performed to determine the behavior of the target, capture matrix and specific activity as a result of scale up when using a higher neutron flux and longer irradiation time.

References

1. Safavi-Tehrani, L., Miller, G. E. & Nilsson, M. Production of high specific activity radiolanthanides for medical purposes using the UC Irvine TRIGA reactor. *J. Radioanal. Nucl. Chem.* **303,** 1099–1103 (2014).
2. Mausner, L. F. & Mirzadeh, S. Reactor Production of Radionuclides.*Handbook of Radiopharmaceuticals* 87–117 (John Wiley & Sons, Ltd, 2002). doi:10.1002/0470846380.ch3
3. Committee on State of the Science of Nuclear Medicine & National Research Council. Advancing Nuclear Medicine Through Innovation. *National Center for Biotechnology Information* (2007).
4. World Nuclear Association. Radioisotopes in Medicine. Available at: http://www.world-nuclear.org/information-library/non-power-nuclear-applications/radioisotopes-research/radioisotopes-in-medicine.aspx.
5. Zeisler, S.K., Weber, K. Szilard-Chalmers effect in holmium complexes. *J. Radioanal. Nucl. Chem.* **227,** 0–4 (1998). doi: 10.1007/BF02386438
6. Dadachova, E., Mirzadeh, S., Lambrecht, R. M., Hetherington, E. L. & Knapp, F. F. Separation of Carrier-free^{166}Ho from Dy_2O_3 Targets by Partition Chromatography and Electrophoresis. *J. Radioanal. Nucl. Chem.* **199,** 115–123
7. Bakht, M. K. & Sadeghi, M. Internal Radiotherapy Techniques using Radiolanthanide Praseodymium-142: A review of production routes, brachytherapy, unsealed source therapy. *Annals of Nuclear Medicine* (2011). doi:10.1007/s12149-011-0505-z
8. Horwitz, E. P., McAlister, D. R., Bond, A. H., Barrans, R. E. & Williamson, J. M. A Process for the Separation of ^{177}Lu from Neutron Irradiated ^{176}Yb Targets. *Appl. Radiat. Isot.* (2005). doi:10.1016/j.apradiso.2005.02.005
9. Chakraborty, S., Unni, P. R., Venkatesh, M. & Pillai, M. R. Feasibility Study for Production of ^{175}Yb: a Promising Therapeutic Radionuclide. *Appl. Radiat. Isot.* **57,** 295–301 (2002).
10. Volkert, W.A., Goeckeler, W. F., Ehrhardt, G. J. & Ketring, a R. Therapeutic Radionuclides: Production and Decay Property Considerations. *J. Nucl. Med.* **32,** 174–185 (1991).
11. Volkert, W.A., Hoffman, T.J... Therapeutic Radiopharmaceuticals. *Chem. Rev.* **99,** 2269–2292 (1999).
12. Radiochemistry Society. Nuclear Medicine. Available at: http://www.radiochemistry.org/nuclearmedicine/index.shtml.
13. Evans, W. J. Organometallic lanthanide chemistry. *Adv Organometal Chem* **24,** 131–177 (1985).
14. Fricker, S. P. The therapeutic application of lanthanides. *Chem. Soc. Rev.* **35,** 524–533 (2006).
15. Kretsinger, R. H., Uversky, V. N. & Permyakov, E. A.. Encyclopedia of Metalloprotiens 1098–1103 (Springer New York, 2013). doi:10.1007/978-1-4614-1533-6_151
16. Ma, D., Ketring, A.R., Ehrhardt, G.J., Jia, W. Production of Radiolanthanides and Radiotherapy Research at MURR. *Budapest J. Radioanal. Nucl. Chem. Artic.* **206,** 119–126 (1996).
17. Rösch, F. Radiolanthanides in endoradiotherapy: An overview. *Radiochim. Acta* **95**, 303-311 (2007). doi:10.1524/ract.2007.95.6.303

18. Uusijärvi, H., Bernhardt, P., Rösch, F., Maecke, H. R. & Forssell-Aronsson, E. Electron- and Positron-Emitting Radiolanthanides for Therapy: Aspects of Dosimetry and Production. *J Nucl Med* **47,** 807–814 (2006).
19. Louw, W. K. A. *et al.* Evaluation of Samarium-153 and Holmium-166-EDTMP in the Normal Baboon Model. *Nucl. Med. Biol.* **23,** 935–940 (1996).
20. Sartor, O. Overview of samarium Sm-153 lexidronam in the treatment of painful metastatic bone disease. *Rev. Urol.* **6 Suppl 10,** S3–S12 (2004).
21. Goeckeler, W. F. *et al.* Skeletal Localization of Samarium-153 Chelates: Potential Therapeutic Bone Agents. *J. Nucl. Med.* **28 ,** 495–504 (1987).
22. Serafini, A. N. Systemic Metabolic Radiotherapy with Samarium-153 EDTMP for the Treatment of Painful Bone Metastasis. *Q. J. Nucl. Med.* **45,** 91–99 (2001).
23. Finlay, I. G., Mason, M. D. & Shelley, M. Radioisotopes for the Palliation of Metastatic Bone Cancer: a Systematic Review. *Lancet. Oncol.* **6,** 392–400 (2005).
24. Goeckeler, W. F. *et al.* ^{153}Sm Radiotherapeutic Bone Agents. *Int. J. Rad. Appl. Instrum. B.* **13,** 479–482 (1986).
25. Nayak, D. & Lahiri, S. Application of Radioisotopes in the Field of Nuclear Medicine I. Lanthanide series elements. *J. Radioanal. Nucl. Chem.* **242,** 423–432 (1999).
26. Bayouth, J. E. *et al.* Pharmacokinetics, Dosimetry and Toxicity of Holmium-166-DOTMP for Bone Marrow Ablation in Multiple Myeloma. *J. Nucl. Med.* **36,** 730–737 (1995).
27. Mumper, R. J., Ryo, U. Y. & Jay, M. Neutron-Activated Holmium-166-poly (L-lactic acid) Microspheres: A Potential Agent for the Internal Radiation Therapy of Hepatic Tumors. *J. Nucl. Med.* **32,** 2139–2143 (1991).
28. Breitz, H., Wendt, R., Stabin, M., Bouchet, L. & Wessels, B. Dosimetry of High Dose Skeletal Targeted Radiotherapy (STR) with ^{166}Ho-DOTMP. *Cancer Biother. Radiopharm.* **18,** 225–230 (2003).
29. Giralt, S. *et al.* ^{166}Ho-DOTMP plus Melphalan followed by Peripheral Blood Stem Cell Transplantation in Patients with Multiple Myeloma: Results of two phase 1/2 trials. *Blood* **102,** 2684–2691 (2003).
30. Mäkelä, O., Sukura, A., Penttilä, P., Hiltunen, J. & Tulamo, R.-M. Radiation Synovectomy With Holmium-166 Ferric Hydroxide Macroaggregate in Equine Metacarpophalangeal and Metatarsophalangeal Joints. *Vet. Surg.* **32,** 402–409 (2003).
31. Costa, R. F. *et al.* Production of Microspheres Labeled with Holmium-166 for Liver Cancer Therapy: the Preliminary Experience at IPEN/CNEN-SP. *International Nuclear Atlantic Conference Innovations in nuclear technology for a sustainable future, Brazil (2009).*
32. Frantisek, M. Preparation of Ho-166 Labeled Compounds for Endoradiotherapy and Skin Cancer Therapy. *Nuclear physics institute, Radiopharmaceuticals Department Prague,CZ*
33. World information service on Energy & Nuclear information and resource service. Medical Radioisotopes Production without a Nuclear Reactor. (2010). Available at: http://www.nirs.org/mononline/nm710.pdf.
34. Mirzadeh, S., Mausner, L. F. & Garland, M. A. Handbook of Nulcear Chemistry. 1857–1902 (Springer US, 2011). doi:10.1007/978-1-4419-0720-2_38
35. Qaim, S. M. Handbook of Nuclear Chemistry 1903–1933 (Springer US, 2011). doi:10.1007/978-1-4419-0720-2_39

36. Köster, D. H. U. Production of Medical Radioisotopes with High Specific Activity in Photonuclear Reactions with γ -beams of High Intensity and Large Brilliance. *Appl Phys B* (2011) **103**: 501–519 (2011). doi:10.1007/s00340-010-4278-1

37. Nassan, L., Achkar, B. & Yassine, T. Nuclear Chemical Transformations of Ytterbium and Lutetium Radionuclides following (n,gamma) and Beta Decay Reactions in Tris(2,2,6,6-tetramethyle-3,5-heptanedionato)Yb(III). *Appl. Radiat. Isot.* (2012). doi:10.1016/j.apradiso.2011.11.060
38. Bushberg, J. T., Seibert, A. J., Leidholdt, E. M. & Boone, J. M. The Essential Physics of Medical Imaging. (2011).
39. IAEA. Production and Supply of Molybdenum-99. Available at: https://www.iaea.org/About/Policy/GC/GC54/GC54InfDocuments/English/gc54inf-3-att7_en.pdf
40. Tilbury, R. S. & Laughlin, J. S. Cyclotron Production of Radioactive Isotopes for Medical Use. *Semin. Nucl. Med.* **4,** 245–255 (1974).
41. De Goeij, J. J.M. Nuclear, Physical and Chemical Aspects in Cyclotron Production of Radionuclides. *Nucl. Instruments Methods Phys. Res. Sect. B Beam Interact. with Mater. Atoms* **139,** 91–97 (1998).
42. Szilard, L. & Chalmers, T. A. Chemical separation of the radioactive element from its bombarded isotope in the Fermi effect. *Nature* **134,** 462 (1934).
43. Zeisler, S.K., Becker, D.W., Weber, K. Szilard-Chalmers reaction in praseodymium compounds. *J. Radioanal. Nucl. Chem.* **240***,* 637-641 (1999). doi:10.1007/BF02349425
44. Zhernosekov, K. P., Filosofov, D. V. & Rösch, F. The Szilard-Chalmers Effect in Macrocyclic Ligands to Increase the Specific Activity of Reactor-Produced Radiolanthanides: Experiments and Explanations. *Radiochim. Acta* **100,** 669–674 (2012).
45. Jia, W., Ehrhardt, G.J. Enhancing the Specific Activity of ^{186}Re Using an Inorganic Szilard-Chalmers Process . *Radiochim. Acta* **79,** 131-136 (1997).
46. Nassan, L., Yassine, T. & Achkar, B. Production of ^{166}Ho and ^{153}Sm using Hot Atom Reactions in Neutron Irradiated Tris(cyclopentadienyl) Compounds. *Nukleonika* **56,** 263–267 (2011).
47. Mausner, L. F., Mirzadeh, S. & Srivastava, S. C. Improved Specific Activity of Reactor Produced ^{117m}Sn with the Szilard-Chalmers Process. *Int. J. Radiat. Appl. Instrumentation. Part* (1992). doi:10.1016/0883-2889(92)90053-H
48. Revay, Z. & Belgya, T. in Handbook of Prompt Gamma Activation Analysis with Neutron *Beams* (ed. Molnar, G. L.) (Kluwer Academic Publishers, 2004).
49. Zhang, Z., Wang, X., Wu, Y., Liu, Y., Zheng, W., Wang, K. Preparation of ^{186}Re and ^{188}Re with high specific activity by the Szilard–Chalmers effect. *J. Label. Compd. Radiopharm.* **43,** 55–64 (2000).
50. Hetherington, E.L., Sorby, P.J., Camakaris, J. The preparation of high specific activity copper-64 for medical diagnosis. *Int. J. Radiat. Appl. Instrum. Appl. Radiat. Isot.* **37**, 1242-1243 (1986). doi:http://dx.doi.org/10.1016/0883-2889(86)90014-6
51. Tomar, B.S., Steinebach, O.M., Terpstra, B.E., Bode, P., Wolterbeek, H.T. Studies on production of high specific activity ^{99}Mo and ^{90}Y by Szilard Chalmers reaction. *Radiochim. Acta* **98**, 499-506 (2010). doi:10.1524/ract.2010.1744
52. Wolterbeek, H.T., Bode, P. Process for the production of no-carrier added ^{99}Mo. U.S.

Patent 12/996,209, May 19, 2011.

53. Jia, W., Ehrhardt, G.J. Production of ^{186}Re, ^{188}Re and other radionuclides via inorganic szilard-chalmers process. U.S. Patent 09/151,874, April 24, 2001.
54. Jansen, D.R., Krijger, G.C., Kolar, Z.I., Zeevaart, J.R. Method of producing radionuclides. European Patent EP20110711686, January 22, 2014.
55. Campbell, D. Isotope enrichment process for lanthanide and actinide elements. U.S. Patent US3708392 A, January 2, 1973.
56. IAEA. Database for Prompt Gamma-ray Neutron Activation Analysis (2007).
57. IAEA. Database of Prompt Gamma Rays from Slow Neutron Capture for Elemental Analysis. (2007).
58. Friedlander, G., Kennedy, J. W., Macias, E. S. & Miller, J. M. Nuclear and Radiochemistry. (1981).
59. American Chemical Society. Worldwide Shortage of Isotopes for Medical Imaging Could Threaten Quality of Patient Care (2010).
60. Van Noorden, R. Radioisotopes: The Medical Testing Crisis. *Nature* **504,** 202–204 (2013).
61. IAEA. Averting a Medical Radioisotope Shortage. (2014).
62. Rosenthal, M. S. Ethical Issues in Radioisotope Shortages: Rationing and Priority Setting. *J. Nucl. Med. Technol.* **38,** 117–120 (2010).
63. Szabo, L. Radioisotope Shortage could Force Delays in Medical Tests. *USA Today* (2008).
64. The Department of Energy. *Expert Panel : Forecast Future Demand for Medical Isotopes* (1999). Available at: http://energy.gov/ne/downloads/expert-panel-forecast-future-demand-medical-isotopes
65. Simon, P. The Feasibility of Domestic Medical Isotope Production for Clincal Imaging Qualifying Project. Available at: https://www.wpi.edu/Pubs/E-project/Available/E-project-122013-151910/unrestricted/IQP_draft.pdf
66. World Nuclear Association. Radioisotopes in Industry. (2014). Available at: http://www.world-nuclear.org/information-library/non-power-nuclear-applications/radioisotopes-research/radioisotopes-in-industry.aspx
67. ANSTO. What are Radioisotopes. Available at: http://www.ansto.gov.au/NuclearFacts/AboutNuclearScience/Radioisotopes/
68. Updegraff, D., Hoedl, S. a & Ph, D. Nuclear Medicine without Nuclear Reactors or Uranium Enrichment. *American Association for the Advancement of Science.*(2013).
69. National Isotope Development Center. Isotope Production Methods. Available at: https://www.isotopes.gov/sites/production.html
70. Australian Nuclear Science and Technology Organisation. OPAL Research Reactor Available at: http://www.ansto.gov.au/AboutANSTO/OPAL/ (2015).
71. United States Nuclear Regulatory Commission. Backgrounder on Research and Test Reactors. (2015). Available at: http://www.nrc.gov/reading-rm/doc-collections/fact-sheets/research-reactors-bg.html.
72. World Nuclear Association. Resarch Reactors. Available at: http://www.world-nuclear.org/information-library/non-power-nuclear-applications/radioisotopes-research/research-reactors.aspx
73. IAEA. Radioisotope Production and Radiation Technology. Available at: http://www-naweb.iaea.org/na/RIRT/rirt.html.
74. Rosenman, J. Medical Isotopes. Available at: http://www.egeneration.org/medical-

isotopes/.
75. Chuvilin, D. Y., Khvostionov, V. E., Markovskij, D. V., Pavshouk, V. A. & Zagryadsky, V. A. Low-Waste and Proliferation-Free Production of Medical Radioisotopes in Solution and Molten-Salt Reactors. *Radioactive Waste* (2012).
76. Management Information Services. The Untold Story: The Economic Benefits of Nuclear Technologies. Available at: http://pbadupws.nrc.gov/docs/ml0037/ML003719644.pdf
77. Aloise, G. Managing Critical Isotopes: DOE's Isotope Program Needs Better Planning for Setting Prices and Managing Production Risks (2011).
78. Serafini, A. N. Samarium Sm-153 Lexidronam for the Palliation of Bone Pain Associated with Metastases. *Cancer* **88,** 2934–2939 (2000).
79. Lamb, H. M. & Faulds, D. Samarium ^{153}Sm Lexidronam. *Drugs Aging* **11,** 413–8; discussion 419 (1997).
80. Taylor, D. W. Economic and Clinical Net Benefits from the Use of Samarium Sm-153 Lexidronam Injection in the Treatment of Bone Metastases. *International Journal of Tumor Therapy*. **2,** 10–17 (2013).
81. Committee on Medical Isotope Production Without Highly Enriched Uranium & National Research Council. Medical Isotope Production without Highly Enriched Uranium. Available at: http://www.nap.edu/catalog/12569/medical-isotope-production-without-highly-enriched-uranium (2009).
82. Zeisler, S. K. & Weber, K. Szilard-Chalmers Effect in Holmium Complexes. *J. Radioanal. Nucl. Chem.* (1998). doi:10.1007/BF02386438
83. Australian Nuclear Science and Technology Organization (ANSTO). Annual Report 2012-2013. Available at: http://www.ansto.gov.au/cs/groups/corporate/documents/document/mdaw/mdez/~edisp/acs043245.pdf
84. IAEA. Research Reactor Database. Available at: https://nucleus.iaea.org/RRDB/RR/ReactorSearch.aspx?rf=1.
85. European Observatory on the Supply of Medical Radioisotopes. Capacity and Infrastructure Development. Available at: http://ec.europa.eu/euratom/observatory_radioisotopes.html (2014).
86. Olmsted, J. & Williams, G. Chemistry: The Molecular Science (2nd Edition). (1997).
87. Tomar, B.S., Steinebach, O.M., Terpstra, B.E., Bode, P., Wolterbeek, H.T. Studies on production of high specific activity ^{99}Mo and ^{90}Y by Szilard Chalmers reaction. *Radiochim. Acta* **98**, 499-506 (2010). doi:10.1524/ract.2010.1744
88. Sillen, L. G. & Martell, A. Stability Constants on Metal-Ion Complexes. (1964).
89. Gupta, R. D., Manku, G. S., Bhat, A. N. & Jain, B. D. Determination of the Stability Constants of Lanthanon(III) Complexes with 8-hydroxyquinoline and Some of its 5, 7-disubstituted Derivatives. *J. Less Common Met.* **20,** 345–352 (1970).
90. Mumper, R. J. & Jay, M. Formation and Stability of Lanthanide Complexes and Their Encapsulation into Polymeric Microspheres. *J. Phys. Chem.* **96,** 8626–8631 (1992).
91. Bains, A.P.. Lanthanide Contraction. *UC-DAVIS ChemWiki (2014).*
92. Choppin, G., Liljenzin, J.-O. & Rydberg, J. Radiochemistry and Nuclear Chemistry.
93. ROHM and HAAS. Amberlite XAD4 Industrial Grade Polymeric Adsorbent. Available at: http://www.dow.com/assets/attachments/business/process_chemicals/amberlite_xad/amberlite_xad4/tds/amberlite_xad4.pdf

94. Bhattacharyya, A. *et al.* Extraction Chromatographic Study on the Separation of Am^{3+} and Eu^{3+} using Ethyl-BTP as the Extractant. *J. Radioanal. Nucl. Chem.* (2011). doi:10.1007/s10967-010-0971-0
95. Singh, B. N. & Maiti, B. Separation and Preconcentration of U(VI) on XAD-4 Modified with 8-hydroxy quinoline. *Talanta* **69,** 393–6 (2006).
96. Rawat, B. N., Bhattacharyya, A., Ghosh, S. K., Gadly, T. & Tomar, B. S. Thermodynamics of Complexation of Lanthanides with 2,6-bis(5,6-diethyl-1,2,4-triazin-3-yl) pyridine. *Radiochim. Acta* **99,** 705–712 (2011).
97. Wei, Y., Sabharwal, K. N., Kumagai, M. & Asakura, T. Preparation of Novel Silica-Based Nitrogen Donor Extraction Resins and Their Adsorption Performance for Trivalent Americium and Lanthanides *J. Nucl. Sci. Tech* **37, 1108-1110 (2012)**.
98. Hoshi, H., Wei, Y.-Z., Kumagai, M., Asakura, T. & Morita, Y. Separation of trivalent actinides from lanthanides by using R-BTP resins and stability of R-BTP resin. *J. Alloys Compd.* **408-412,** 1274–1277 (2006).
99. Ecole Polytechnique Federale De Lausanne & Institute of chemical Sciences and Engineering. NMR Database.
100. Vente, M. A. D. *et al.* Neutron Activation of Holmium Poly(L-lactic acid) Microspheres for Hepatic Arterial Radioembolization: a Validation Study. *Biomed. Microdevices* **11,** 763–772 (2009).
101. Mumper, R. J. & Jay, M. Poly(L-lactic acid) Microspheres Containing Neutron-Activatable Holmium-165: a Study of the Physical Characteristics of Microspheres Before and after Irradiation in a Nuclear Reactor. *Pharm. Res.* **9,** 149–154 (1992).
102. Zielhuis, S. W. *et al.* Production of GMP-grade Radioactive Holmium Loaded Poly(L-lactic acid) Microspheres for Clinical Application. *Int. J. Pharm.* **311,** 69–74 (2006).
103. Nijsen, J. F. *et al.* Holmium-166 Poly Lactic Acid Microspheres Applicable for Intra-arterial Radionuclide Therapy of Hepatic Malignancies: Effects of Preparation and Neutron Activation Techniques. *Eur. J. Nucl. Med.* **26,** 699–704 (1999).
104. Bult, W. *et al.* Microspheres with Ultrahigh Holmium Content for Radioablation of Malignancies. *Pharm. Res.* **26,** 1371–1378 (2009).
105. Atwood, D. The rare earth elements : fundamentals and applications. (2012).
106. Choppin, G., Musikas, C., Sekine, T. & Rydberg, J. Solvent Extraction Equilibria in *Solvent Extraction Principles and Practice, Revised and Expanded* (CRC Press, 2004). doi:10.1201/9780203021460.ch4
107. Kislik, V. S. Chemistry of Metal Solvent Extraction in *Solvent Extraction* (ed. Kislik, V. S.) 113–156 (Elsevier, 2012). doi:http://dx.doi.org/10.1016/B978-0-444-53778-2.10003-2
108. Rizkalla, E. N. & Choppin, G. R. Hydration and Hydrolysis of Lanthanides. *J. of Alloys and Compounds* **180,** 325–336 (1992).
109. KUSAKA, Y. & MEINKE, W. W. Rapid Radiochemical Separations. *Sci. York* (1961).
110. Harbottle, G. Chemical Effects of Nuclear Transformations in Inorganic Solids. *Annu. Rev. Nucl. Sci.* **15,** 89–124 (1965).
111. Nassan, L., Yassine, T. & Achkar, B. Post-recoil thermal annealing study of ^{177}Lu, ^{169}Yb, ^{175}Yb, ^{166}Ho and ^{153}Sm in different organometallic compounds. *Nukleonika* **56,** 185–190 (2011).
112. National Aeronautics and Space Administration (NASA). What is Plutonium-238. Available at: https://solarsystem.nasa.gov/rps/docs/APP%20RPS%20Pu-238%20FS%2012-10-12.pdf

113. Witze, A. Nuclear Power: Desperately Seeking Plutonium. *Nat. News* (2014).
114. Los Alamos National Laboratory. Nuclear-Powered Cardiac Pacemakers. doi:http://osrp.lanl.gov/pacemakers.shtml
115. Huffman, F. N. & Norman, J. C. Nuclear-fueled cardiac pacemakers. *Chest* **65,** 667–672 (1974).
116. Howe, S. D., Crawford, D., Navarro, J. & Ring, T. Economical Production of Pu-238. *Nucl. Emerg. Technol. Sp. (NETS 2013)* (2013).

Appendix

A.1: SEM/ EDX Supplement

Sample 1: Uncoated XAD-4 resin

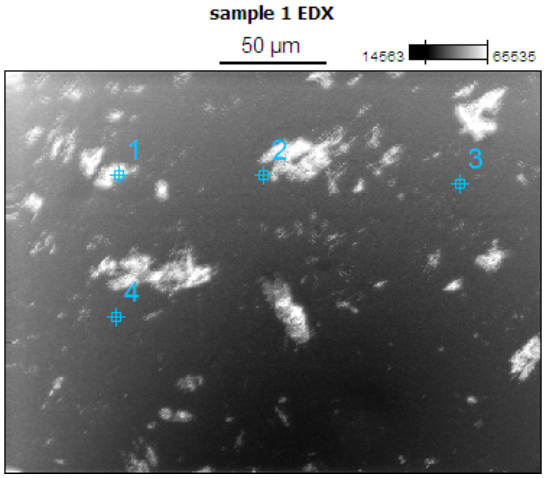

Image Name:	sample 1 EDX
Image Resolution:	512 by 384
Image Pixel Size:	0.49 µm
Acc. Voltage:	10.0 kV
Magnification:	1000

sample 1 EDX_pt1

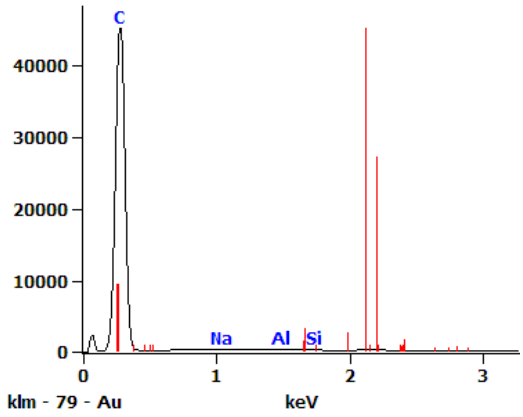

sample 1 EDX_pt2

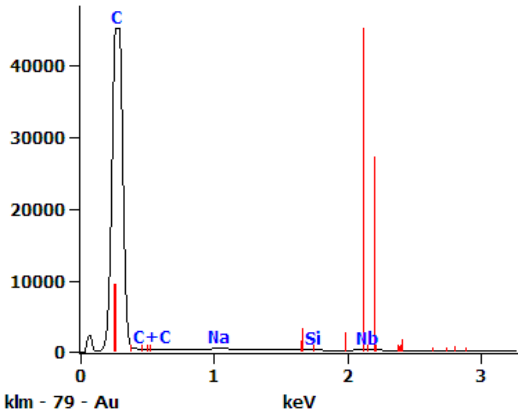

sample 1 EDX_pt3

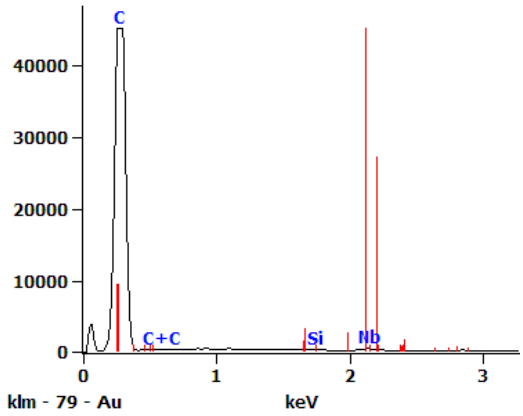

sample 1 EDX_pt4

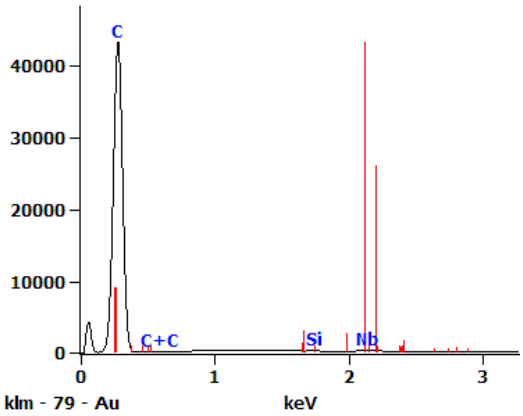

Sample 2: HoAcAc PVA XAD-4 resin

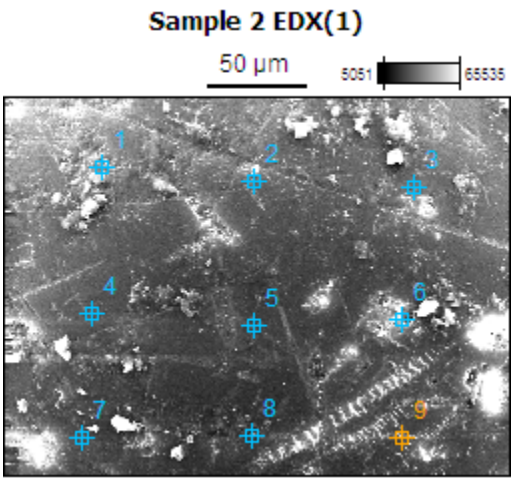

Image Name:	Sample 2 EDX(1)
Image Resolution:	512 by 384
Image Pixel Size:	0.49 µm
Acc. Voltage:	20.0 kV
Magnification:	1000

Sample 2 EDX(1)_pt1

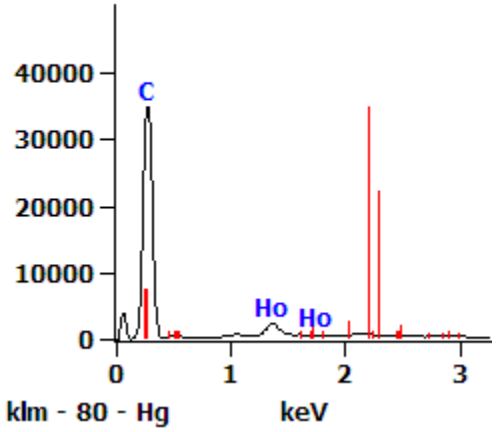

Sample 2 EDX(1)_pt2

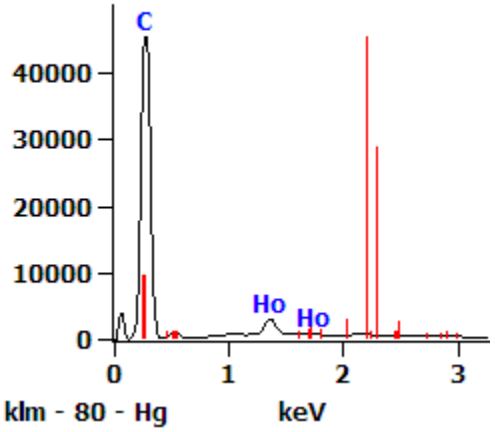

Sample 2 EDX(1)_pt3

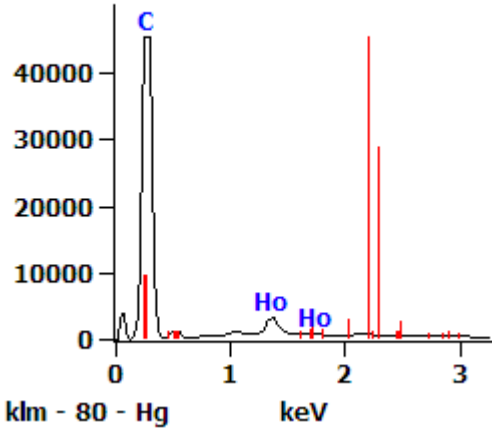

Sample 2 EDX(1)_pt4

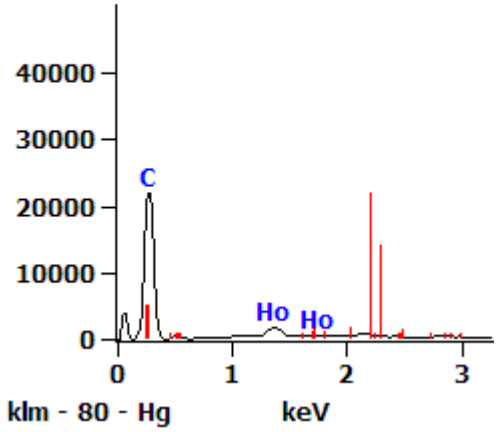

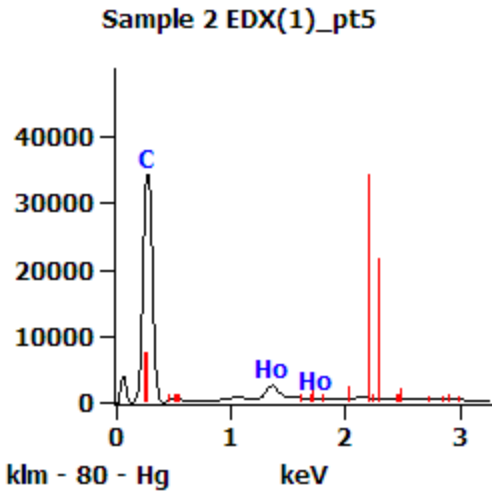
Sample 2 EDX(1)_pt5
40000
30000
20000
10000
0
C
Ho
Ho
0
1
2
3
klm - 80 - Hg
keV

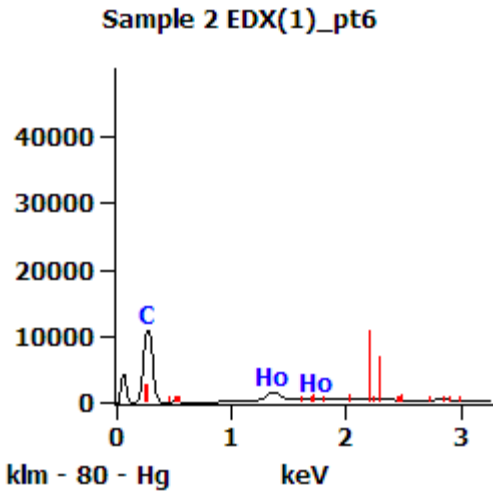
Sample 2 EDX(1)_pt6
40000
30000
20000
10000
0
C
Ho
Ho
0
1
2
3
klm - 80 - Hg
keV

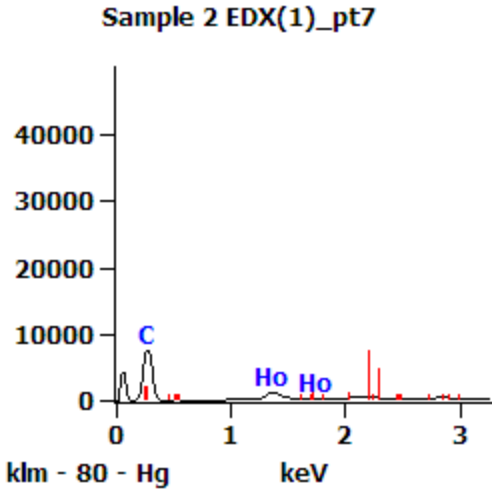
Sample 2 EDX(1)_pt7
40000
30000
20000
10000
0
C
Ho
Ho
0
1
2
3
klm - 80 - Hg
keV

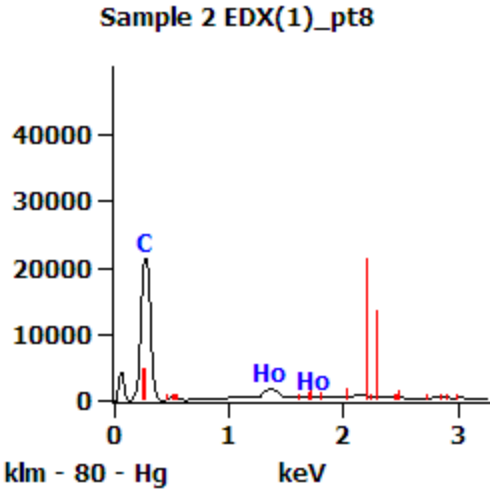
Sample 2 EDX(1)_pt8
40000
30000
20000
10000
0
C
Ho
Ho
0
1
2
3
klm - 80 - Hg
keV

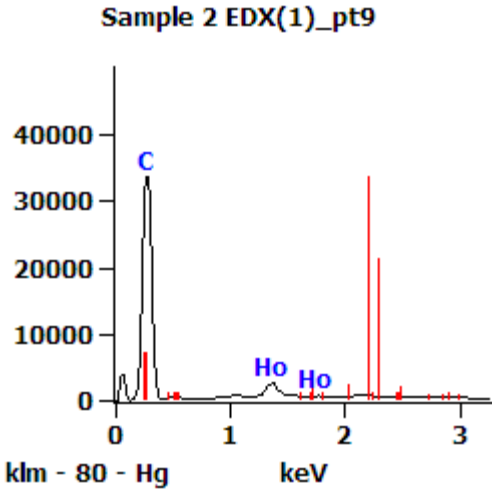
Sample 2 EDX(1)_pt9
40000
30000
20000
10000
0
C
Ho
Ho
0
1
2
3
klm - 80 - Hg
keV

Sample 3: Ho8HQ PVA XAD-4 resin

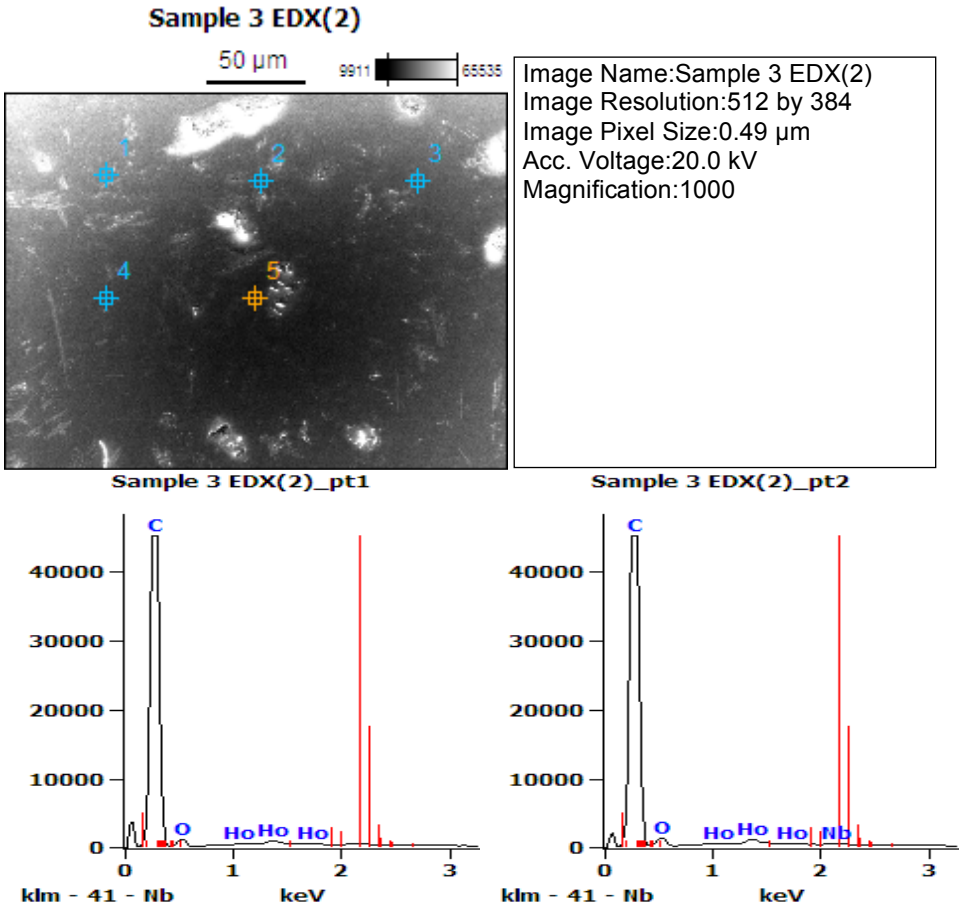

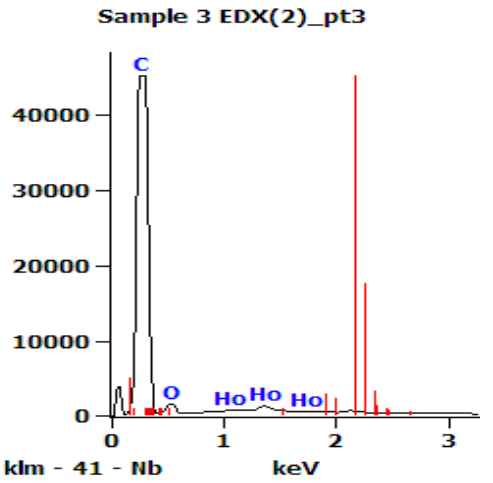
Sample 3 EDX(2)_pt3
C
O
Ho Ho Ho
40000
30000
20000
10000
0
0
1
2
3
klm - 41 - Nb
keV

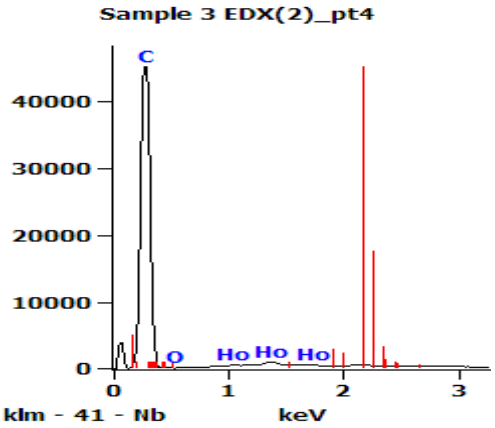
Sample 3 EDX(2)_pt4
C
O
Ho Ho Ho
40000
30000
20000
10000
0
0
1
2
3
klm - 41 - Nb
keV

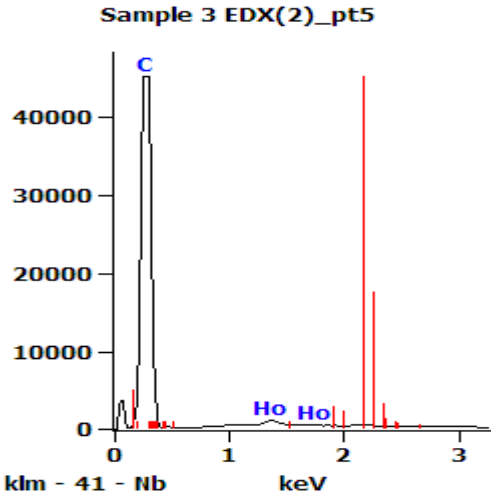
Sample 3 EDX(2)_pt5
C
Ho Ho
40000
30000
20000
10000
0
0
1
2
3
klm - 41 - Nb
keV